Evaluating state-of-the-art remotely sensed data and methods for mapping wetlands in Minnesota

A DISSERTATION
SUBMITTED TO THE FACULTY OF THE GRADUATE SCHOOL
OF THE UNIVERSITY OF MINNESOTA
BY

Lian Pamela Rampi

IN PARTIAL FULFILLMENT OF THE REQUIREMENTS
FOR THE DEGREE OF
DOCTOR OF PHILOSOPHY

Dr. Joseph F. Knight, Advisor

December 2013

Acknowledgements

I want to acknowledge all my colleagues, past and present, from the Remote Sensing and Geospatial Analysis Laboratory. Each has inspired me through their dedicated work in the field of remote sensing and geographic information systems.

I want to thank the American Society for Photogrammetry and Remote Sensing, and the Minnesota Department of Natural Resources. These professional and governmental entities have provided important data and networking opportunities to expand my research with meaningful information.

Also, I would like to acknowledge the core sources of funding for my Research assistantship at the University of Minnesota: the Legislative Citizen Commission on Minnesota Resources, the Minnesota Environment and Natural Resources Trust (ENRTF), the Minnesota Department of Natural Resources (MNDNR), and the United States Fish and Wildlife Services,

I would like to give a special thank you to my advisor Joseph Knight for always being patience and a consistent source of encouragement throughout all these last five years. This research was funded by (USFWS: Award 30181AJ194).

Dedication

This dissertation is dedicated to my husband Joshua Rampi. Joshua has been a continuous source of support and unconditional love that has allowed for me to reach for the stars in my professional career. I am grateful for you and our son Daniel Rampi, both have encouraged me to continue and finish my doctoral studies.

I would like to give a special thanks to my sisters Vania and Jasmin, my brother Carlos, my sister-in-law Geydi and my parents Maria and Carlos in Honduras. Their emotional support has allowed me to be filled and refresh along my journey.

Also, I would like to give another special thanks to my adoptive mother Becky Glewwe and my in-laws from Minnesota, Susan, Robert, Mia, Patrick, Jenny, John, Kemi and MaryAnn. My Minnesota family has provided me affection and spiritual support every time I needed it.

Finally, I would like to thank all my friends in Minnesota and my Honduras friends: Yery de Espinal, Sindy Palma, Meilyn de Moncada, Mauricio Moncada, Mario Nuñez, Lilian Morazán de Ruíz, Lincy Mejia, Otto Castillo, Eliezer Pavon, Roberto Barrientos, and all my friends in Zamorano University for always encouraging me to go beyond what I thought was possible!

Abstract

Appropriate management of our natural resources requires constant improvement and update of natural resource inventories. Remote sensing data and techniques offer an effective way to map and estimate changes in our current natural resources.

The research presented in this dissertation will demonstrate state-of-the art remote sensing based methods for mapping natural and man-made features, including wetlands, general land cover, and building footprints. High resolution remotely sensed data used in this research included: lidar (light detection and ranging) data (low and high lidar posting density) and multispectral (NIR, blue, green and red bands) leaf-off aerial imagery.

This research examined high resolution lidar data through the evaluation of various lidar posting densities and their influence on the accuracy of building footprints and DEMs. The lidar DEM analysis was extended by creating a Compound Topographic Index (CTI) from the DEM to evaluate the potential of the CTI's information for identifying wetland's location. Finally, the results from the second chapter were integrated into the third chapter by combining CTI, high resolution imagery, Digital Surface Model (DSM) and lidar intensity for mapping four land cover classes, including: wetlands, urban, agricultural and forest. A state-of-the-art remote sensing technique known as Object-Based Image Analysis (OBIA) was used to integrate lidar derived products and high resolution imagery.

Results and findings of this research are important in two ways: First, advancing the understanding of lidar and lidar derivatives for mapping natural and manmade landscape features. Second, providing needed information to the scientific and civilian community, particularly in the state of Minnesota, to help with the process of updating wetland inventories such as the NWI and increasing the accuracy of mapping wetlands efforts with state-of-the-art techniques.

Table of Contents

List of Tables

Chapter 1

Chapter 2

Chapter 3

List of Figures

Chapter 1

Chapter 2

Chapter 3

Introduction - Overview of Dissertation

Conservation and management of our valuable natural resources requires updated knowledge of the locations of these resources. We cannot conserve what we do not map. For example, in Minnesota, United States, approximately 53% of the original wetlands have been lost since the mid-1800s through drainage and filling processes for agricultural or urban development purposes (Dahl 2006; Stedman and Dahl, 2008). Minnesota's Wetlands Conservation Act mandates "no net loss" in wetland acres in the state; thus reliable methods to monitor wetlands (and other natural resources) are needed.

Updated inventories of our natural resources, particularly wetlands, can help managers including the local government, local stakeholders and federal agencies to take correct decisions based on accurate information for the preservation, monitoring and restoration of these valuable ecosystems. Also, accurate wetland inventory maps can help to determine better location for wildlife and fishing activities, creation of emergency plans in places that tend to have high risk of flooding and reduce some of the negative effects, protection and monitoring of wetlands with the purpose of regulate the climate change (Anteau and Afton, 2009; Töyrä and Pietroniro, 2005; Turner et al., 2000).

At this time, the most commonly used public wetland inventory maps in the United States, including Minnesota, are the National Wetlands Inventory (NWI). The NWI maps were created from aerial imagery collected in the years of 1979-1988 (LMIC, 2007). It has been already over 20 years since these maps were created and many landscape elements have changed.

High resolution remotely sensed data and remote sensing techniques offer efficient automated techniques that can help to updated wetland inventory maps (Knight et al., 2013; Lang et al., 2009; Maxa and Bolstad, 2009). Past studies that have used remote sensing techniques have traditionally focused on the use of low-to-medium resolution data and pixel based methods for mapping wetlands (Baker et al., 2006; Fournier et al., 2007; Lunetta and Balogh, 1999; Ozesmi and Bauer, 2002).

As a result, these studies have not been able to obtain high accuracy on mapping wetlands because of the mixed nature of these ecosystems and insufficient spatial resolution in the imagery used.

Some of the current solutions presented to the traditional pixel-based remote sensing techniques are the integration of high resolution data and high resolution elevation data (Jenkins and Erazier, 2010; Knight et al., 2013; Lang et al., 2012).

Acquisition of high resolution elevation data such as lidar (light detection and ranging) has become lately of great interest to many countries including the United States. Minnesota has joined the nationwide effort through the recent collection of lidar data for the entire state (MnGEO, 2013).

Lidar is an active remote sensing technology that captures accurate elevation information with a geographic coordinate location. The high vertical and horizontal accuracy of lidar data has gained the attention of researchers to explore and investigate the use of this data for a variety of environmental, geological and engineering applications (Awrangjeb et al., 2013; Banskota et al., 2011; Bilskie and Hagen, 2013; Haugerud et al., 2003). Wetland mapping studies have confirmed the importance of using lidar data in conjunction with other ancillary data in the process of mapping wetlands (Antokarakis et al., 2008; Knight et al., 2013 Lang et al. 2013).

The goal of this research was to explore the use and accuracy of high resolution data including lidar and multispectral leaf-off aerial imagery to map natural and man-made features on the landscape, including wetlands and structures. This goal was achieved through a detailed examination of the lidar data and integration of lidar data with other data. The detailed examination was carried out through the evaluation of several lidar posting densities and their effects on the accuracy of building footprints and DEMs.

Once it was determined that a reasonably accurate DEM can be derived from low lidar posting densities; several DEM derivatives were tested over different ecoregions and integrated elevation information with optical data. The integration of data was done using a state-of-the-art remote sensing technique known as Object-Based Image Analysis

(OBIA). The main idea behind the OBIA technique is to create statistically homogenous image objects from pixels (Baatz et al., 2008; Benz et al., 2004; Blaschke, 2010).

Furthermore, the OBIA approach has the capability to incorporate remote sensing data, contextual information, human knowledge and experience to interpret more accurately the objects of interest (Blaschke, 2003; Fourniert et al., 2007; O'Neil-Dunne et al., 2012).

The expected products of this research are methods and results that indicate the accuracy of lidar data and other data types for mapping natural and man-made features, including wetlands. The practical goal of this research was to present valuable and significant information to the scientific community and general public regarding the use of high resolution data for mapping wetlands and man-made features.

From an environmental point of view, the purpose of informing stakeholders, scientific and civilian community regarding the accuracy and applications of this free high resolution data is to allow for better management decisions regarding these valuable natural ecosystems.

This dissertation presents a framework of three major projects, including: **Chapter 1:** *Lidar posting density effects on the accuracy of building footprints and ground elevation* (Manuscript in preparation); **Chapter 2:** *Comparison of flow direction algorithms in the application of the CTI for mapping wetlands in Minnesota* (Manuscript in review); and **Chapter 3:** *Wetland mapping in the Upper Midwest United States: An object-based approach integrating lidar and imagery data* (Paper in press).

The Chapter 1 results indicated that lidar posting densities ranging from 1.3 pt/m² to 11.4 pt/m² are acceptable to create accurate Digital Elevation Models (DEMs) and building footprints compared to traditional methods such as ground survey collection and manual digitization. These finding are potentially educational and useful for the scientific and civilian community in Minnesota because of the existing statewide lidar data and lidar derived products accessible to users at no cost.

Chapter 2 expands into a hydrological application of lidar DEMs for mapping wetlands in three different ecoregions in Minnesota. A lidar DEM was derived and used to evaluate the accuracy of two Single Flow Direction (SFD) and five Multiple Flow

Direction (MFD) algorithms in the application of the compound topographic index (CTI) for mapping wetlands. Results of this chapter showed that wetlands in different ecoregions can be correctly identified using a lidar derived CTI, and MFD algorithms should be chosen over SFD algorithms for wetland mapping.

Chapter 3 offers a practical remote sensing based method to integrate lidar data and high resolution multispectral leaf-off aerial imagery for mapping wetlands. These data were integrated using an OBIA approach and tested in three different ecoregions in Minnesota. The results showed that high overall accuracy results in the range of 96-98% can be reached for mapping wetlands larger than 0.20 ha (0.5 acres). These results may allow for an increased accuracy of mapping wetlands efforts over traditional remote sensing methods.

.

Chapter 1: Lidar posting density effects on the accuracy of building footprints and ground elevation*

This study investigated the effects of low vs. high lidar posting density on the accuracy of lidar-derived buildings footprints and Digital Elevation Models (DEM). The lidar density analysis was tested in nine study areas across the Twin Cities metro region in Minnesota. Lidar densities ranging from 1.3 pt/m² to 11.4 pt/m² were tested on lidar building footprint and DEMs. We assessed the accuracy of lidar building footprints against building outlines created from manual photo-interpretation and heads-up digitization.

We evaluated the accuracy of the lidar DEM values by looking at the consistency of changes from point-to-point within the lidar DEM and ground survey points for the same locations. Results indicate that lidar building footprint and elevation values derived from low and high lidar density in Minnesota were not statistically significant different overall, though some large errors were found. The findings are potentially informative and beneficial for the scientific and civilian community in Minnesota because statewide lidar data and lidar derived products are available to users at no cost.

* Manuscript in preparation for publication: Rampi, L., Knight, J., Klassen, J., Pelletier, K., Wang, Y., Journal TBD, 2013.

Introduction

Lidar (light detection and ranging) is an active remote sensing technology that measures and captures three dimensional (latitude, longitude, and elevation) point cloud information of surface features on the earth. Lidar development began in France in 1935 but stopped during World War II. Lidar remained in the laboratory stage during the 1960s, and the first lidar measurements of the upper atmosphere were made in 1963 (Fiocco and Smullin, 1963). Finally, at the turn of the 21st century lidar developed into a strong remote sensing data type suitable for earth surface applications (Ackermann, 1999; Flood, 2001).

Lidar data is collected from a sensing platform, either airborne (fixed wing aircraft), spaceborne (satellite), or ground-based. The laser pulse is transmitted from the sensor to the target, and some of the radiation emitted is reflected back to the sensor as multiple returns of the ground, natural features or man-made features. The elevation values of these multiple returns are calculated based on the time delay between the pulse emitted and the return from that pulse to the sensor (Wehr and Lohr, 1999).

Lidar data are characterized by precise vertical and horizontal point accuracy (Aguilar et al., 2010; Anderson et al., 2006; Hodson and Bresnahan, 2004). High accuracy has made lidar a very attractive and significant data type for several applications. Examples of some lidar applications include: generation of Digital Elevation Model (DEM) and Digital Surface Model (DSM) (Lee and Younan, 2003; Liu et al., 2007; Ma, 2005), building extraction (Awrangjeb et al., 2013; Lohani and Singh, 2008; Tournaire et al., 2010), aboveground biomass mapping (Banskota et al., 2011; Chen, 2010), wetland mapping (Knight et al., 2013; Rampi and Knight, 2013), floodplain mapping (Bilskie and Hagen, 2013; Deshpande, 2013; Webster et al., 2004), forest characterization (Coops et al., 2004; Dubayah and Drake, 2000; Means et al., 1999), mapping tectonic fault scarps and morphology (Cavalli et al., 2008; Haugerud et al., 2003).

Regardless of the multiple and significant benefits that lidar data can offer to the scientific and civilian community, lidar data is often not freely available to the public.

Moreover, in many countries including the United States lidar data is not available in many areas. Currently, in the United States, the United States Geological Survey (USGS), in collaboration with other agencies, has taken the lead to plan and execute a nationwide lidar dataset (USGS, 2013). Also, many states have initiated their own statewide lidar acquisition.

The Minnesota effort started in July of 2009 when the Minnesota Legislature allocated $8.3 million from the Minnesota's Clean Water, Land, and Legacy Amendment to collect lidar data statewide. The Minnesota Department of Natural Resources (DNR) supervised this lidar acquisition through the Minnesota Elevation Mapping Project. Lidar collection started in 2010, and all the lidar flights were completed in 2012. Lidar data for the entire state were available in June of 2013 through the Minnesota Geospatial Information Office (MnGeo) FTP site.

Lidar density target specifications were in the range of 0.25 pt/m²-8 pt/m² (2m-0.35 m nominal point spacing (NPS)) for the entire state. High density lidar data was collected for the metro area and lower lidar density for the rest of the state (MnGEO, 2013). These contracted lidar point density specifications were satisfied and in some cases the point density was even greater than the established requirement. The Minnesota DNR has made this statewide lidar collection available to the public at no cost. Additionally, the DNR has created lidar-derived products including DEMs, contour data, and building footprints for the majority of the counties in Minnesota.

Availability of lidar data in Minnesota has awakened the interest of many governmental and non-governmental institutions to explore and use these data for many environmental, engineering and urban planning applications. It is important to inform the public about the accuracy of the lidar data and derived products because this will have an impact of their final use or application. The Minnesota DNR has already started assessing the accuracy of statewide lidar data acquisition with the assistance of many county surveys.

Specific requirements for the lidar accuracy are 1 m RMSE for the horizontal accuracy, ≤ 15 cm RMSE for vertical accuracy in non-vegetated areas, and 27 cm RMSE in vegetated areas for vertical accuracy (MnGEO, 2013). These vertical and horizontal

requirements are based on the USGS specification (Heidemann, 2012). All these target specifications for vertical and horizontal accuracies were met for the statewide lidar collection.

In contrast, there is no quality control or assessment of building footprints derived from lidar data, created by the Minnesota DNR. Furthermore, there is no lidar density comparison of the accuracy of the building footprints and ground elevations. A general assumption is that lidar derived products such as building footprints and DEM created from higher lidar density would yield greater accuracy results, than building footprints and DEM created from created from lower lidar density. However, this assumption is very subjective to lidar acquisition parameters and how the lidar data is going to be used for different applications.

For example, numerous studies have found that flying at low or high altitude has little or no effect on the accuracy of forest structure derived from lidar data (Goodwin et al., 2006; Næsset, 2004). Other studies, have investigated the effects of lidar posting densities and accuracy (Aguilar et al., 2010, Liu and Zhang, 2008; Raber et al., 2007; Rutzinger, 2009; Zhang et al., 2006), but most of these studies have been limited to using lidar densities ranging from 0.25 pt/m²-1.3 pt/m², simulating lower lidar densities and focusing more on the accuracy of a DEM.

These studies have provided helpful insights regarding the effect of lidar density and accuracy. However, there are two main motivations for extending the aforementioned work with this study: 1) Minnesota stakeholders will be most interested in the accuracy of their data and derived products, rather than those acquired in other areas; and 2) Previous studies examined differing resolutions by simulating lower resolution data from higher resolution data. This study uses adjacent datasets that were acquired at different resolutions.

Thus, this study investigates the effects of low vs. high lidar posting density on the accuracy of lidar derived buildings footprints and lidar derived Digital Elevation Model (DEM) in Minnesota. The context for this study was commercial buildings in very dense urban areas within the Twin Cities metro region. The main goal of this study was accomplished through the following specific objectives:

1. Compare the accuracy of lidar building footprints created from low and high lidar densities against building outlines created by manual photo-interpretation and heads-up digitization using high resolution orthoimagery.
2. Evaluate the accuracy of the lidar DEM values by looking at the consistency of changes from point-to-point between the lidar DEM and coincident ground survey points.

Study Area and Data

Study Area Description

Nine areas within the Twin Cities metro region in Minnesota were studied. For the building area comparison analysis the following study areas were chosen based on their lidar density: Woodbury-Oakdale, Anoka, and Belle Plain have a lidar density of 1.3, 1.4, and 1.5 points per square meter (pt/m²), respectively. Burnsville and Hastings have a lidar density of 1.9, and 2.0 pt/m², respectively. Eagan, Falcon Heights-Saint Paul, and Maple Grove have a lidar density of 11.0, 11.4, and 11.5 pt/m², respectively (Figure1-1). For the elevation analysis the following area was selected based on lidar density: New Brighton with two lidar densities: 1.3 and 11.4 pt/m² (Figure1-2).

Study area # 1: Woodbury-Oakdale has an area of about 18 km² and is located between the cities of Woodbury and Oakdale in Washington County. Study area # 2: Anoka has an area of about 6.8 km² and is located in the city of Anoka within Anoka County. Study area # 3: Belle Plaine has an area of about 5 km² and is located in the city of Belle Plain within Scott County. Study area # 4: Burnsville has an area of 21 km² and is located in the city of Burnsville within Dakota County. Study area # 5: Hastings has an area of 12 km² and it is located in the city of Hastings within Dakota County.

Study area # 6: Eagan has an area of 34.00 km² and is located in the city of Eagan within Dakota County. Study area # 7 Falcon Heights-Saint Paul study area has an area of about 5.30 km² and is located between the cities of Falcon Heights and Saint Paul in Ramsey County. Study area # 8: Maple Grove has an area of about 5.1 km² and is located in the city of Maple Grove in Hennepin County. The elevation across these eight study

areas ranges from 182 m to 375 m above sea level. Land use is dominated by urban development including residential and commercial areas of various sizes and types.

Finally, the last study area #9: New Brighton was chosen for the elevation analysis because of the variation in topography and availability of two different lidar densities collections within this small area. The New Brighton site has an area of about 3,995.0 m² and is located in the city of New Brighton within Ramsey County. Elevation ranges from 291 m to 299 m with slopes averaging of 7%. The nine study areas are located within the central hardwood forest ecoregion in the state of Minnesota.

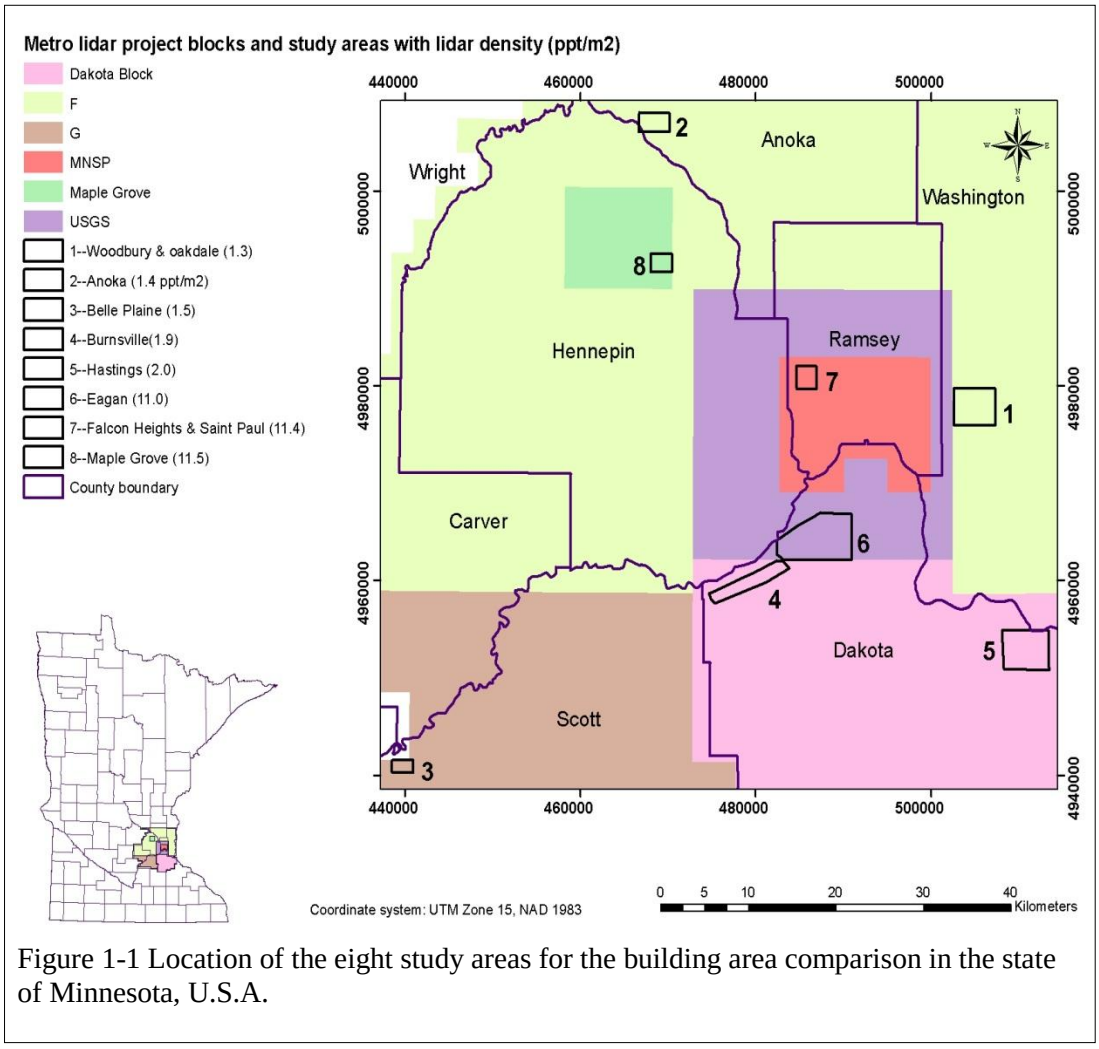

Figure 1-1 Location of the eight study areas for the building area comparison in the state of Minnesota, U.S.A.

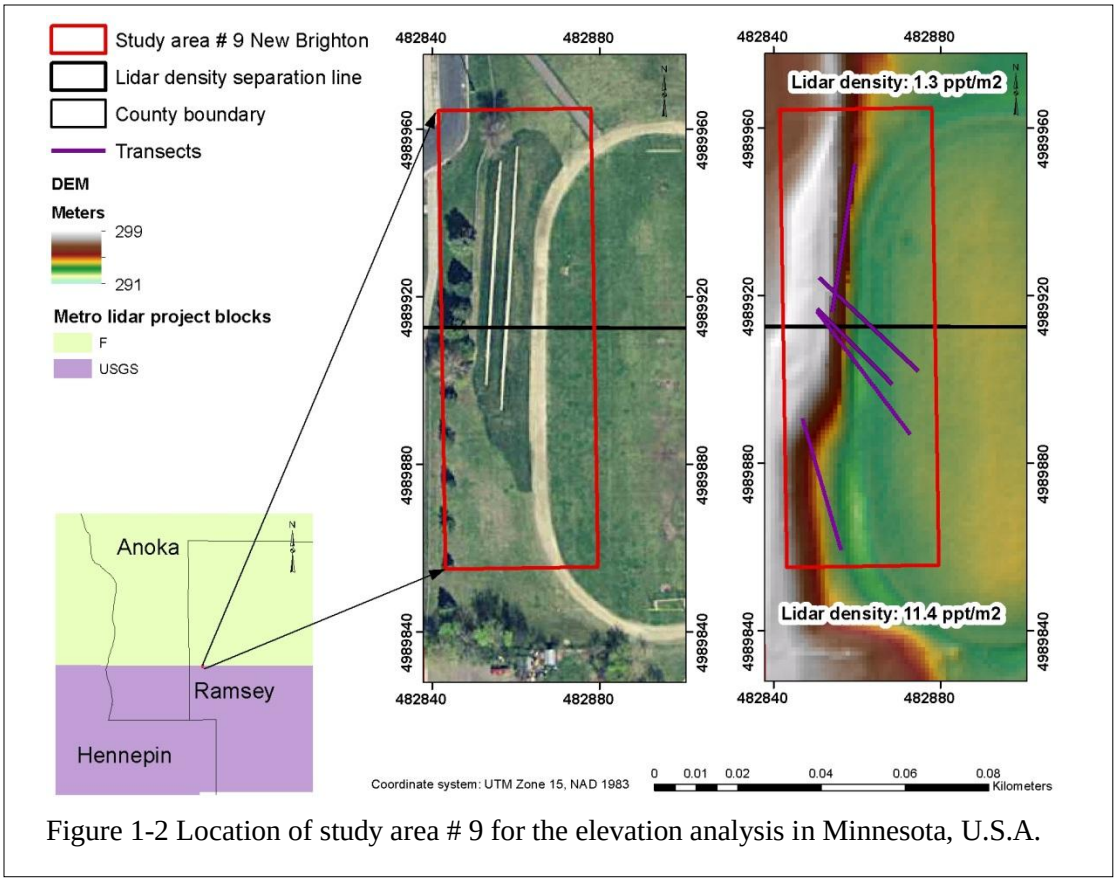

Figure 1-2 Location of study area # 9 for the elevation analysis in Minnesota, U.S.A.

Lidar Data

The lidar data used for the metro region in this study was downloaded from the Minnesota Geospatial Information Office (MnGeo) FTP site. The lidar data were collected by Fugro Horizons, Inc. and delivered to the Minnesota DNR as classified LAS formatted point cloud data. All the lidar data are in the UTM Zone 15 coordinate system, NAD83 NAVD88 Geoid09 meters. The tiling scheme is 16th USGS 1:24,000 quadrangle tiles. The lidar data were collected in the Spring and Fall of 2011, with some reflights in Spring 2012. The specific dates for the areas located within the lidar blocks used in this study are the following:

1. Block F (Woodbury-Oakdale, Anoka, and New brighton-low density) 11-13-11 to 11-17-11, reflight 3-25-12
2. Block G (Belle Plain): 11-11-11 to 11-12-11, reflight 3-24-12

3. Dakota Block (Hastings and Burnsville): 11-12-11 to 11-15-11
4. MNSP (Falcon Heights-Saint Paul and New brighton-high density), USGS (Eagan), and Maple Grove Block (Maple grove): 11-02-11 to 11-15-11

The horizontal accuracy for these data meets or exceeds 0.6 m RMSE (root mean square error), 95% confidence level. The vertical accuracy of this lidar data was assessed using the guidelines developed by the NDEP (National Digital Elevation Program) and then implemented by the American Society for Photogrammetry and Remote Sensing (ASPRS).

The vertical accuracy for our study areas were the following: Woodbury-Oakdale, Anoka, New Brighton-low density, and Belle Plain (RMSE of 12.5cm); Dakota Block (RMSE of 10.8 cm), USGS and MNSP (RMSE of 5 cm), and Maple Grove (RMSE of 8.3 cm).

The lidar data collected for study areas contained within Block F and Block G used a lidar system with a Leica sensor ALS50-II MPiA, and provided acquisition at 2,012.0 meters above mean terrain (AMT), 130 knots, pulse rate 99,500Hz, scan rate 27.28Hz, 40 degree field of view, 4,805ft swath width. This sensor was equipped with IPAS inertial measuring unit (IMU) and a dual frequency airborne GPS receiver.

The lidar data collected for study areas confined within Dakota Block used a lidar system with a FLI-MAP sensor, and provided acquisition at 823 meters AMT, 145 knots, 30% side lap, 150kHz, 60% degree field of View, 950 meters swath width. This sensor was equipped with an IMU and a dual frequency airborne GPS receiver.

The lidar data collected for study areas confined within MNSP and USGS (metro block) used a lidar system with a FLI-MAP sensor, and provided acquisition at 640 meters AMT, 130 knots, 60% side lap, 200 kHz, 60% degree field of View, 739 meters swath. This sensor was equipped with an IMU and a dual frequency airborne GPS receiver.

High resolution orthoimagery

High resolution orthoimagery was used to create a set of reference data for each the study areas used for the building outline analysis. Orthoimagery, collected in the spring of 2012 by Digital Aerial Solutions, LLC was used in the following study areas: Woodbury-Oakdale, Anoka, Falcon Heights-Saint Paul, Burnsville, Eagan, and Maple Grove. This orthoimagery has a 30 cm spatial resolution, natural color, collected during leaf-off condition on 25 March and 29 March, and 3 April – 4 April 2012. This orthoimagery was acquired with a (Sensor Head 52) Digital Camera Imagery Control - Airborne GPS/IMU, obtained at an altitude of 2,880.36 m above ground level. The horizontal positional accuracy for this imagery is 0.52 m RMSE (NSSDA 95% confidence level).

The vendor delivered the data imagery to the EROS data center, U.S Geological Survey, and USGS distributed to MnGeo in TIFF format with a NAD 1983 UTM zone 15N projection. MnGeo serves the images over the web via a WMS (Web Mapping Service) server in JPG format. For our analyses, we accessed this orthoimagery via MnGeo's Image Server WMS through ArcMap version 10.2.

Orthoimagery for the other two study areas: Belle Plaine (Scott county) and Hastings (Dakota County) was collected in the spring of 2010 by Surdex Corporation. The spatial resolution of this orthoimagery for most areas is 30 cm, but for Scott and Dakota Counties is 15 cm.

This orthoimagery was acquired during leaf-off conditions in mid-April 2010, with an Intergraph DMC (Digital Mapping Cameras), four bands (RGBI), at an altitude of 3,048.0 m for most areas and for Scott and Dakota county at 1,524.0 m AMT. The horizontal positional accuracy for this imagery was assessed using a total of 87 control points and obtaining a 0.85 m, CE95 (Circular standard error at 95% confidence level).

The vendor delivered the data imagery to the Minnesota Department of Natural Resources, and MnGeo serves the images over the web via a WMS server in JPG format. For our analyses, we accessed this orthoimagery via MnGeo's Image Server WMS through ArcMap version 10.2

Field data Collection (Surveying)

We conducted a ground-based elevation survey during the Fall 2013 to compare the relative change in elevation between the points generated using a total station survey unit and the elevation points generated from two different lidar datasets (1.3 and 11.4 pt/m^2). A team from the Remote Sensing and Geospatial Analysis Laboratory at the University of Minnesota surveyed 168 points, every 50-60 cm along four transects in the New Brighton study area (Figure 2) in Ramsey County. We used an electronic total station Sokkia SET5WS with a survey rod mounted with a reflective prism.

To create a positional reference to the state plane coordinate system and provide verification of positional accuracy, we collected the total station coordinates in an arbitrary Cartesian coordinate system located at (0, 0). Also, we centered the total station over a known control point and centered the prism over another set of known control points. These set of control points were collected with a Trimble Juno GPS and Pro XT receiver at four locations concurrent with surveyed locations in a UTM geographic coordinates (NAD83 CORS96 UTM15N). The GPS points were differentially corrected using Office Pathfinder resulting in an average accuracy of 15-30cm.

These two points were needed to establish the state plane coordinate grid (0,0), and all other points requiring location were methodically measured as side shots by sighting on the prism that the rodman accurately fixed over each required survey point. We used the electronic data collector in the total station equipment to record data for each point, including the horizontal and vertical angles, and slope distances. Finally, we downloaded these point measurements to a local computer for processing. The arbitrary coordinates were transformed to a UTM geographic coordinate system using 2D linear conformal transformation. Two GPS coordinates (known control points) were used for defining parameters for rotation, scaling and translation of the arbitrary coordinate system to the geographic coordinate system.

The points were rotated using a positive anticlockwise angle (270), scaled by a factor of ($s = 0.9988606$), a rotation angle of $\theta = 4.34019$, and translation factors of $T_X =$ 482856.13, and $T_Y = 498859.1$ (Ghilani and Wolf, 2012). We calculated E and N coordinates of the noncontrol points from their X and Y values using the following

formula given by Ghilani and Wolf (2012): E coordinate = sX cosθ - sY sinθ + Tx; N coordinate = sX sinθ + sY cosθ + Ty. The resultant transformed points were visually compared to features identified at the study area and in the high resolution digital orthoimagery acquired in spring 2012, via MnGeo's WMS through ArcMap version 10.2.

Methods

To determine the influence of lidar data density on the accuracy of two lidar derived products (buildings footprints and DEMs) from different densities, we first compared building footprints created from lidar data against buildings outlines created from high resolution aerial imagery. Second, we compared lidar elevation points from two different lidar densities collection against total station survey ground points.

The first subsection of this methods section describes the analysis carried out to compare building outlines from different lidar densities. The next subsection explains the analysis carried out to compare the consistency in elevation changes from point-to-point within the ground survey points and lidar DEM from two different lidar densities. The last subsection describes the statistical analyses employed to evaluate the results of both comparisons.

Building footprint analysis

For the building analysis comparison, we selected 30 buildings (randomly independent stratified by size selection) for each study area (total n = 240 buildings), including only commercial buildings with area size ≥ 500 m². The lidar building footprints used in this study for each study area were obtained directly as a vector layer from the MnGeo FTP site. These buildings were created by the Minnesota DNR staff by extracting points classified as buildings (class=6) from the LAS files. Building points were regrouped within 3 m of each other into a single cluster.

Finally an outline was created around those points. All these processes were performed in ArcMap software using standard tools. The main difference between the lidar-derived building footprints used in this study is the lidar density used to create them. For this study, we had buildings outlines that were created from the following lidar

densities: 1.3 (Woodbury-Oakdale), 1.4 (Anoka), 1.5 (Belle Plaine), 1.9 (Burnsville), 2.0 (Hastings), 11.0 (Eagan), 11.4 (Falcon Heights-Saint Paul), and 11.5 (Maple Grove) pt/m².

Reference data digitization for buildings outline areas

A set of building outlines for each study area was created via manual digitization in Arc Map 10.1. The high resolution orthoimagery available for each study area was used to create each set of reference data (total n = 240) buildings. The reference data digitization was used to evaluate the accuracy of the lidar building's area for each study area.

Building statistical analysis

We assessed the accuracy of the lidar buildings areas and the reference digitization buildings areas using three indicators: A building area index, an analysis of variance (ANOVA) and the Tukey Honest Significant Difference (HSD) test.
The building area accuracy index was calculated using the following formula:

$$Building\ area\ index = \left(\frac{Area\ (Ref\ building) - Area\ (lidar\ building)}{Area\ (Ref\ building)}\right) \times 100$$

where Area (Ref building) is the area of the reference polygon and the Area (lidar building) is the area of the lidar footprint polygon. This index indicates the amount of area in percentage that has been overestimated or underestimated compared to the reference data building polygon area and the difference between the reference building polygon and the lidar building polygon in percentage.

Comparisons of means of the building area index for all the study areas were carried out to detect if the means between all the eight study areas were equal or different between them. The majority of our data met the normality requirements.

We used a one-way Analysis of Variance (ANOVA), with a significance level of α=0.05 to determine statistical differences between the study areas. Our null hypothesis was that the mean building area index scores for the eight groups were equal.

Additionally, to determine which specific study area was significantly different at a significance level of $\alpha=0.05$ from all the groups, we used a multiple pairwise comparison technique named the Tukey HSD test. This test, calculates the honest significant difference between two means using the studentized range distribution to build simultaneous confidence intervals for differences of all pairs of means (Oehlert, 2010). We used R statistical software to perform the ANOVA and Tukey HSD analyses

Elevation analysis

For the relative change in elevation analysis, we compared the total station survey elevation points and lidar DEM elevation points for five transects in the New Brighton study area. Three of the transects contained points that were located within the 1.3 pt/m² and 11.4 pt/m² collection. The other two were located only in one of the two lidar density collection regions.

We used the Cognition Network Language (CNL) within the software package Definiens eCognition Developer version 8.8.0 to create a 1m lidar DEM for the New Brighton study area using both point cloud densities. We used a ruleset to create the DEM using the Lidar file converter, fill pixel value and export algorithms.

For the Lidar file converter algorithm the following parameter were used to convert the point cloud files to a raster layer: Result mode: average, returns: all, point filter by class: ground and model key points only. The fill pixel value algorithm was used to create a value for those pixels that were not filled in the raster previously created from the lidar point cloud.

The following parameters were used with the fill pixel algorithm: calculation mode: Inverse Distance Weighting (IDW), IDW distance weight: Two. The IDW interpolation method calculates the value of a point by averaging the value of sample data points within its neighborhood by giving more weight to adjacent points than to distant points (Bartier and Keller, 1996; Caruso and Quarta, 1998). We exported the DEM as an IMG raster file for the elevation analysis.

Elevation accuracy analysis

A point-to-point accuracy assessment was calculated to evaluate the consistency of change within the ground survey reference locations and within the interpolated elevation (DEM) locations. First, we calculate the difference from point-to-point within the ground survey reference location using the following formula:

Difference in elevation between two adjacent survey points **(DiE survey-pt)**

$DiE\ survey - pt = \ Zsurvey\ pt\ (\mathrm{i1}) - \mathrm{Zsurvey\ pt(i2)}$

Where Zsurvey pt(i1) is the elevation surveyed at the first reference location point, and Zsurvey pt (i2) is the elevation surveyed at the second reference location point. This subtraction of difference between points is done from point-to-point until the last point surveyed in each transect.

Second, we calculate the difference from point-to-point within the interpolated elevation (DEM) locations using the same formula above:

Difference in elevation between two adjacent lidarDEM points **(DiE lidarDEM-pt)**

$\boldsymbol{DiE\ lidarDEM - pt} = \ ZlidarDEM\ pt\ (\mathrm{i1}) - \mathrm{ZlidarDEMpt(i2)}$

Where ZlidarDEM pt (i1) is the interpolated elevation at the first lidar elevation location point, and ZlidarDEM pt (i2) is the interpolated elevation at the second lidar elevation location point.

Finally, we assessed the consistency in changes for the survey points (DiE survey-pt) locations vs the changes in the lidar interpolated elevation (DiE lidarDEM-pt) locations.

To evaluate the consistency in changes in both datasets we compute a relative vertical error from point-to-point using the following formula:

Relative vertical error between the survey and lidar points (RVE):

$\boldsymbol{RVE} = \ \mathrm{DiE\ survey(pt}\ X1 \ldots i) - \mathrm{DiE\ lidarDEM(pt}\ X1 \ldots i)$

The RVE determines if the changes in elevation that occur from point-to-point in the survey points are consistent with the changes that occur in the interpolated lidar elevation from point-to-point.

Elevation Statistical analysis

Biases between the differences in elevation from point-to-point within the survey points and within the lidar DEM points were assessed by comparing mean values of both datasets. To compare the means of both datasets we performed a two-sample t-test with a significance level of $\alpha=0.05$. The null hypothesis tested was that the mean difference in elevation of both dataset was the same. The assumptions of normality and independence for both datasets were satisfied.

Results

Results for the nine study areas are summarized in Tables 1-1 through 1-4, and Figures 1-3 and 1-7. For the building analysis the eight study areas reported both overestimation and underestimation of the lidar building footprints compared to the reference building outline areas. Lidar building outlines that were created from high lidar density points (11.0-11.5 pt/m²) tended to overestimate areas in average by 0.2 – 1.5% compared to the reference data. On the other hand, Lidar building outlines that were calculated from the low lidar density points (1.3-2.0 pt/m²) showed a tendency to underestimate areas in average by 0.5-6.3% compared to the reference data.

Table 1-1 shows the results on the ANOVA for the building area index comparison between all the study areas. The ANOVA F statistic is 3.9 with a $P<0.001$. This ANOVA result shows strong evidence that the mean of the building area index scores differed for all the study areas. This indicates that there is at least one of the study areas that is very different in their building area index score compared to the rest of the study areas. Figure 1-3 illustrate a boxplot of the distribution of the building area index for each study area and reinforces the ANOVA results that not all the group have the same mean building area index score.

The Tukey (HSD) results (Table 1-2) show which study area was significantly different from all the study areas at a level of $\alpha=0.05$. From the Tukey (HSD) analysis we can determine that Belle Plain study area was the only study area that was significantly different from the three study areas with high lidar density and the only one with low

lidar density (Woodbury-Oakdale). The Tukey (HSD) results help us to understand that even though there is an overestimation and underestimation of building outline areas in all the study areas by a small percentage (0.2-6.3%), this percentage difference is not significantly different for all the study areas.

Table 1-3 indicates by how much on average each study area has overestimated or underestimated (negative symbol) the area size of the buildings. Figure 1- 4 supports the results of table 1-3 by showing a graphical comparison of the mean values and 95% Confidence Intervals (CI) of the building area index for all the lidar densities. Despite the fact that only one study area showed a significance difference between all the groups, Figure 1-5 shows that there may be a qualitative difference in the shape of the building outlines polygons derived from the different lidar densities.

Table 1-4, 1-5, and Figure 1-6 to Figure 1-9 show the results for the relative change in elevation analysis. Table 1-4 shows the descriptive statistics for the relative vertical error change in elevation differences for the lidar DEM and ground survey points for the New Brighton areas. Results from Table 1-4 indicate that the changes in elevation from point-to-point that occur in the lidar data were similar to the changes from point-to-point that occur in the survey ground point.

The changes in elevation from point-to-point for the lidar DEM data ranged from -1.22 m to 0.386 m, with a mean value of 0.083 m. The changes in elevation from point-to-point for the Survey data ranged from -1.197 m to 0.256 m, with a mean value of 0.089 m. The Relative Vertical Error determined the consistency of the changes occurred in the lidar and ground survey data. From Table 1-4 we can determine that the changes in both dataset were consistent with a small variation in average of 0.006 m difference.

Figure 1-6, exemplify the Relative Vertical Error difference where the lidar DEM points are plotted along each transect have overestimated or underestimated the change in elevation compared to the ground survey changes. For example, for all the transects, the lidar DEM have overestimated and underestimated the differences in change from point-to-point that happened in the ground survey point-to-point analysis. On average the lidar DEM changes in elevation were underestimated by 0-1.5 m compared to the ground survey.

Also, the lidar DEM changes were overestimated by 0-0.91 m compared to the ground survey. The RVE give us a range of values where the error between changes in differences for both data have been overestimated or underestimated. However, Table 1-5 shows the two sample t-test results for the two lidar densities and individual lidar density test results.

These results indicate that there is not a statistically significance difference between the changes in elevation from point-to-point that occurred in the lidar and the ground survey points. Also, Table 1-5 results prove that the lidar density effect (1.3 vs. 11.4 pt/m^2) on the accuracy of the lidar DEM by evaluating the consistency in changes was not different for any of the two densities in all the points.

Figure 1-7 shows a boxplot of the RVE along all the points for the two lidar densities. This boxplot indicates that the mean differences values for the changes that occurred in both datasets are very close to zero.

Figure 1-8 shows the a graphical representation of the five transects along the elevation differences from point-to-point for each of the dataset (lidar DEM and ground survey points). Figure 1-9 shows the RVE difference for each transect and for each lidar density. Figure 1-8 and 1-9 provide evidence that the changes in elevation that occurred from point-to-point in the ground survey points are similar to the changes that occur in the same location lidar points. Furthermore, the relative vertical error variation difference ranged from -0.4 m to 0.7 m for the low lidar density DEM and -1.5 m to 0.91 m for the high lidar density DEM points.

Table 1-1 ANOVA for the building analysis of the eight study areas

Analysis of Variance Table					
Response: Building area index					
	Df	Sum Sq	Mean Sq	F value	Pr(>F)
County	7	1350.9	191.021	3.9094	**0.0004747 *****
Residuals	232	11452.9	49.366		
Signif. codes: 0 ‘***’ 0.001 ‘**’ 0.01 ‘*’ 0.05 ‘.’ 0.1 ‘ ’ 1					

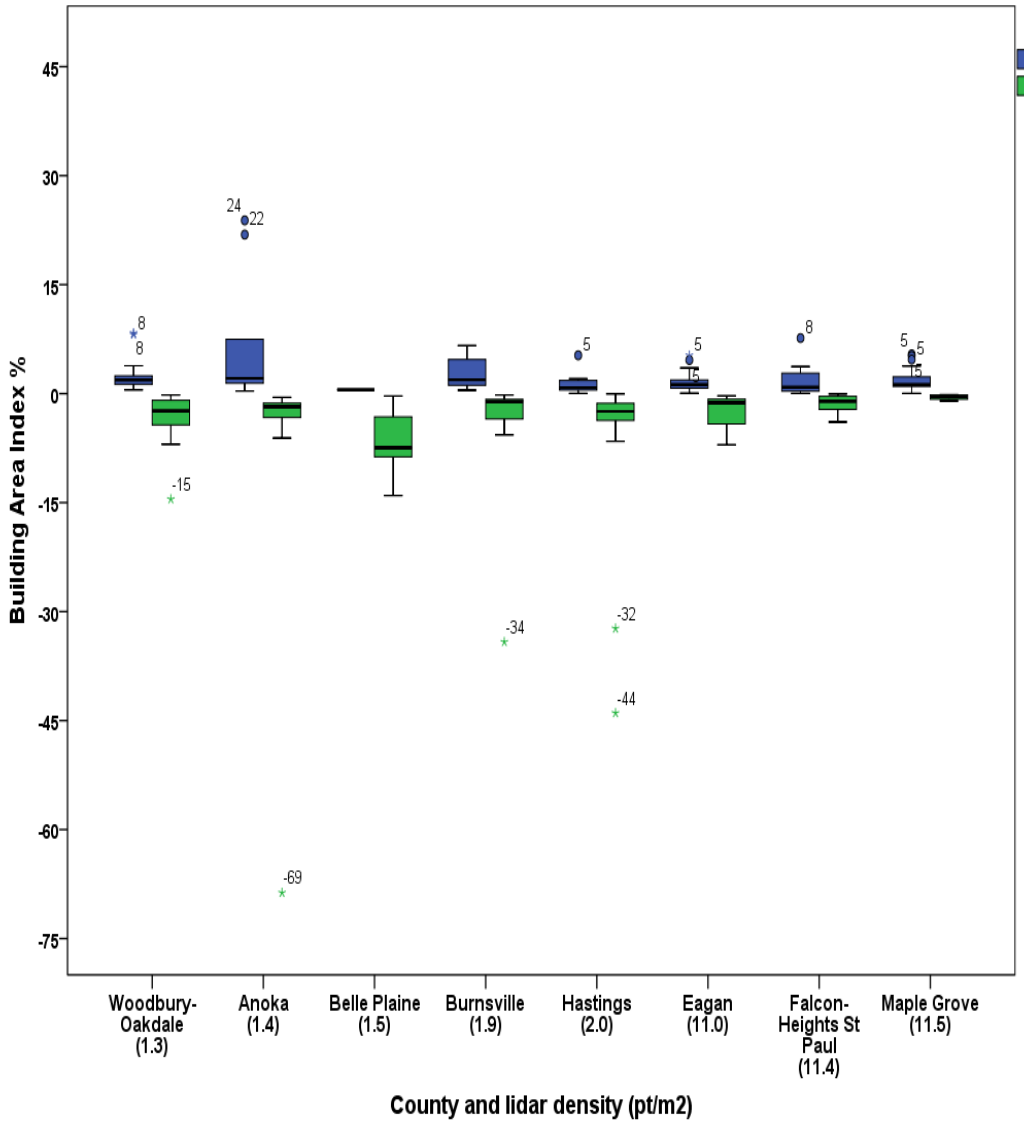

Figure 1-3 Boxplot of the distribution of the county and lidar density along the building area index.

Table 1-2 Results of the multiple pairwise comparison Tukey Honest Significant Difference (HSD) test .

County	Density	Diff	Lwr	Upr	p adjusted
Maple Grove -Belle Plaine	11.5-1.5	-7.73	-13.28	-2.19	0.0007600 ***
Eagan -Belle Plaine	11-1.5	-7.27	-12.81	-1.72	0.0021024 ***
Falcon Heights-St Paul – Belle Plaine	11.4-1.5	-6.40	-11.95	-0.86	0.0115758 *
Woodbury-Oakdale –Belle Plaine	1.3-1.5	-5.70	-11.25	-0.15	0.0391146 *
Burnsville -Belle Plaine	1.9-1.5	-5.07	-10.61	0.48	0.1019614
Maple Grove -Hastings	11.5-2 .0	-4.94	-10.49	0.61	0.1208099
Maple Grove -Anoka	11.5-1.4	-3.04	-8.59	2.51	0.7024327
Woodbury-Oakdale - Hastings	1.3-2.0	-2.91	-8.46	2.64	0.7477273
Hastings -Belle Plaine	2-1.5	-2.79	-8.34	2.75	0.7847919
Maple Grove - Burnsville	11.5-1.9	-2.67	-8.22	2.88	0.8219145
Eagan -Anoka	11-1.4	-2.57	-8.12	2.98	0.8481991
Eagan -Burnsville	11-1.9	-2.20	-7.75	3.35	0.9275006
Falcon Heights-St Paul - Anoka	11.4-1.4	-1.71	-7.26	3.84	0.9813892
Falcon Heights-St Paul - Burnsville	11.4-1.9	-1.34	-6.89	4.21	0.9957257
Maple Grove - Falcon Heights-St Paul	11.5-11.4	-1.33	-6.88	4.22	0.9959058
Woodbury-Oakdale - Anoka	1.4-1.3	-1.01	-6.56	4.54	0.9992957
Maple Grove - Eagan	11.5-11	-0.47	-6.02	5.08	0.9999961
Burnsville - Anoka	1.9-1.4	-0.37	-5.92	5.18	0.9999992
Woodbury-Oakdale - Falcon Heights-St Paul	1.3-11.4	0.70	-4.85	6.25	0.9999384
Falcon Heights-St Pau l- Eagan	11.4-11	0.86	-4.69	6.41	0.9997547
Woodbury-Oakdale - Eagan	11-1.3	1.56	-3.99	7.11	0.9890781
Hastings - Anoka	2-1.4	1.90	-3.65	7.45	0.9665869
Woodbury-Oakdale – Maple Grove	1.3-11.5	2.03	-3.52	7.58	0.9520007
Hastings -Burnsville	2-1.9	2.27	-3.28	7.82	0.9150998
Hastings -Falcon Heights-St Paul	2-11.4	3.61	-1.94	9.16	0.490685
Hastings -Eagan	2-11.0	4.47	-1.08	10.02	0.2159281
Belle Plaine - Anoka	1.5-1.4	4.69	-0.86	10.24	0.1659548

Table 1-3 Mean building area index.

County and lidar Density(pt/m²)	Mean Index (%)	Note
Maple Grove (11.5)	1.5	Overestimated
Eagan (11.0)	1.0	Overestimated
Falcon Heights-Saint Paul (11.4)	0.2	Overestimated
Woodbury-Oakdale (1.3)	-0.5	Underestimated
Burnsville (1.9)	-1.2	Underestimated
Anoka (1.4)	-1.6	Underestimated
Hastings (2.0)	-3.5	Underestimated
Belle Plaine (1.5)	-6.3	Underestimated

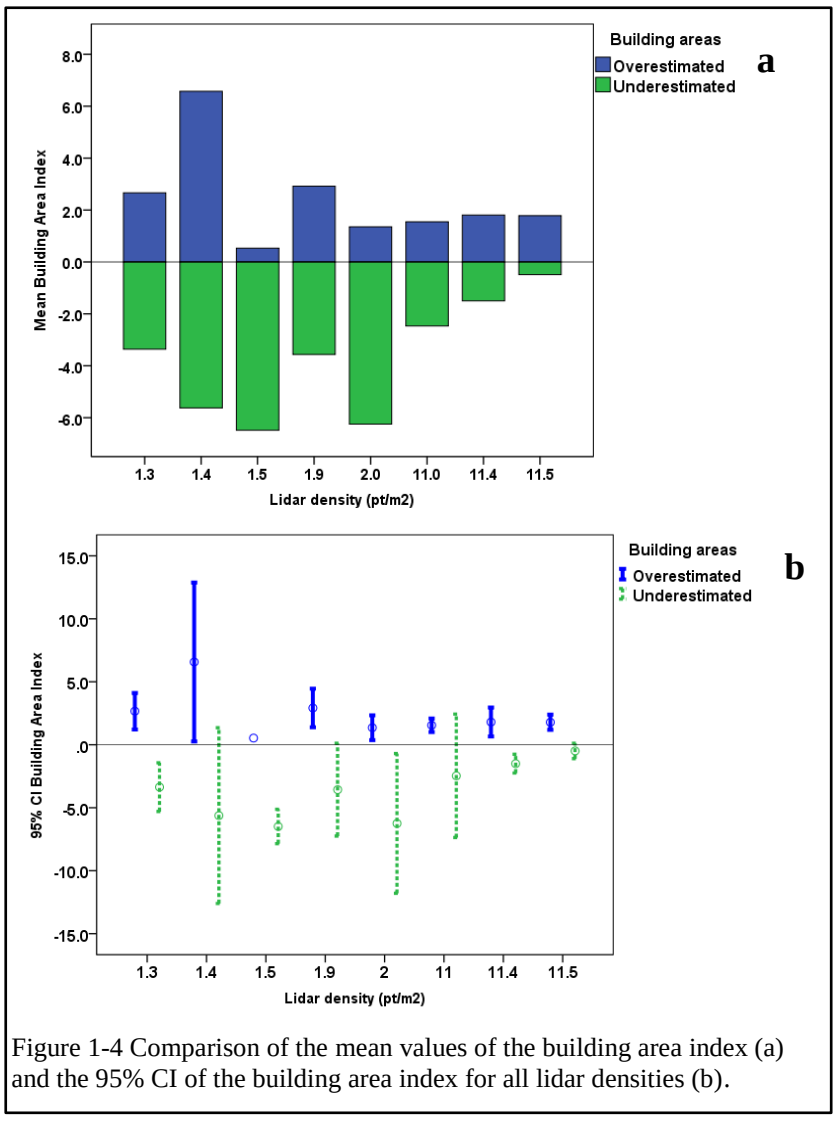

Figure 1-4 Comparison of the mean values of the building area index (a) and the 95% CI of the building area index for all lidar densities (b).

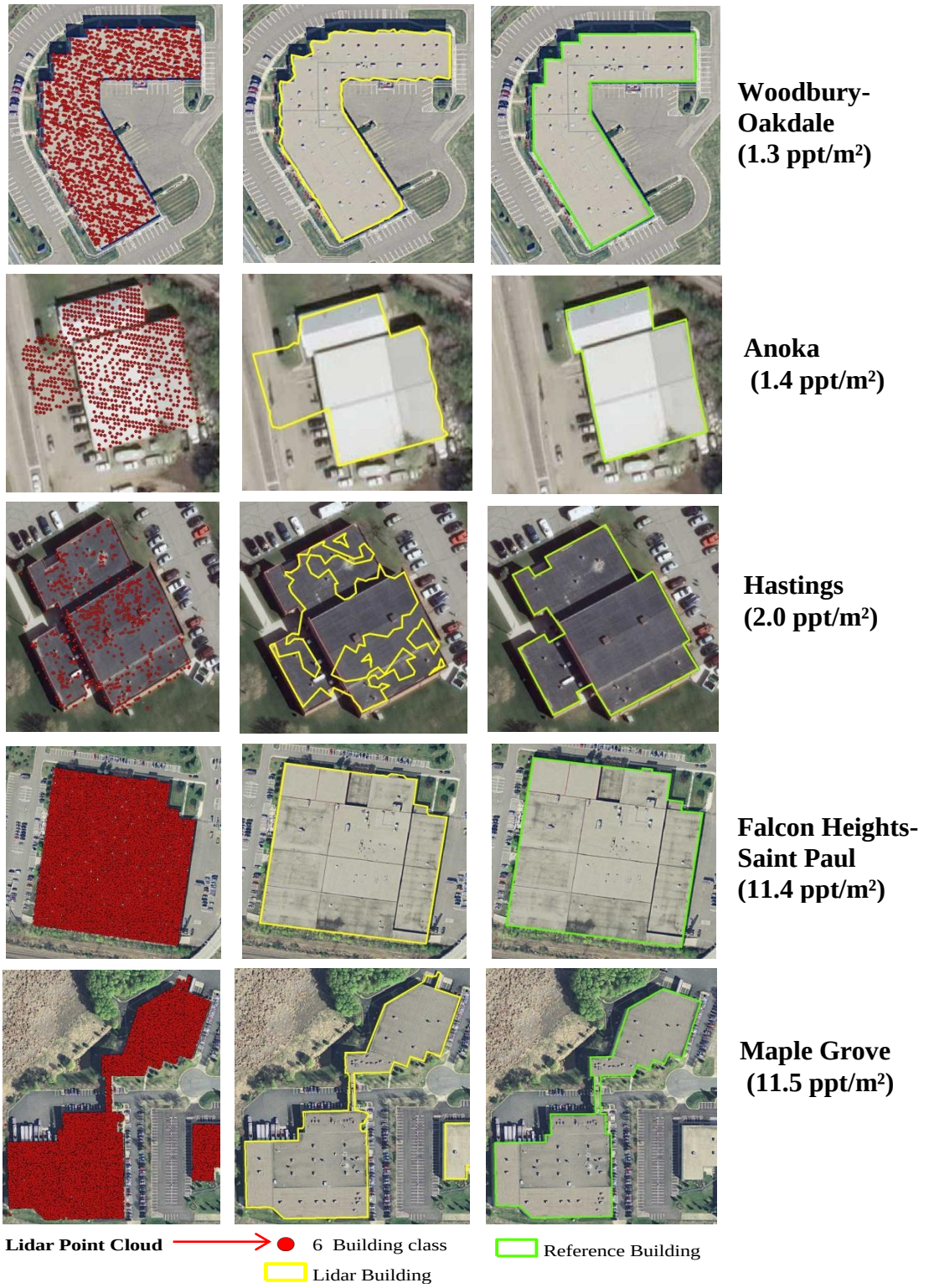

Figure 1-5 Lidar density comparison for lidar building footprints and reference data buildings.

Table 1-4 Descriptive statistics of the Relative Vertical Error (RVE) and change in elevation differences for ground survey and lidar DEM points

	N	Minimum	Maximum	Mean	Std. Deviation
Relative Vertical Error (RVE)	169	-1.58	0.92	0.006	0.23
Change in elevation Lidar DEM	169	-1.22	0.39	0.083	0.024
Change in elevation ground survey	169	-1.20	0.26	0.090	0.22

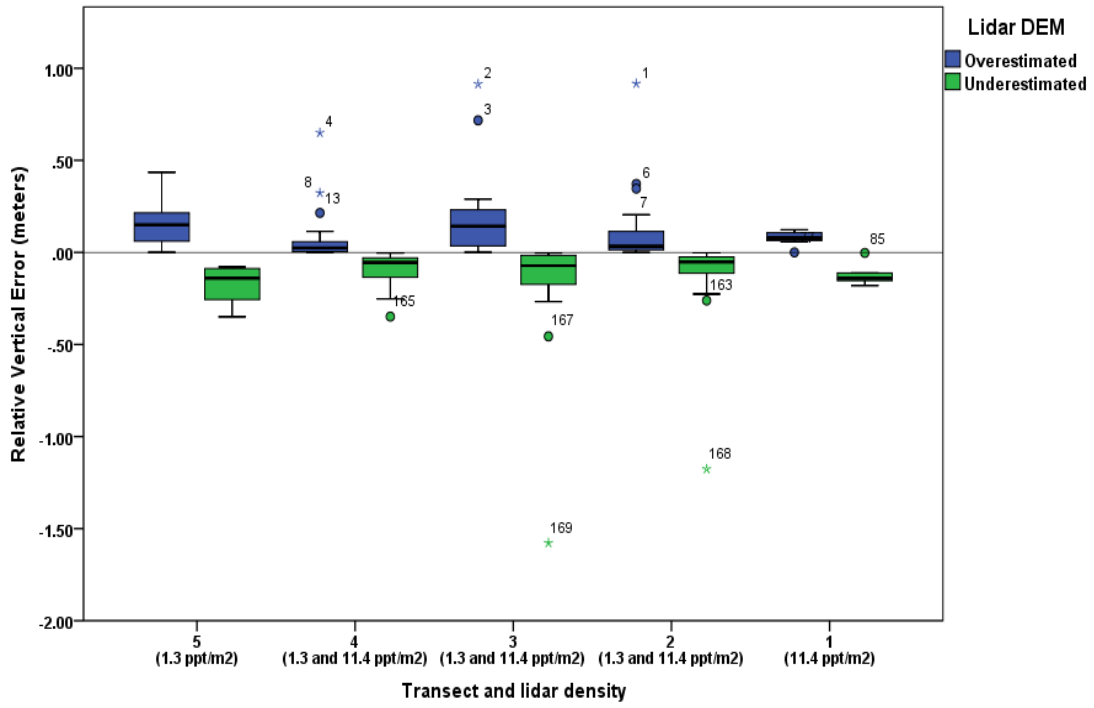

Figure 1-6 Boxplot of the five transects showing the RVE, where the lidar DEM has overestimated or underestimated the change compared to the ground survey data

Table 1-5 T-test results for the relative change in elevation difference between the lidar

Welch Two Sample t-test including the two lidar density	
t = 0.25, df = 331, p-value = 0.80	
95 % CI: -0.043 - 0.056	
sample estimates:	
mean of x (Survey) 0.090	mean of y (lidar DEM) 0.083
Welch Two Sample t-test for 11.4 lidar density	
t = 0.26, df = 214, p-value = 0.79	
95 % CI: -0.05 - 0.071	
sample estimates:	
mean of x (Survey) 0.091	mean of y (lidar DEM) 0.083
Welch Two Sample t-test for 1.3 lidar density	
t = 0.071, df = 117, p-value = 0.9	
95 % CI: -0.08 - 0.087	
sample estimates:	
mean of x (Survey) 0.087	mean of y (lidar DEM) 0.084

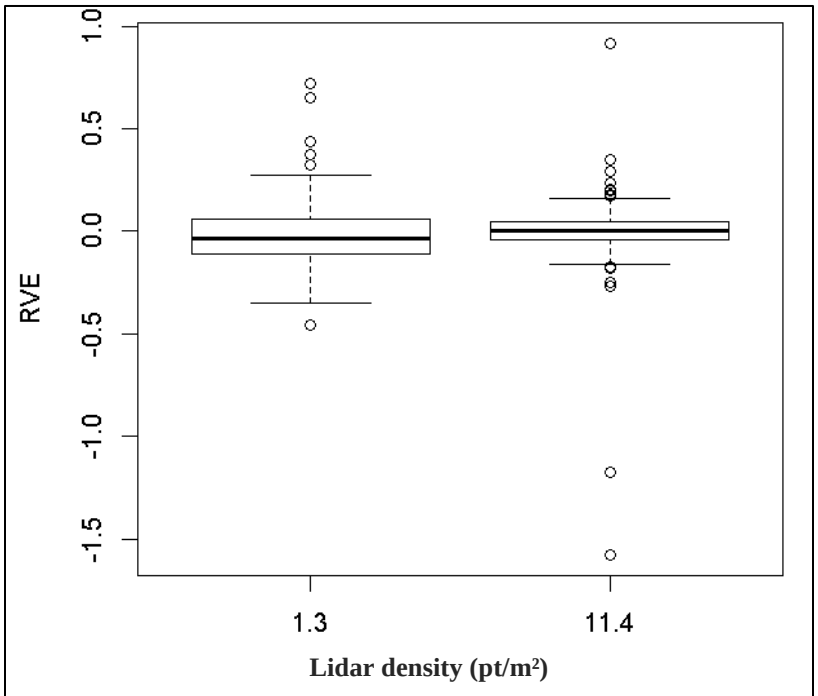

Figure 1-7 Boxplot of the Relative Vertical Error (RVE) along all points for the two lidar densities elevation points.

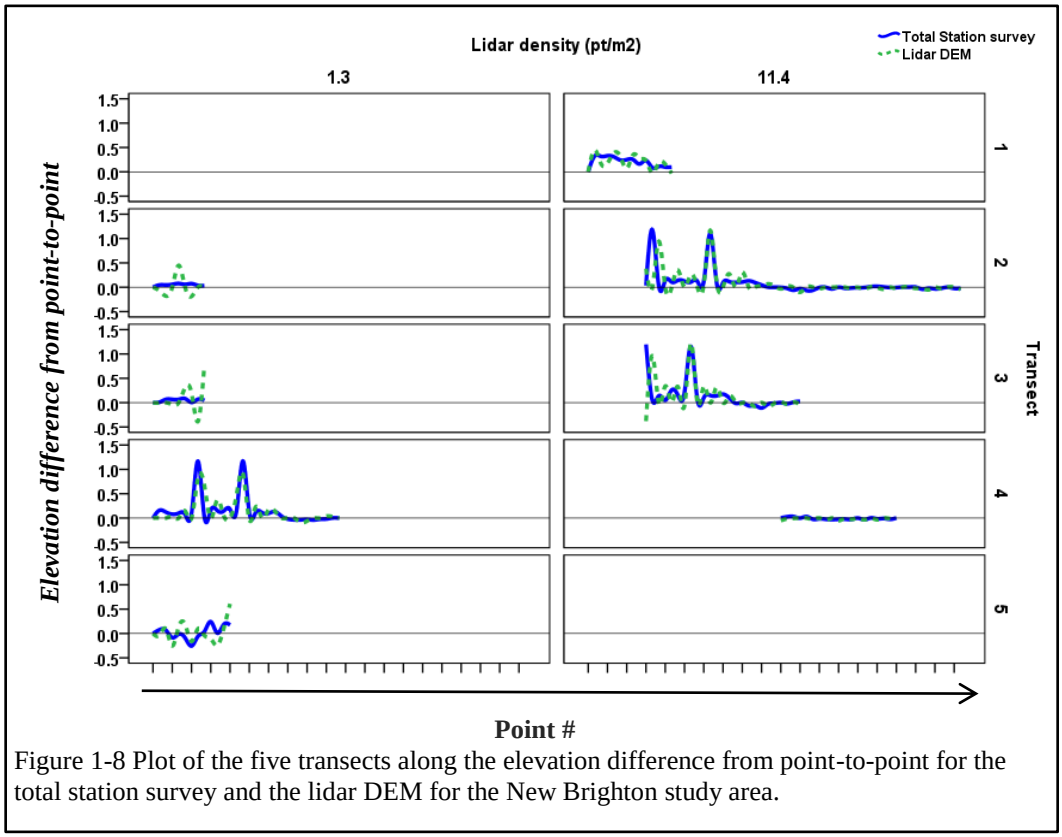

Figure 1-8 Plot of the five transects along the elevation difference from point-to-point for the total station survey and the lidar DEM for the New Brighton study area.

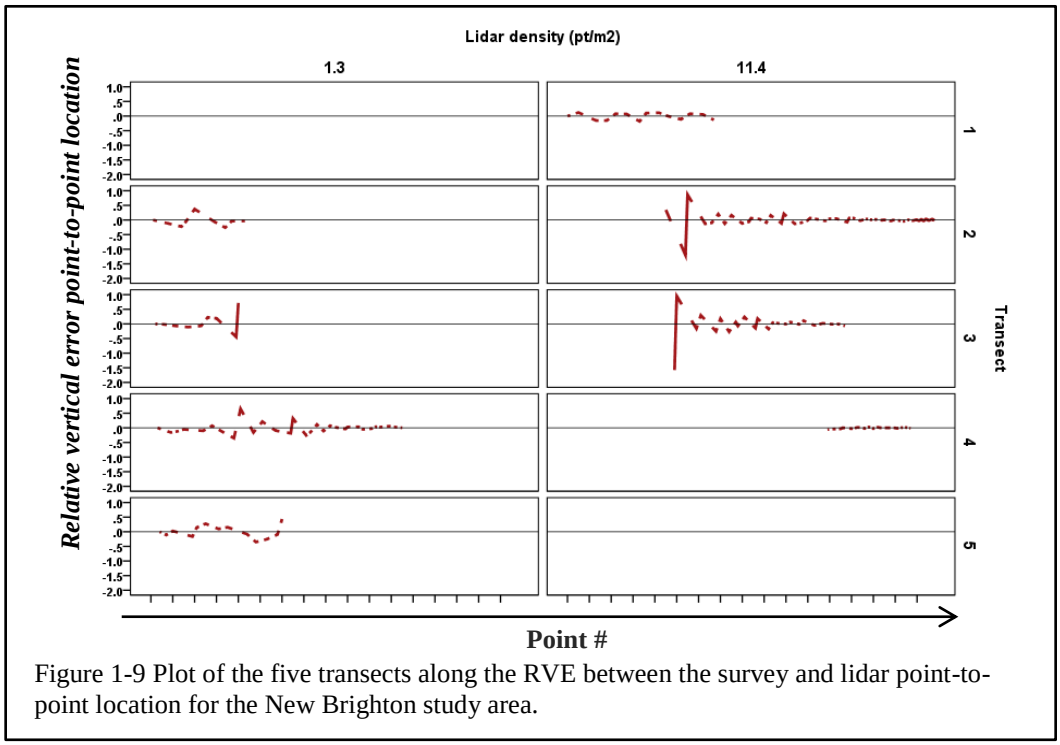

Figure 1-9 Plot of the five transects along the RVE between the survey and lidar point-to-point location for the New Brighton study area.

Discussion and Conclusions

In this study, we evaluated the influence of lidar posting density of the accuracy of building footprint and ground elevation points across the Twin Cities metro region in Minnesota. The accuracy assessment indicators used in this study were used to determine any significant differences between lidar derived products and reference data. For the nine study areas tested for the effect of lidar density on the accuracy of building footprint, there was a small percentage (0.2%-6.3%) of building areas being overestimated or underestimated.

The ANOVA results showed that there was a significant difference for at least one of the study areas, but the Tukey (HSD) test helped to determined which areas were significantly different. From the Tukey (HSD) test only Belle Plain was found to be statistically significant different compared to the other study areas. These results approved and confirm the accuracy and quality of building footprint created by the Minnesota DNR.

Building analysis results indicate that creating building footprint from lidar density ranging from (1.3-11.5 pt/m^2) will give a very close approximation of the real building area size. In contrast, our visual quality assessment comparison of building footprints (Figure 5) indicates that the quality of building footprint varies at different lidar densities. These quality comparison point out the need to further improve the edges of building footprints created from lower lidar densities. Building footprints created from high lidar density have sharper edges which make these buildings to look more aesthetically pleasing compared to building created from lower densities.

Other studies reinforced our findings regarding the effect of lidar density on the accuracy and visual quality of building footprints. Lohani and Singh (2008) used simulated lidar data to examine the influence of different lidar density (1pt/m^2-12pt/m^2), flying height(500m-1500m), and scan angles (10°-30°) on the accuracy of building identification. The Lohani and Singh (2008) results indicated that the most significant parameter that affected the accuracy of the building extracted from lidar data was the

lidar density used. Also, they found that there is not significant improvement on the accuracy and quality of the building after 8pt/m² lidar density.

Zhang et al., (2006) assessed the effect of lidar point density on building footprints that were created from 0.25 ppt/m² and 1 ppt/m² lidar density. The Zhang et al., (2006) results also indicate that the higher lidar point density (1 ppt/m²) produced more accurate building footprints because small building surfaces were retained with the higher lidar density.

Our results confirm these previous studies and suggest that the Minnesota DNR lidar-derived building footprints are close approximation of the area size of existing commercial buildings across the metro region. Additionally, these free lidar building footprints offer an alternative data type for commercial building inventory compared to traditional and time consuming Geographic Information System (GIS) techniques such as photo-interpretation and heads-up digitization to create building outlines.

For the ground elevation analysis, the influence of the lidar posting densities on the accuracy of the ground elevation points was assessed by looking at the consistency of changes that occur from point-to-point in the lidar DEM and in the ground survey points.

This consistency was evaluated by looking at the RVE difference values and assessing whether the variation between both datasets were statistically significant different. First, our results demonstrated that the changes that were calculated from point-to-point within the lidar DEM points were similar to the range observed within the ground survey points.

The changes in elevation that occurred in the lidar DEM ranged from -1.22 m to 0.38 m, these values were close to the ground survey changes observed: -1.97m to 0.25 m. A small difference was seen between that changes that occurred in both dataset, this was calculated by the RVE indicator. The RVE shows that the changes were very consistent in both dataset almost zero difference, only with a small variation in average of 0.006 m. In some extreme cases a minimum of -1.5 m was observed, indicating that the lidar DEM data was underestimating the change in elevation compared to the ground survey.

In the same way, a maximum of 0.91 m was observed, indicating that the lidar DEM data was overestimated the change in elevation compared to the ground survey. The Two sample t-test results helped us to determine if these small variation in elevation changes were significant different. Our statistical results indicated there was not a statistically significant difference between lidar DEM and the ground survey points at a confidence level of $\alpha = 0.05$.

The t-test analysis was performed for individual lidar densities and the results also demonstrated that there was not a statistically significant difference between the lidar DEM derived from 1.3 pt/m² and 11.4 pt/m² compared to the ground survey points. Although our methodology to assess the effect of lidar density on the accuracy of a lidar DEM was a different from that used in other studies (Anderson et al., 2006; Guo et al., 2010; Hodson and Bresnahan, 2004; Smith et al., 2004), we provided a new way to look at the accuracy of a lidar DEM by evaluating the consistency of changes across the lidar DEM elevations and the reference data ground elevations. We conclude that both datasets for each transect had small insignificant relative vertical error variations. These results provide valuable regarding the influence of low or high lidar density on the accuracy of elevations derived from a lidar DEM.

The accuracy and quality visual assessment perfomed in this study have demostrated that low and high lidar density in the state of Minnesota will provide accurate lidar products, particurlaly for the lidar derive DEM wheter it comes from 1.4 – 11.4 pt/m² lidar density. This free high resolution lidar data can be beneficial to many governmental and non-governmental organizations interested in urban, engineering, and enviromental applications.

Acknowledgements

This research was funded by the Minnesota Environment and Natural Resources Trust (ENRTF), the Minnesota Department of Natural Resources (MNDNR), and the United States Fish and Wildlife Services (USFWS: Award 30181AJ194).

References

Anderson E.S., Thompson J., Crourse D.A., Austin R.E., 2006. Horizontal resolution and data density effects on remotely sensed lidar-based DEM. Geoderma. 132, 406–15.

Ackermann F., 1999. Airborne laser scanning-present status and future expectations. ISPRS Journal of Photograpmmetry and Remote Sensing. 54,64-67.

Awrangjeb M., Zhang C., Fraser C.S., 2013. Automatic extraction of buildings roofs using LIDAR data and multispectral imagery. ISPRS Journal of Photogrammetric and Remote Sensing. 83, 1-18.

Aguilar F.J., Agüera F., Aguilar M.A., Fernando C., 2005. Effects of terrain morphology, sampling density**,** and interpolation methods on grid DEM accuracy. Photogrammetric Engineering & Remote Sensing. 7, 805–816.

Aguilar F.J., Mills J.P., Delgado J., Aguilar M.A., Negreiros J.G., Perez J.L., 2010. Modelling vertical error in LiDAR-derived digiral elevation models. ISPRS Journal of Photogrammetric and Remote Sensing. 65, 103-110.

Bilskie M.V., Scott C.H., 2013. Topographic accuracy assessment of bare earth lidar-derived unstructured meshes. Advances in water resources. 52, 165-177.

Banskota A., Wynne R. H., Johnson P., Emessiene B., 2011. Synergistic use of very high-frequency radar and discrete-return lidar for estimating biomass in temperate hardwood and mixed forests. Annals of Forest Science. 68, 347–356.

Cavalli M., Tarolli P., Marchi L., Fontana G.D., 2008. The effectiveness of airborne LiDAR data in the recognition of channel-bed morphology. Catena. 73, 249-260.

Bartier P.M., Keller C.P., 1996. Multivariate interpolation to incorporate thematic surface data using inverse distance weighting (IDW). Computers & Geosciences. 22, 795–799.

Caruso C., Quarta F., 1998. Interpolation methods comparison, Computers and Mathematics with Applications. 35,109–126.

Coops N.C., Wulder M.A., Culvenor D.S., St-onge B., 2004. Comparison of forest attributes extracted from fine spatial resolution multispectral and lidar data. Canadian Journal of Remote Sensing. 30, 855-866.

Chen Q., 2010.Retrieving vegetation height of forests and woodlands over mountainous areas in the Pacific Coast region using satellite laser altimetry," Remote Sensing of Environment. 114, 1610–1627.

Chow T.E.,Hodson M.E., 2009. Effects of lidar post-spacing and DEM resolution to mean slope estimation, International Journal of Geographical Information Science. 23, 1277-1298. DOI: 10.1080/13658810802344127

Deshpande S.S., 2013. Improved Floodplain Delineation Method Using High-Density LiDAR Data. Computer-Aided Civil and Infrastructure Engineering. 28, 68–79.

Dubayah R.O., Drake J.B., 2000. Lidar remote sensing for forestry. Journal of Forestry. 98, 44-46.

Fiocco G., Smullin L.D., 1963. Detection of scattering layers in the upper atmosphere (60-140 kn) by optical radar. Nature. 199, 1275-1276. doi:10.1038/1991275a0

Flood M., 2001. Laser altimetry, from science to commercial lidar mapping. Photogrammetric Engineering and Remote Sensing. 67, 1209-1217.

García-Quijano M.J., Jensen J.R., Hodgson M.E., Hadley B.C., Gladden J.B., Lapine L.A., 2008. Significance of Altitude and Posting Density on Lidar-derived elevation accuracy on Hazardous waste sites. Photogrammetric Engineering and Remote Sensing. 74, 1137-1146.

Ghilani C.D., Wolf P.R., 2012. Elementary surveying: an introduction to geomatics. 13th edition, Prentice Hall.

Goodwin N.R., Coops N.C., Culvenor D.S., 2006. Assessment of forest structure with airborne LiDAR and the effects of platform altitude. Remote Sensing of Environment. 103, 140–152.

Guo Q., Li W., Yu H., Alvarez O., 2010. Effects of topographic variability and Lidar sampling density on several DEM interpolation methods. Photogrammetric Engineering and Remote Sensing. 76, 701-712.

Haugerud R.A., Harding D.J., Johnson S.Y., Harless J.L., Weaver C.S., Sherrod B.L., 2003. High-resolution lidar topography of the Puget Lowland-A bonanza for earth science. Geological Society of America Today. 13, 4–10.

Heidemann H. k., 2012. Lidar Base Specification version1.0: U.S. Geological Survey Techniques and Methods, Book 11. United States Geological Survey, Washington D.C.

Hodson M.E., Bresnahan, P., 2004, Accuracy of airborne lidar-derived elevation, empirical assessment and error budget. Photogrammetric Engineering and Remote Sensing. 70, 331–339.

Knight J.F., Tolcser B.T., Corcoran J.M., Rampi L.P., 2013. The effects of data selection and thematic detail on the accuracy of high spatial resolution wetland classifications, Photogrammetric Engineering and Remote Sensing. 79, 613-623.

Lee H., Younan N.H., 2003. DEM extraction of lidar returns via adaptive processing. IEEE Transactions on Geoscience and Remote Sensing. 41,2063–2069.

Liu X., Zhang Z., 2008. LIDAR data reduction for efficient and high quality DEM generation Paper presented at the ISPRS Congress Beijing 2008, Beijing, China (http://eprints.usq.edu.au/4569/)

Liu X., Zhang Z., Peterson J., Chandra S., 2007. Lidar-derived high quality ground control information and DEM for image orthorectification. GeoInformatica. 11,37–53.

Lohani B., Singh R., 2008. Effect of data density, scan angle, and flying height on the accuracy of building extraction using LiDAR data. Geocarto International. 23, 81-94. DOI: 10.1080/10106040701207100

Lloyd C.D., Atkinson P.M., 2002. Deriving DSMs from lidar data with kriging. International Journal of Remote Sensing. 23, 2519–2524.

Ma R. 2005. DEM generation and building detection from lidar data. Photogrammetric Engineering and Remote Sensing.71, 847-854.

Minnesota Geospatial Information Office (MnGeo). Minnesota Geospatial Information Office. www.mngeo.state.mn.us. Accessed 2013 October 15.

Means J. E., Acker S. A., Harding D. J., Blair J. B., Lefsky M. A., Cohen W. B., Harmon M. E., McKee W. A., 1999. Use of large-footprint scanning airborne lidar to estimate forest stand characteristics in the Western Cascades of Oregon. Remote Sensing of Environment. 67, 298–308

Næsset 2004. Effects of different flying altitudes on biophysical stand properties estimated from canopy height and density measured with a small-footprint airborne scanning laser. Remote Sensing of Environment. 9, 243–255

Oehlert G. W., 2010.A First Course in Design and Analysis of Experiments. New York: W. H. Freeman and Company. http://users.stat.umn.edu/~gary/book/fcdae.pdf

Raber G.T., Jensen J.R., Hodgson M.E., Tullis J.A., Davis B.A., Berglund J., 2007. Impact of lidar nominal post-spacing on DEM accuracy and flood zone delineation. Photogrammetric Engineering & Remote Sensing. 73, 793–804.

Rampi L.P., Knight J.F., 2013. Wetland mapping in the Upper Midwest United States: An object-based approach integrating lidar and imagery data. PhotogrammetricEngineering and Remote Sensing. In review.

Rutzinger M., Rottensteiner F., Pfeifer N., 2009.A Comparison of Evaluation Techniques for Building Extraction From Airborne Laser Scanning. IEEE Journal of selected topics in applied earth observations and remote sensing. 2, 11-20.

Smith S.L., Holland D.A., Longley P.A., 2004. The importance of understanding error in lidar digital elevation models. International Archives of the Photogrammetry, Remote Sensing and Spatial Information Sciences. 35, 996–1001.

Tournaire O., Brédif M., Boldo D., Durupt M., 2010. An efficient stochastic approach for building footprint extraction from digital elevation models. ISPRS Journal of Photogrammetry and Remote Sensing. 65, 317-327.

USGS Center for LIDAR Information Coordination and Knowledge. http://lidar.cr.usgs.gov/. Accessed 2013 October 15.

Webster T.L., Forbes, D.L., Dickie, S., 2004. Using topographic lidar to map flood risk from storm-surge events from Charlottetown, Prince Edward Island. Canadian Journal of Remote Sensing. 30, 64–76.

Wehr, A., Lohr U., 1999. Airborne laser scanning-An introduction and overview. ISPRS Journal of Photograpmmetry and Remote Sensing 54:68-82.

Zhang K., Yan j., Chen S., 2006. Automatic Construction of Building Footprints From Airborne LIDAR Data. IEEE Transactions on geoscience and remote sensing. 44, 2523-2533.

Chapter 2: Comparison of flow direction algorithms in the application of the CTI for mapping wetlands in Minnesota*

Topography has been traditionally used as a surrogate to model spatial patterns of water distribution and variation of hydrological conditions. In this study, we investigated the use of light detection and ranging (lidar) elevation data to derive two Single Flow Direction (SFD) and five Multiple Flow Direction (MFD) algorithms in the application of the compound topographic index (CTI) for mapping different types of wetlands. We evaluated the following flow direction algorithms: SFD (D8 and Rho8), and MFD (DEMON, D-∞ MD-∞, Mass Flux, and FD8) in three ecoregions in Minnesota. Numerous studies have found that MFD algorithms better represent the spatial distribution of water compared to SFD. CTI wetland/upland maps were compared to field collected and image interpreted reference data using traditional remote sensing accuracy estimators. Overall accuracy results in the three study areas for the majority of CTI based algorithms were in the range of 81-92%, with low errors of wetland omission. The results of this study provide evidence that 1) different types of wetlands can be accurately identified using a CTI derived from lidar data across three ecoregions, and 2) MFD algorithms should be preferred over SFD algorithms in most cases.

* Manuscript in review: Rampi, L.P., Knight, J., Lenhart C., Comparison of flow direction algorithms in the application of the CTI for mapping wetlands in Minnesota, Wetlands, 2013.

Introduction

Wetlands are distinctive ecosystems as a result of their hydrologic conditions, chemistry, and transitional bridge between terrestrial and aquatic life. The U.S. Fish and Wildlife service define wetlands as " lands of transitional between terrestrial and aquatic systems where the water table is usually at or near the surface or the land is covered by shallow water…Wetlands must have one or more of the following attributes: (1) at least periodically, the land supports predominantly hydrophytes; (2) the substrate is predominantly undrained hydric soil; and (3) the substrate is non-soil and is saturated with water or covered by shallow water at some time during the growing season of each year" (Cowardin et al.,1979; Mitsch and Gosselink, 2000).

Wetland benefits include wildlife habitat, fishing activities, educational activities, protection of shorelines, reduction of negative effects of floods and drought, recharge of groundwater aquifers, cleansing of contaminated waters and climate regulation. For example, peatland is a type of wetland that has the ability to regulate climate change through carbon sequestration. Peatlands may hold up to 540 gigatons of carbon, representing in approximately 1.5% of the total estimated global carbon storage (Anteau and Afton, 2009; Bridgham et al., 2008; Charman, 2009).

Despite their benefits, many wetlands have not been protected but instead have been drained and filled for agricultural or urban development. For example, the United States has lost about 53% of the original wetlands since the mid-1800s. Those wetlands were converted to agricultural, urbanization and other commercial landuses (Dahl and Johnson, 1991; Stedman and Dahl, 2008). Similar change was seen in the state of Minnesota from the 1780s to the mid-1980s where about 42% of the original wetlands were drained, ditched, filled and converted to other land uses (Dahl, 2006).

Currently the most widely used quantitative source of wetland inventory in the majority of the United States, including Minnesota, is the National Wetlands Inventory (NWI). However, many NWI maps are outdated, having been completed in the late 1980's, and many changes in the landscape have occurred. Furthermore, the NWI maps were created from aerial imagery (some black and white) collected from 1979 to1988

(LMIC, 2007). Thus, it is important and necessary to update wetland inventories with accurate locations of wetlands. An updated wetland inventory is beneficial to make correct decisions for the preservation, protection and restoration of these valuable ecosystems.

The use of topography data provides a fast and cost-effective way to analyze watershed morphology, and compute terrain indices useful for improving river, lake, and wetland identification (Corcoran et al., 2011; Chaplot and Walter, 2003; Grabs et al., 2009; Lang et al., 2012). Digital Elevation Models (DEMs) are preferred to calculate terrain attributes because of the visual representation of these features and the easy computer implementation of algorithms to calculate terrain features (Gunter et al., 2004; Knight et al., 2013; Shoutis et al., 2010; Sørensen and Seibert, 2007).

For example, flow direction algorithms can be calculated directly from DEMs, to determine in which direction the outflow from a given cell will be distributed to one or more neighboring downslope cells. Flow direction algorithms are important for the calculation of topographic indices such as the Compound Topographic Index (CTI), also known as the Topographic Wetness Index (TWI). One of the valuable benefits of using indices such as the CTI is the ability to represent the distribution and flow of water (saturated vs. non-saturated areas) based only on topographic data (Guntner et al., 2004; Moore et al., 1993; Wilson and Gallant, 2000).

The CTI can identify parts of the landscape where sufficient wetness could allow the formation of wetlands particularly depressional wetlands. The CTI is based on the formula proposed by Beven and Kirkby (1979): $CTI = \ln [(\alpha)/ (\tan (\beta)]$, where α represents the local upslope contributing area per unit contour draining through each cell, and β represents the local slope gradient. Upslope contributing areas are calculated using a flow direction algorithm; thus, the choice of flow direction algorithm is important because it influences the spatial pattern of the CTI values.

Flow direction algorithms are divided in two main groups based on how they distribute flow from one grid cell to another cell (Erskine et al., 2006; Gruber and Peckham, 2008; Wilson et al., 2008). The first group consists of single flow direction (SFD) algorithms, which allow flow to pass to only one neighboring cell downslope. The

following algorithms are examples of the SFD group: the Deterministic D8 algorithm proposed by O'Callaghan and Mark (1984), and the random single direction algorithm Rho8 described by Fairfield and Leymarie (1991).

The second group consists of multiple flow direction (MFD) algorithms, which allow flow to pass to more than one neighbor cell downslope. This group is further subdivided into algorithms that allow flow to be distributed to a maximum of two, three, four, and eight neighbor cells downslope. Examples of algorithms that allow flow to be distributed to a maximum of two cells include the Digital Elevation Model Network (DEMON) proposed by Costa-Cabral and Burges (1994), and the Deterministic Infinite (D ∞) algorithm suggested by Tarboton (1997).

The Braunschweiger relief model proposed by Bauer et al., (1985) is an example of an algorithm that allows flow to be distributed to a maximum of three neighbor cells. The Mass Flux (MF) algorithm proposed by Gruber and Peckham (2008) is an example of algorithms that allow flow to pass into a maximum of four neighbors cells. Examples of algorithms that allow flow to be distributed to a maximum of eight neighbor cells include the Triangular Multiple Flow direction algorithm (MD ∞) proposed by Seibert & McGlynn (2007), and the Divergent Flow algorithm (FD8) proposed by Freeman (1991).

Studies related to hydrological applications across disciplines have used SFD algorithms such as the D-8 more often than MFD algorithms. Although several studies have confirmed that MFD algorithms can provide more accurate results in calculating the distribution and flow of water, the use of SFD algorithms continues (Pan et al., 2004; Wilson and Gallant, 2000, Zhou and Liu, 2002).

Numerous studies have shown differences between SFD and MFD algorithms for stream network applications and statistical distribution of primary and secondary terrain attributes (Endreny and Wood, 2003; Gunter et al., 2004; Tarboton, 1997). However, little research has been done to assess the accuracy of these types of algorithms using high resolution elevation data in the application of the CTI for identifying wetlands in the upper Midwest, U.S.A. In recent years, the acquisition of high resolution elevation data using Light Detection and Ranging (lidar) has increased.

Lidar is an active remote sensing technology that uses laser light to produce accurate land elevation data. Numerous studies have confirmed the importance of lidar data to improve the process of mapping wetlands (Jenkins and Erazier 2010; Knight et al. 2013; Lang et al. 2013). Lang and McCarty (2009) mapped forested wetlands using lidar intensity and obtained a high overall acccury of 96.3%. They compared their lidar intensity results to NIR photointerpretation of wetlands, which had an overall accuracy of 70% for the same area. Antokarakis et al., (2008) also achieved high overall accuracy results of 95%-99% for mapping open water features using a combination of lidar intensity and lidar derived terrain attributes. Thus, the goal of this paper was to assess the accuracy of a selection of two Single Flow Direction (SFD) and five Multiple Flow Direction (MFD) algorithms for use in creating several CTIs from lidar data for wetland mapping in three ecoregions in the state of Minnesota, U.S.

Study Areas Description

This study was conducted in three study areas within three different ecoregions in the state of Minnesota (Figure 1). The first study area is located in the Northern Glaciated Plains ecoregion and consists of five watersheds of a 12-digit-level Hydrologic Unit Code (i.e., HUC-12). The five watersheds include Big Stone Lake, Big Stone Lake State Park, Barry Lake, Fish Creek, and Salmonson Point, all within Big Stone County. The total area of the five watersheds together is 293 km² with primarily loamy soils and a mixture of well and poorly drained soils. Land use within these watersheds is predominantly agricultural with grain crops, including corn and soybeans. The topography of these watershed ranges from 290 m to 364 m above sea level.

The average annual precipitation in this area is 640 mm and throughout the growing season is 360 mm (May to September). These watersheds are part of the prairie pothole region in Minnesota, characterized by having many small depressional wetlands known as prairie pothole wetlands. Wetlands in this ecoregion are of vital importance for fostering wildlife habitat, storage of surface water, groundwater recharge and discharge

sites, flow-through systems, and reduction in the risk of downstream flooding (LaBaugh et al., 1998; Winter and Rosenberry, 1995).

The second study area is located in the Central Hardwood Forest ecoregion and contains five watersheds of a 12-digit level Hydrologic Unit Code (i.e., HUC-12). The five watersheds include Upper Lake Minnetonka, Riley Creek, Purgatory Creek, Lower Lake Minnetonka and the City of Shakopee-Minnesota River. These watersheds are located within Hennepin and Carver counties. The total area of the five watersheds is 69 km^2, with fine to moderately coarse textures and well drained soils.

Land use is dominated by urban development including medium density residential, with some areas for commercial growth and open space. The elevation across these watersheds is 209-332 m above sea level. The average annual precipitation is 762 mm and during the growing season (May to September) is 508 mm. The majority of the wetlands types in these watersheds are shallow marshes and wet meadows (City of Chanhassen Surface Water Management Plan, 2006).

The third study area is located within the Northern Lakes and Forest ecoregion and includes four watersheds of a 12-digit level Hydrologic Unit Code (i.e., HUC-12). The four watersheds include Big Lake, the City of Cloquet-St. Louis River, Otter Creek and the Thompson Reservoir-St. Louis River. These watersheds are located between St. Louis and Carlton counties. The total area of the four watersheds together is 265 km^2 with poorly drained soils and near-surface water tables. The main land use in these watersheds is mixed forested land dominated by conifer forest, mixed hardwood-conifer forest and conifer bogs and swamps.

The topography in these areas ranges between 307 m and 436 m above sea level. The average annual precipitation is 710 mm and during the growing season (May to September) the average precipitation is 440 mm. Wetlands types in these watersheds are primarily forested wetlands covered by coniferous and tall shrubby vegetation (Minnesota Department of Natural Resources, 2010).

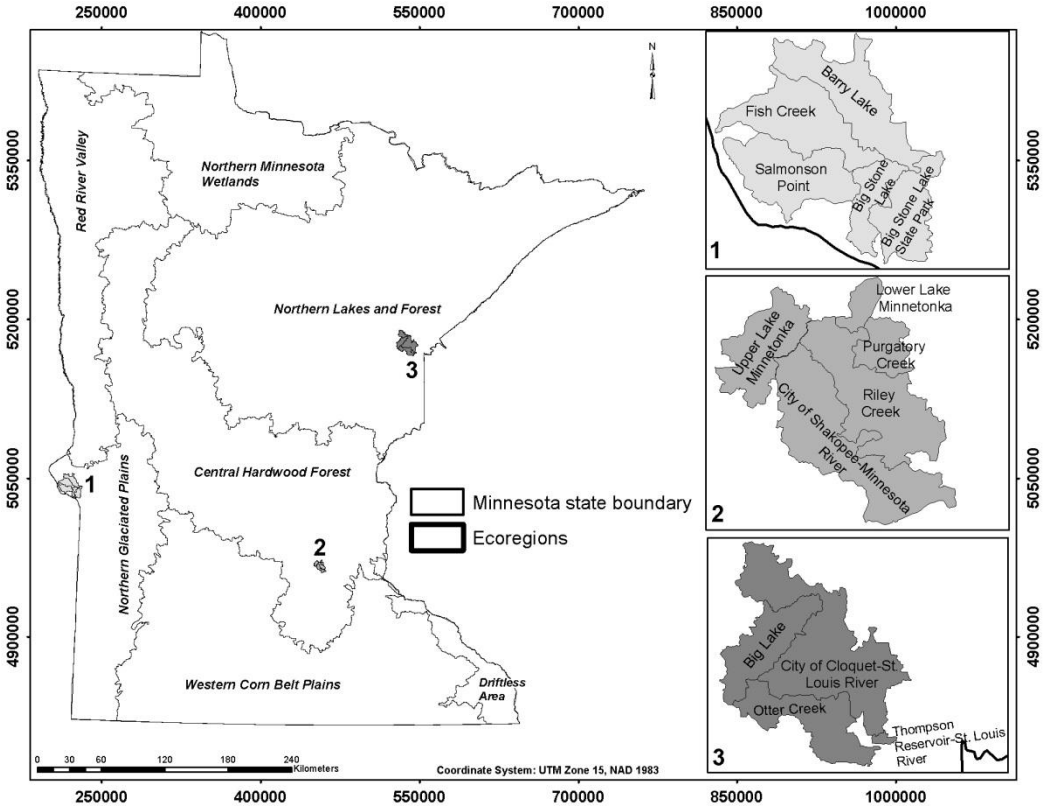

Figure 2-1 Location map of the three study areas in the state of Minnesota, U.S.A

Lidar Data

We used a 3 m lidar DEM for each study area to compute seven different flow direction algorithms. The 3m lidar DEM for the Northern Glaciated Plains study area was obtained from the International Water Institute (IWI) lidar download portal. The DEM was created by interpolating the bare earth point LAS files using the 'Raster to ASCII' command in the Environmental Systems Research Institute (ESRI) ArcGIS software.

Collection of the lidar data used to create the DEM occurred during the spring of 2010 (leaf-off conditions) by Fugro Horizons Inc. with an average post spacing of 1.35 m. The lidar data horizontal accuracy was of +/- 1 m (95% confidence level), with a vertical accuracy RMSE of 15.0 cm.

The 3m lidar DEM for the Central Hardwood Forest study area was downloaded from the Minnesota Geospatial Information Office (MnGeo). This lidar DEM was produced by the Minnesota DNR by extracting bare earth points from the point cloud data. The DEM was hydro flattened using the edge of the water breaklines. Collection of the lidar point cloud data took place between Nov 11 and Nov 17, 2011 by Fugro Horizons Inc. with an average post spacing of 1.5 m. The horizontal accuracy for these data was of +/- 0.6 m (95% confidence level), and a vertical accuracy RMSE of 5 cm.

The 3m lidar DEM for the Northern Lakes and Forest study area was also acquired from the Minnesota Geospatial Information Office (MnGeo). The 3m DEM was produced by the Minnesota DNR by extracting bare earth points from the point cloud data. The DEM was also hydro flattened using the edge of the water breaklines. Acquisition of the lidar data took place between May 3 and May 5, 2011 by Woolpert Inc. with an average post spacing of 1.5 m. The horizontal accuracy of the lidar data was +/- 1.2 m (95% confidence level), with a vertical accuracy RMSE of 5 cm.

Analysis Methods

The first subsection of this method section describes the pre-processing steps applied to the lidar DEMs. The second subsection describes the steps and software used to calculate each of the lidar derived terrain attributes required for the CTI calculation CTIs. The last subsection explains the accuracy assessment procedures used to assess the results for each study area.

Lidar DEM Pre-processing

Each lidar DEM was subset to a shapefile watershed boundary that was obtained from the Minnesota Department of Natural Resources (DNR). Sinks or pits that did not have a surface water outlet were moderately filled to avoid irregularities that could interfere with correct hydrologic flow (trapping flow). We used the tool *fill sinks XXL* implemented in the free open source software System for Automated Geoscientific Analysis (SAGA) v. 2.1.0. We chose this tool because it offers the option to fill sinks fully or partially by keeping a minimum slope gradient along the flow path. Otherwise, if

no minimum slope gradient value is specified all the sinks will be filled to the spill elevation which will create completely flat areas. Due to the high resolution of our lidar DEMs we avoided filling surface depressions completely by preserving a minimum slope gradient of 0.001 between cells. The resultant sink-moderately-filled DEM for each study area was used to compute the required terrain attributes for calculation of the upslope contributing areas.

Derived Terrain Surfaces

The following flow direction algorithms were implemented in different software packages for the computation of seven upslope contributing areas: The D8, Rho8 and DEMON algorithms were implemented using the SAGA software; the FD8 and MD-∞ algorithms were implemented using Whitebox Geospatial Analysis Tools v. 1.0.7 open source software; the Mass Flux algorithm was implemented using the River Tools v. 3.0.3, GIS software; the D∞ algorithm was implemented using the Terrain Analysis Using Digital Elevation Models (TAUDEM) v. 5.0 toolbox in ArcGIS 9.3.1; and the seven upslope contributing areas for each study area were used to calculate the seven CTIs in ArcGIS v. 10.1.

We computed a slope grid in degrees from the pre-filled DEM using the spatial analyst tool in ArcGIS v. 10.1. We modified the resultant slope by adding a minimum value of 0.0001 to avoid division by zero for CTI calculations. The raster calculator in ArcGIS v. 10.1 was used to modify the slope and impose the minimum value. Finally, we calculated all the CTIs based on the formula proposed by Beven and Kirkby (1979). The CTI computations were carried out in ArcGIS v. 10.1 using the raster calculator from the Spatial Analyst toolbox.

Accuracy Assessment

We evaluated the CTI results for each study area based on traditional accuracy assessment methods, including error matrices, overall accuracy, producer's accuracy, user's accuracy, and kappa statistic (k-hat) for upland and wetland classes. We also executed a significance test of error matrices known as the Z Pair-Wise statistical test

described by Congalton and Green (2009). This Z-test was used to determine whether there was a statistically significant difference between the various CTIs at an alpha level of 0.05. The Z-test was also performed between every CTI and the NWI wetland map using the same classification scheme (upland/wetland).

We used a threshold value to separate the CTI results into two classes: uplands and wetlands. Our unpublished accuracy assessment showed that after evaluating several CTI threshold values, the most accurate CTI threshold values to separate wetness (potential wetland) from dryness (upland) was the mean plus ½ standard deviation of the CTI range of values. CTI's threshold values were assessed using traditional accuracy assessment methods, including error matrices, overall accuracy, producer's accuracy, and user's accuracy using field reference data.

The CTIs and NWI were assessed against a set of independent randomly generated sample points for each study area. These reference data used for the Northern Glaciated Plain and Central Hardwood Forest study areas were collected from a few sources that included: randomly generated field sites visited by trained field crews in the summers of 2009 and 2010, plots generated by the MN Department of Natural Resources Wetland Status and Trend Monitoring Program (WSTMP) using centroids from polygons of 2006 and 2008 updates, and randomly generated points using photo interpretation by our experienced analyst.

The reference data used for the Central Hardwood Forest study area was developed by the City of Chanhassen using a combination of photo-interpretation and field data collection during the fall of 2004, and the growing season of 2005. The field data collected for the three study areas contained the following information: Plant type and percent coverage, land-cover/land-use type, UTM coordinates, 5-6 photos per site, and the Cowardin wetland type (Cowardin et al., 1974).

Upland types included crop fields, other agriculture, forests, grasslands, urban areas, construction areas, bare areas, and others. We used 2000 reference data points for the Northern Glaciated Plains study area, 9,994 for the Central Hardwood Forest study area and 2,000 for the Northern Lakes and Forest study area.

Results

Accuracy assessment results and significance tests of the three study areas are summarized in Tables 2-1 through 2-6. Maps of the seven CTIs and NWI wetland/upland classification are displayed in Figures 2 through 7. Overall accuracy results for all the CTIs tested across the three study areas were in the range of 69-92%.
Wetlands larger than 0.20 ha (0.5 acres) throughout the three study areas were identified by the majority of the algorithms, with producer's and user's accuracies of 67-97% and 65-98% respectively.

Also, a comparison assessment of the seven CTIs and the original NWI was performed for each study area, using the same two classes (wetland/upland). The comparison assessment was done using the kappa-statistic (Z- test) proposed by Congalton and Green (2009). The majority of the CTIs based flow direction algorithms derived from lidar data for identifying wetlands; produced higher accuracy results compared to the NWI results that were in the range of 75-88% for overall accuracy, 73-97% for user's accuracy and 71-87% for producer's accuracy across the three study areas.

Results for the Northern Glaciated Plains study area

Table 2-1 shows accuracy estimates of the two classes for the Northern Glaciated Plains study area. The overall accuracy for all the CTIs evaluated in this area was in the range of 71-92%, with overall kappa scores in the range of 0.42-0.84. Producer's and user's accuracies for all the CTI's were in the range of 67-97% and 70-98% respectively.

The majority of CTIs, with the exception of the CTI Rho8, presented low errors of commission and omissions for the wetland class. The NWI accuracy assessment results were lower than the majority of CTIs for predicting wetland locations in this study area. Table 2-2 displays only the significance test (Z-test) results of those CTI and NWI results that were found to be statistically different at a 95% confidence level.

These Z-test results revealed that the CTI FD8, CTI Rho8 and NWI maps were significantly different compared to every CTI evaluated.

This statistical difference for the CTI FD8, CTI Rho8 and NWI suggests that the other algorithms are more suitable for identifying wetland occurrences in this ecoregion.

Figure 2 shows a visual comparison of the seven CTI algorithms and NWI polygons for a small portion of the Northern Glaciated Plains study area.

Figure 2-3 displays a map of a NIR image and CTI map of the entire study area. This qualitative comparison revealed more details of the differences between the algorithms and the original NWI polygons for representing flow water distribution in wetlands in that area. Overall, the D8, D-∞, and Mass Flux CTIs were the only algorithms for this study area that showed excellent agreement with the reference data in the visual and quantitative assessment, with the highest overall accuracy results in the range of 91-92%.

Results for the Central Hardwood Forest study area

Table 2-3 shows accuracy estimates of the two classes for the Central Hardwood Forest study area. Overall accuracy percentages for all the CTIs assessed in this study area were in the range of 70-88%, with overall kappa scores in the range of 0.41-0.77. Producer's and user's accuracies for all the CTI's were in the range of 71-93.% and 70-88%, respectively. The majority of CTI algorithms excluding the Rho8 and FD8 reported low errors of commission and omissions for the wetland class. NWI producer's accuracy was relatively low compared to the majority of CTIs, which resulted in higher rates of wetland omission in this area. Table 2-4 shows the significance test (Z-test) results of those CTIs and NWI maps that were found to be significantly different at a 95% confidence level.

The CTI FD8, CTI Rho8 and CTI D8 were found to be statistically significant compared to the rest of the CTI and NWI results. Figure 2-4 illustrates a detailed visual comparison of the seven algorithms, wetland polygons created by the City of Chanhassen, and NWI polygons for a small portion of this study area. Figure 2-5 shows a CTI map and NIR image of the entire study area.

This visual comparison exposes many differences between the polygons created by the City of Chanhassen, the NWI polygons and the straight flow water patterns of the

single flow direction algorithms. In general, out of all the algorithms tested, the D-∞ and MD-∞ CTIs indicated excellent agreement with the reference data in the visual and quantitative assessment for this study area. These CTIs had high overall accuracy results in the range of 86-87%, with low errors of wetland omissions and commission.

Results for the Northern Lakes and Forest study area

Table 2-5 shows accuracy assessment results for the two classes for the Northern Lakes and Forest study area. Overall accuracy results for all the CTI's based algorithms evaluated in this study area were in the range of 69-82% with kappa scores between 0.38-0.64. Producer's and user's accuracies for all the CTI's were in the range of 80-86 % and 65-81%, respectively. NWI accuracy assessment estimators were lower compared to the majority of the CTI algorithms for this area. Lower accuracy assessment results of the NWI revealed the inaccuracy of the polygons in this forested area for identifying wetlands, particularly forested wetlands.

Table 2-6 displays significance tests (Z-tests) for only CTI algorithms that were found to be statistically different at a 95% confidence level. The CTI FD8, CTI Rho8 and CTI D8 were found to be statistically significant different compared to the rest of the CTI and NWI results for mapping wetlands. Figure 2-6 is a visual comparison of the seven CTI algorithms and NWI polygons for a small portion of this study area.

Figure 2-7 displays a CTI map and NIR image of the entire study area. A detailed visual comparison of the algorithms in this area revealed the differences between the different algorithms and NWI polygons for predicting forested wetlands. In general, the D-∞, MD-∞, and Mass Flux CTIs were the only algorithms that presented excellent agreement with the reference data in the visual and quantitative assessment for this study area. These three algorithms had the highest overall accuracy results in the range of 81-82%, with relatively low errors of wetland omissions and commission.

Table 2-1Accuracy estimators of the seven CTIs algorithms and the NWI for the Northern Glaciated Plains study area (Classification scheme: wetland/upland).

CTI algorithm	Threshold used	Overall accuracy	Wetland User's accuracy	Upland User's accuracy	Wetland Producer's accuracy	Upland Producer's accuracy	Overall Kappa
D8	6.0	92	87	98	97	87	0.84
Rho8	6.7	71	70	72	67	75	0.42
DEMON	8.1	92	87	97	96	88	0.84
D-∞	7.2	92	87	97	97	87	0.84
MD-∞	6.1	92	87	97	97	87	0.83
Mass Flux	6.1	91	98	85	85	98	0.82
FD8	11.0	86	87	85	82	89	0.71
NWI	1	88	87	89	87	88	0.76
Total # points used for the accuracy assessment: 2000							

Table 2-2. Significance Test (Z-test) for comparing the seven algorithms and the NWI for the Northern Glaciated Plains study area (Classification scheme: wetland/upland).

CTI Type	Kappa1 vs. Kappa2	Z-Value
D8 vs. Rho8	0.84 vs. 0.42	17.6*
D8 vs. FD8	0.84 vs. 0.71	6.7*
D8 vs. NWI	0.84 vs. 0.76	4.5*
Rho8 vs. DEMON	0.42 vs. 0.83	17.5*
Rho8 vs. D-∞	0.42 vs. 0.84	17.6*
Rho8 vs. MD-∞	0.42 vs. 0.83	17.2*
Rho8 vs. Mass Flux	0.42 vs. 0.82	16.6*
Rho8 vs. FD8	0.42 vs. 0.71	10.9*
Rho8 vs. NWI	0.42 vs. 0.76	13.2*
DEMON vs. FD8	0.83 vs. 0.71	6.5*
DEMON vs. NWI	0.83 vs. 0.76	4.3*
D-∞ vs. FD8	0.84 vs. 0.71	6.6*
D-∞ vs. NWI	0.84 vs. 0.76	4.4*
MD-∞ vs. FD8	0.83 vs. 0.71	6.2*
MD-∞ vs. NWI	0.83 vs. 0.76	4.0*
Mass Flux vs. FD8	0.82 vs. 0.71	5.6*
Mass Flux vs. NWI	0.82 vs. 0.76	3.4*
Fd8 vs. NWI	0.71 vs. 0.76	2.24*

* A Z-value over 1.96 indicates that there is a significant difference at the 95% confidence level.

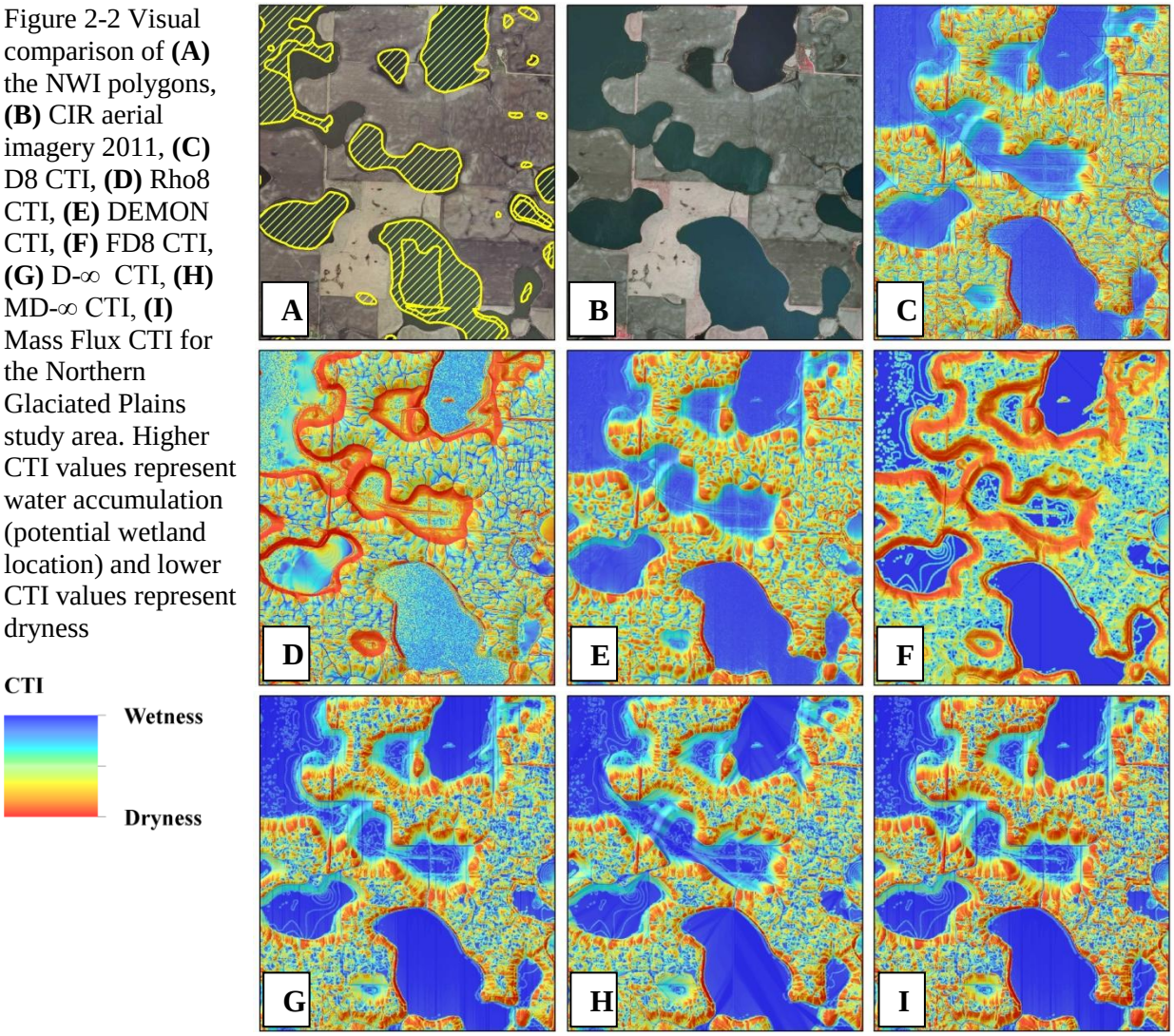

Figure 2-2 Visual comparison of **(A)** the NWI polygons, **(B)** CIR aerial imagery 2011, **(C)** D8 CTI, **(D)** Rho8 CTI, **(E)** DEMON CTI, **(F)** FD8 CTI, **(G)** D-∞ CTI, **(H)** MD-∞ CTI, **(I)** Mass Flux CTI for the Northern Glaciated Plains study area. Higher CTI values represent water accumulation (potential wetland location) and lower CTI values represent dryness

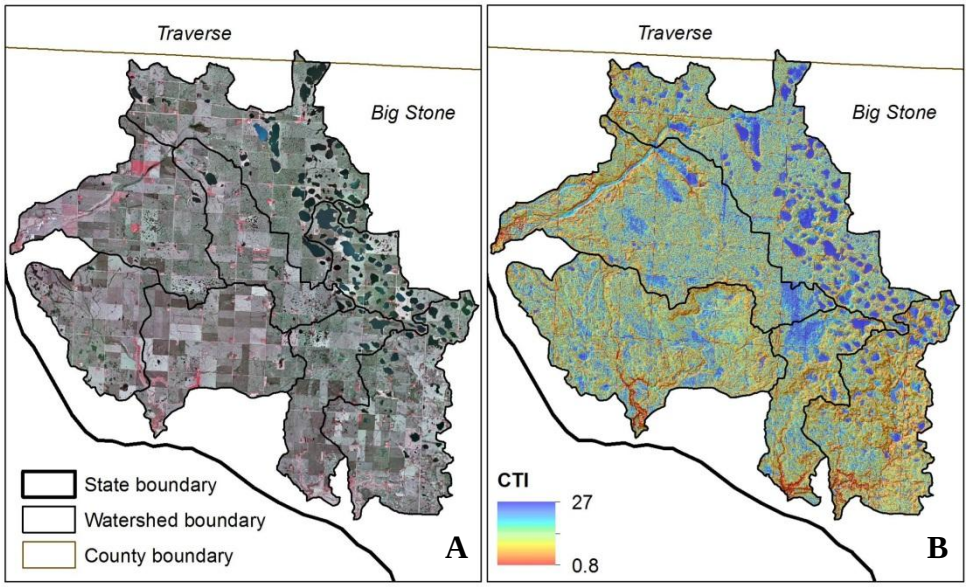

Figure 2-3 **(A)** CIR aerial imagery 2011 map, and **(B)** MD-∞ CTI map for the Northern Glaciated Plains study area

Table 2-3 Accuracy estimators of the seven CTIs algorithms and the NWI for the Central Hardwood Forest study area (Classification scheme: wetland/upland).

CTI algorithm	Threshold used	Overall accuracy	Wetland User's accuracy	Upland User's accuracy	Wetland Producer's accuracy	Upland Producer's accuracy	Overall Kappa
D8	6.1	88	88	89	89	87	0.77
Rho8	5.5	72	71	74	75	70	0.45
DEMON	7.3	85	85	85	85	85	0.71
D-∞	5.4	86	82	92	93	79	0.72
MD-∞	5.1	87	87	87	87	87	0.74
Mass Flux	5.0	85	84	87	87	84	0.71
FD8	5.6	70	70	70	71	70	0.41
NWI	1	85	97	77	71	98	0.70
Total # points used for the accuracy assessment: 9994							

Table 2-4 Significance Test (Z-test) for comparing the seven algorithms and the NWI for the Central Hardwood Forest study area (Classification scheme: wetland/upland).

CTI Type	Kappa1 vs. Kappa2	Z-Value
D8 vs. Rho8	0.77 vs. 0.45	28.7*
D8 vs. DEMON	0.77 vs. 0.71	6.21*
D8 vs. D-∞	0.77 vs. 0.72	4.7*
D8 vs. MD-∞	0.77 vs. 0.74	2.9*
D8 vs. Mass Flux	0.77 vs. 0.71	6.0*
D8 vs. FD8	0.77 vs. 0.41	31.9*
D8 vs. NWI	0.77 vs. 0.70	7.6
Rho8 vs. DEMON	0.45 vs. 0.71	22.5*
Rho8 vs. D-∞	0.45 vs. 0.72	24.15*
Rho8 vs. MD-∞	0.45 vs. 0.74	25.7*
Rho8 vs. Mass Flux	0.45 vs. 0.71	22.7*
Rho8 vs. FD8	0.45 vs. 0.41	3.18*
Rho8 vs. NWI	0.45 vs. 0.70	21.6*
DEMON vs. MD-∞	0.71 vs. 0.74	3.2*
DEMON vs. FD8	0.71 vs. 0.41	25.7*
D-∞ vs. FD8	0.72 vs. 0.41	27.4*
D-∞ vs. NWI	0.72 vs. 0.70	2.8*
MD-∞ vs. Mass Flux	0.74 vs. 0.71	3.0*
MD-∞ vs. FD8	0.74 vs. 0.41	28.9*
MD-∞ vs. NWI	0.74 vs. 0.70	4.5*
Mass Flux vs. FD8	0.71 vs. 0.41	25.9*
Fd8 vs. NWI	0.41 vs. 0.70	24.8*

** A Z-value over 1.96 indicates that there is a significant difference at the 95% confidence level.*

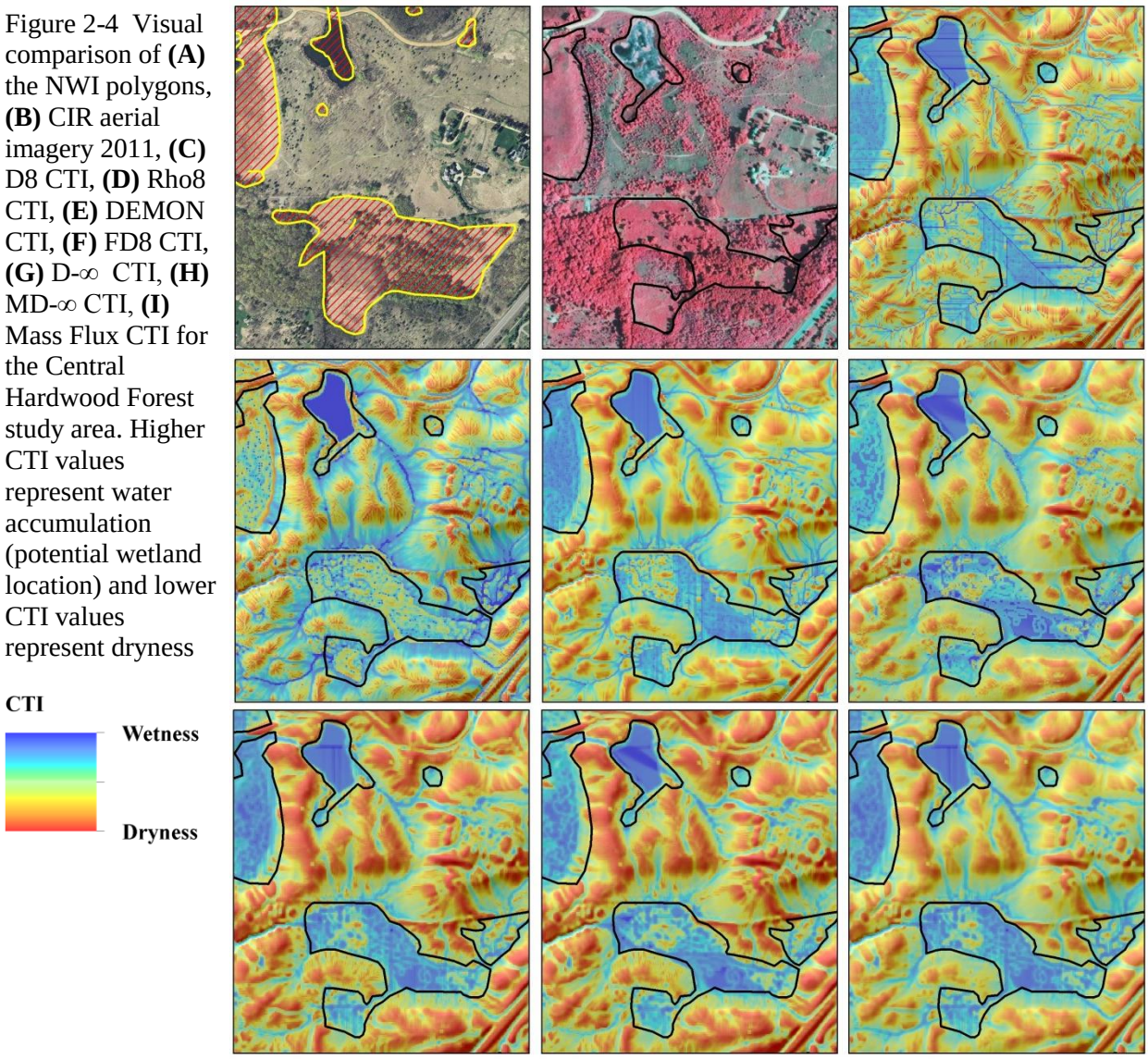

Figure 2-4 Visual comparison of **(A)** the NWI polygons, **(B)** CIR aerial imagery 2011, **(C)** D8 CTI, **(D)** Rho8 CTI, **(E)** DEMON CTI, **(F)** FD8 CTI, **(G)** D-∞ CTI, **(H)** MD-∞ CTI, **(I)** Mass Flux CTI for the Central Hardwood Forest study area. Higher CTI values represent water accumulation (potential wetland location) and lower CTI values represent dryness

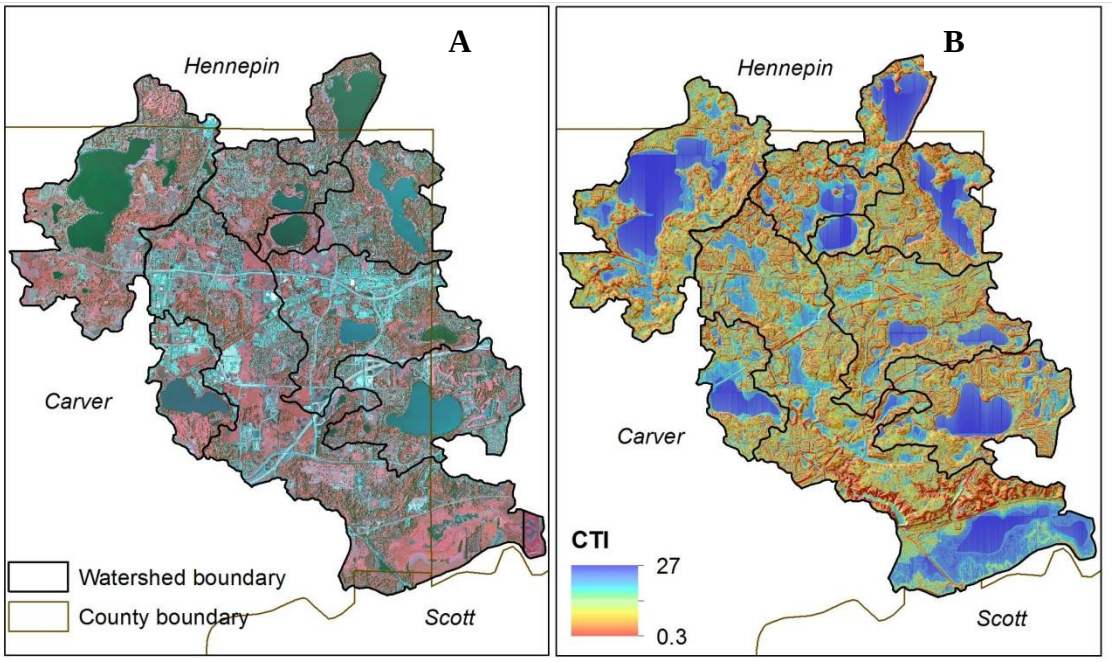

Figure2-5 **(A)** CIR aerial imagery 2008 map, and **(B)** MD-∞ CTI map for the Central Hardwood Forest study area

Table 2-5 Accuracy estimators of the seven CTIs algorithms and the NWI for the Northern Lakes and Forest study area (Classification scheme: wetland/upland).

CTI algorithm	Threshold used	Overall accuracy	Wetland User's accuracy	Upland User's accuracy	Wetland Producer's accuracy	Upland Producer's accuracy	Overall Kappa
D8	5.2	82	80	84	86	78	0.64
Rho8	6.1	69	65	77	84	54	0.38
DEMON	7.1	75	73	77	80	70	0.50
D-∞	7.0	81	81	81	81	81	0.61
MD-∞	5.5	82	80	83	84	80	0.63
Mass Flux	6.0	81	80	81	82	79	0.61
FD8	5.8	81	79	83	83	78	0.61
NWI	1	75	73	78	80	70	0.50
Total # points used for the accuracy assessment: 2000							

Table 2-6 Significance Test (Z-test) for comparing the seven algorithms and the NWI for the Northern Lakes and Forest study area (Classification scheme: wetland/upland).

CTI Type	Kappa1 vs. Kappa2	Z-Value
D8 vs. Rho8	0.64 vs. 0.38	9.78*
D8 vs. DEMON	0.64 vs. 0.50	5.43*
D8 vs. NWI	0.64 vs. 0.50	5.24*
Rho8 vs. DEMON	0.38 vs. 0.50	4.18*
Rho8 vs. D-∞	0.38 vs. 0.61	8.84*
Rho8 vs. MD-∞	0.38 vs. 0.63	9.43*
Rho8 vs. Mass Flux	0.38 vs. 0.61	8.59*
Rho8 vs. FD8	0.38 vs. 0.61	8.80*
Rho8 vs. NWI	0.38 vs. 0.50	4.37*
DEMON vs. D-∞	0.50 vs. 0.61	4.52*
DEMON vs. MD-∞	0.50 vs. 0.63	5.10*
DEMON vs. Mass Flux	0.50 vs. 0.61	4.28*
DEMON vs. FD8	0.50 vs. 0.61	4.48*
D-∞ vs. NWI	0.61 vs. 0.50	4.34*
MD-∞ vs. NWI	0.63 vs. 0.50	4.91*
Mass Flux vs. NWI	0.61 vs. 0.50	4.10*
Fd8 vs. NWI	0.61 vs. 0.50	4.30*

* A Z-value over 1.96 indicates that there is a significant difference at the 95% confidence level.

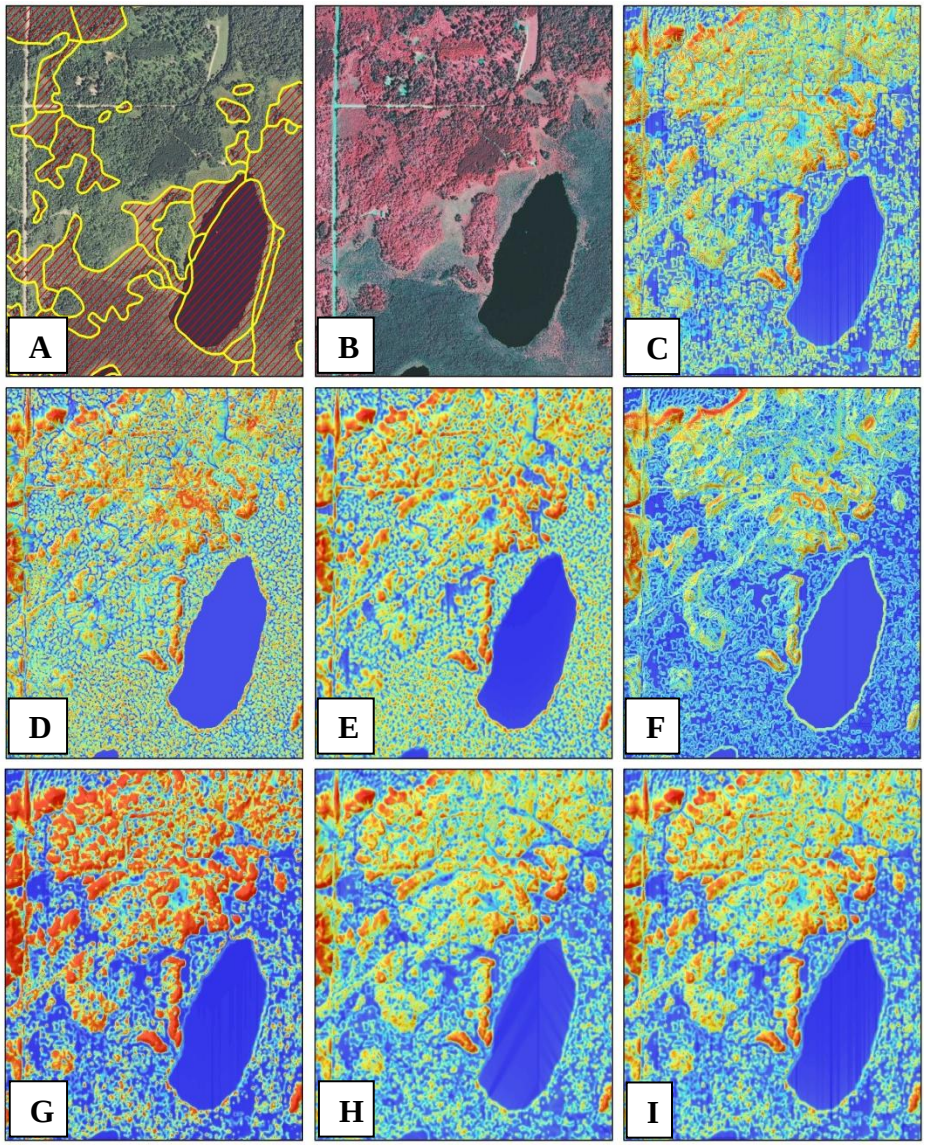

Figure 2-6 Visual comparison of **(A)** the NWI polygons, **(B)** CIR aerial imagery 2011, **(C)** D8 CTI, (D) Rho8 CTI, **(E)** DEMON CTI, (F) FD8 CTI, **(G)** D-∞ CTI, **(H)** MD-∞ CTI, **(I)** Mass Flux CTI for the Northern Lakes and Forest study area. Higher CTI values represent water accumulation (potential wetland location) and lower CTI values represent dryness

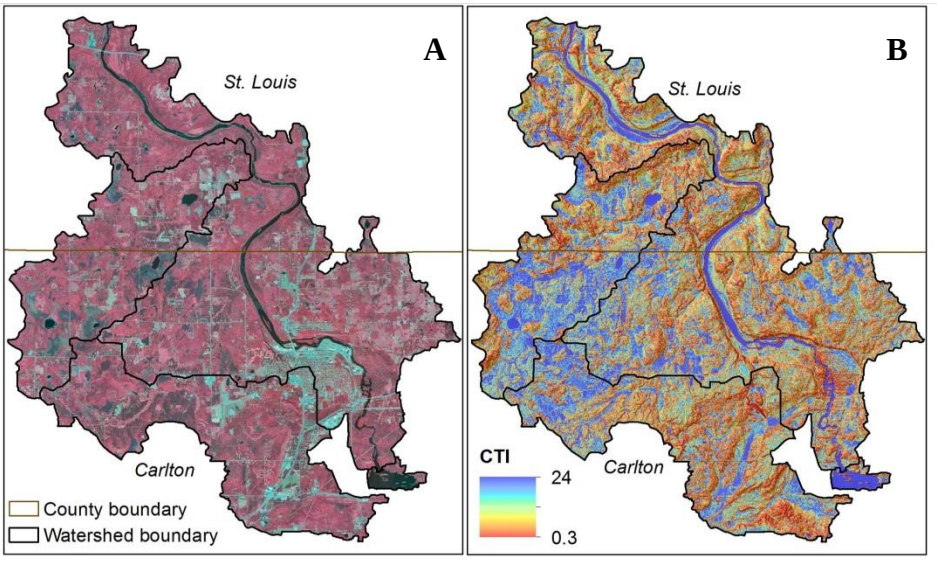

Figure 2-7 **(A)** CIR aerial imagery 2009 map, and **(B)** MD-∞ CTI map for the Northern Lakes and Forest study area

Discussion

We compared and evaluated seven CTI based algorithms derived from lidar DEMs for identifying wetlands across three different ecoregions in Minnesota. The computation of the CTI offered a practical and fast method to identify wetlands greater than 0.20 ha. All CTI based maps showed a relatively high overall percentage of agreement with the reference data for wetland and upland classes (69-92%). Results of this study demonstrate that lidar derived CTIs can significantly improve the accuracy of wetlands classification compared to the NWI across different ecoregions in Minnesota.

Although a direct comparison of the NWI and our CTI results may be not fair because of the differences in data types and techniques used to create these two wetland maps; the CTI-based approach developed here provides an alternative efficient and accurate method to update wetland maps. Available updated wetland maps would be valuable for many governmental and non-governmental entities that currently only used NWI maps as a tool and resource to monitor and take decisions regarding wetlands.

Our results showed the importance of choosing the correct flow direction algorithm for identifying wetlands location visually and quantitatively. Visual comparison of the seven CTI algorithms in the three study areas revealed noticeable

differences that are partially seen in the quantitative accuracy assessment analysis for some algorithms.

We speculate that the quantitative accuracy assessment analysis did not show strong differences for all the algorithms because of the type of reference data used to assess these algorithms (points) instead of polygon reference data types. For example, the D8 SFD algorithm exhibits similar quantitative accuracy results compared to three of the MFD algorithms (D-∞, MD-∞, Mass Flux) in the three study areas; nevertheless, the qualitative visual analysis exposes major difference related to unrealistic parallel flow patterns of the SFD algorithms (D8 and Rho8) for differentiating wetlands from uplands.

Similarities and differences between the two groups of algorithms are also highlighted in the way each of these algorithms tends to distribute the flow and accumulation of water in wetlands and uplands across the three study areas.

The Northern Glaciated Plains study area exhibited similarities in the way the majority of the CTI based algorithms represented water flow and accumulation for wetland mapping. For example, the D8, D-∞, and Mass Flux CTIs showed parallel flow patterns and similarly high accuracy assessment results. Low topography relief and presence of more concave hillslopes in this study area were the two main factors that favored greater flow convergence for the majority of wetlands located in this study area.

These two factors may explain the similarities in performance of the majority of flow direction algorithms in this area. Additionally, this study area had the highest overall accuracy, user's and producer's accuracy results compared to the other two study areas.

High accuracy results can be explained primarily because of the type of wetlands found in this study area, known as prairie pothole wetlands or depressional wetlands (LaBaugh et al., 1998). The majority of flow accumulation that contributes to the hydrology of these wetlands tends to occurs in these topographic depressions that can be identified efficiently using high resolution elevation data. As a result, the CTI method tested in this study is an efficient mapping technique to identify these wetlands because of the topographic nature of this index.

For the Central Hardwood Forest study area marked visual differences between the SFD and MFD algorithms were displayed in this study. For example, parallel flow patterns were very evident on the D8, Rho8 and DEMON CTIs. The Rho8 showed the lowest accuracy assessment results for classifying wetlands and uplands.

This study area had the second relatively high overall accuracy, user's and producer's accuracy results compared to the other two study areas. Visually and statistically the best algorithms for mapping wetlands in this area were the D-∞ and MD-∞ CTIs. Marked differences between algorithms in this study area can be attributed to the presence of medium to high topography relief and more convex hillslopes near or in the type of existing wetlands in this area.

The majority of existing wetlands include open water, shallow and deep marshes, and unconsolidated bottom (Knight et al., 2013). Thus, CTIs based on MFD algorithms were more suitable than SFD algorithm for this area to represent realistic patterns of wetlands areas and greater flow of divergence distribution of water.

The Northern Lakes and Forest study area study area had the lowest overall accuracy, user's accuracy, and producer's accuracy results for all the CTIs maps compared to the other two study areas. This can be explained because of the wetlands types located in this area which includes calcareous fens, sedge meadows, hardwood wetlands, coniferous swamps, and coniferous bogs. The majority of these existing wetlands in this area are groundwater-fed wetlands, and generally high in the landscape.

For example, fens wetlands are groundwater discharge wetlands that occur along topographic or geologic breaks or where groundwater aquifers are exposed near the surface. Thus, these types of wetlands are less sensitive to topography influence and inundation events as they are located at an elevation above floodplain.

Nevertheless, out of all the CTI's based algorithms, the MFD algorithms performed better at visually separating uplands from wetlands. The D-∞, MD-∞, and Mass Flux CTIs had the highest accuracy results for separating wetlands from uplands.

The three MFD algorithms mentioned above allowed for a more divergent and smoother distribution of water in very pronounced convex-steep hillslopes near or close to these wetlands.

Lang et al., (2013) reinforces our results regarding the accuracy and preferences for MFD over SFD algorithms for identifying wetland locations. The Lang et al., (2013) results indicate that the FD8 CTI multiple flow direction algorithm derived from lidar data performed better than other non-distributed flow direction algorithms including the D8 for identifying locations of forested wetlands in the Coastal Plain of Maryland.

Our significance Z-test results for the three study areas confirmed the significant differences between the SFD algorithms and MFD, particularly for the Rho8 CTI, across the three study areas. CTI based algorithms (D8, D-∞, MD-∞, Mass Flux D, and FD8) wetland/upland classification maps in general were significant improvements over the NWI map for two of our study areas. However, for the Central Hardwood Forest study area, the CTI based algorithms (D8, D-∞, MD-∞, and Mass Flux D) outperformed only the NWI. NWI results in this area had high errors of omission because of rapid urban development over the past six years.

This calls into question the accuracy of the outdated NWI maps, but many of these maps are still used by governmental and non-governmental policymakers for wetland management and policy development.

Conclusions

Lidar derived CTIs enable a fast, efficient, and more accurate method to estimate current wetland location compared to NWI maps. Our results provide evidence that different wetland types in varied ecoregions can be identified accurately using lidar derived terrain indices. In general, the seven CTI based algorithms were able to predict wetland locations across different ecoregions. However, there were statistically and visually significant differences in their performance.

Our visual comparison results revealed that CTIs based on MFD algorithms are better than CTIs based on SFD algorithms for separating wetlands from uplands. Based on our results, we suggest the use of the following algorithms: D-∞, MD-∞ or Mass Flux in the application of the CTI for mapping wetlands in areas similar to the ones evaluated

in this study. The MFD algorithms represented the distribution and accumulation of water (wetness) in wetlands in a more visually accurate form compared to SFD algorithms.

Further research is encouraged to investigate the use of the CTI combined with other ancillary data such as optical data for mapping wetlands. Particularly, for wetlands types located an elevation above floodplain where elevation information alone is not influential as it is for depressional wetlands.

Finally, the use of NWI maps continues across different parts of the country because these maps are the most accessible information available. Many of these NWI maps need to be updated. Remote sensing techniques including those based on the CTI offer a fast, cost-effective and reliable method to quickly identify wetland location and update such maps.

Acknowledgements

This research was funded by the Minnesota Environment and Natural Resources Trust (ENRTF), the Minnesota Department of Natural Resources (MNDNR), and the United States Fish and Wildlife Services (USFWS: Award 30181AJ194).

References

Anteau M.J., Afton A.D., 2009. Wetland Use and feeding by lesser Scaup during spring migration across the upper midwest, USA. Wetlands 29,704-712.

Antonarakis A.S., Richards K.S., Brasington J., 2008. Object-based land cover classification using airborne Lidar. Remote Sensing of Environment. 2988-2998

Barling R.D., Moore I.D., Grayson R.B., 1994.A quasi-dynamic wetness index for characterizing the spatial distribution of zones of surface saturation and soil water content. Water Resources Research. 30, 1029-1044.

Bauer J., Rohdenburg H., Bork H.R., 1985. Ein Digitales Reliefmodell als Vorraussetzung fuer ein deterministisches Modell der Wasser- und Stoff-Fluesse. In: Bork, H.R. & Rohdenburg H(eds) Parameteraufbereitung fuer deterministische Gebiets-Wassermodelle, Grundlagenarbeiten zu Analyse von Agrar-Oekosystemen. Technische University Braunschweig. 1-15.

Bridgham S.D., Pastor J., Dewey B., Weltzin J.F., Updegraff K., 2008. Rapid Carbon Response of Peatlands to Climate Change. Ecology. 89, 3041-3048.

Beven K.J, Kirkby M.J., 1979. A physically based, variable contributing area model of basin hydrology. Hydrological Sciences journal. 24, 43-69.

City of Chanhassen Surface Water Management Plan (2006) In: The Second Generation Surface Water Management Plan - Chanhassen, Minnesota: http://www.ci.chanhassen.mn.us/serv/cip/swmp/wetlandsmanagement.htm. Accessed 25 May 2013.

Congalton R.G., Green K., 2009. Assessing the accuracy of remotely sensed data: principles and practices, 2nd edn. Boca Raton, Florida: CRC Press/Taylor and Francis.

Corcoran J.M., Knight J.F., Brisco B., Kaya S., Cull A., Murnaghan K., 2011. The integration of optical, topographic, and radar data for wetland mapping in northern Minnesota. Canadian Journal of Remote Sensing. 37, 564-582.

Costa-Cabral M., Burges S.J., 1994. Digital elevation model networks (DEMON): a model of flow over hillslopes for computation of contributing and dispersal areas. Water Resources Research. 30,1681-1692.

Chaplot V., Walter C., 2003. Subsurface topography to enhance the prediction of the spatial distribution of soil wetness. Hydrological processes. 2567-2580.

Charman D.J., 2009. Peat and Peatlands. Elsevier Inc. 541-548.

Dahl T.E., Johnson C.E., 1991. Status and trends of wetlands in the conterminous United States, mid-1970's to mid-1980's. U.S. Fish and Wildlife Service, Washington, DC. 28.

Dahl T.E., 2006. Status and trends of wetlands in the conterminous United States 1998 to 2004, U.S. Department of the Interior; Fish and Wildlife Service, Washington, D.C. 112.

Erskine R.H., Green T.R., Ramirez J.A., MacDonald L.H., 2006. Comparison of grid-based algorithms for computing upslope contributing area. Water Resources Research. 42, W09416.

Fairfield J., Leymarie P., 1991. Drainage networks from grid digital elevation models. Water Resources Research. 27,709-717.

Guntner A., Seibert J., Uhlenbrook S., 2004. Modeling spatial patterns of saturated areas: An evaluation of different terrain indices. Water Resources Research. 40,W05114.

Grabs T., Seibert J., Bishop K., Laudon H., 2009. Modeling spatial patterns of saturated areas: A comparison of the topographic wetness index and a dynamic distributed model. Journal of Hydrology. 373,15-23.

Gruber S., Peckham S., 2008. Land-surface parameters and objects in hydrology. In: Hengl T, Reuter HI (eds) Geomorphometry: concepts, software, applications, Elsevier, Amsterdam, Netherlands. 171-194.

Jenkins R.B., Frazier P.S., 2010. High-Resolution Remote Sensing of Upland Swamp Boundaries and Vegetation for Baseline Mapping and Monitoring. Wetlands. 30, 531-540.

Knight J.F., Tolcser B.T., Corcoran J.M., Rampi L.P., 2013. The effects of data selection and thematic detail on the accuracy of high spatial resolution wetland classifications, Photogrammetric Engineering and Remote Sensing. 79, 613-623.

LaBaugh J.W., Winter, T. C., Rosenberry, D. O.,1998. Hydrologic Functions of Prairie Wetlands. Great Plains Research: A Journal of Natural and Social Sciences.17-37.

Land Management Information Center (LMIC)., 2007. Metadata for the National Wetlands Inventory, Minnesota.

Lang M.W., McCarty G.W., 2009. Lidar intensity for improved detection of inundation below the forest canopy. Wetlands. 29,1166–1178.

Lang M.W., McDonough O., McCarty G.W., Oesterling R., Wilen B., 2012. Enhanced Detection of Wetland-Stream ConnectivityUsing LiDAR. Wetlands 32:461-473

Lang M.W., McCarty G.W., Oesterling R., Yeo I., 2013. Topographic Metrics for Improved Mapping of Forested Wetlands. Wetlands. 33, 141-155.

Lea N.L., 1992. An aspect driven kinematic routing algorithm. In: Parsons AJ, Abrahams AD, (eds) Overland flow: hydraulics and erosion mechanics, Chapman & Hall, New York. 393–407.

Minnesota Department of Administration (AdminMN) Office of geographic and demographic analysis state demographic center, 2010 census: Minnesota city profiles. http://www.demography.state.mn.us/CityProfiles2010/index.html. Accessed May 20, 2013

Midwest Community Planning LLC (2012) Big Stone County Water Plan. URL: http://www.bigstonecounty.org/environmental/waterplanning/BigStoneCountyWaterPlan.pdf. Accessed April 05, 2013

Mitsch W. J., Gosselink J. G., 2000. Wetlands (Third ed.). New York: Wiley.938

Moore I.D., Gessler P.E., Nielsen G.A., Peterson G.A., 1993. Soil attribute prediction using terrain analysis. Soil Science Society of America Journal. 57, 443-452.

O'Callaghan J.F., Mark D.M.m 1984. The extraction of drainage networks from digital elevation data. Computer Vision, Graphic and Image Processing. 28, 328-344.

Pan F., Peters- Lidar C.D., Sale M.J., King A.W., 2004. A comparison of geographical information system-based algorithms for computing the TOPMODEL topographic index. Water Resources Research. 40,1–11.

Quinn P., Beven K., Chevallier P., Planchon O., 1991. The prediction of hillslope flow paths for distributed hydrological modeling using digital terrain models. Hydrological Processes. 5,59–80.

Seibert J, McGlynn B., 2007. A new triangular multiple flow direction algorithm for computing upslope areas from gridded digital elevation models. Water Resources Research. 43,1-8.

Sørensen R., Seibert J., 2007. Effects of DEM resolution on the calculation of topographical indices: TWI and its components. Journal of Hydrology. 79–89.

Stedman S., Dahl T.E., 2008.Status and trends of wetlands in the coastal watersheds of the Eastern United States 1998 - 2004. National Oceanic and Atmospheric Administration, National Marine Fisheries Service and U.S. Department of the Interior, Fish and Wildlife Service, 32 pages

Schmidt F., Persson A., 2003. Comparison of DEM data capture and topographic wetness indices. Precision Agriculture. 4,179-192.

Shoutis L., Dunca T.P., McGlyn B., 2010. Terrain-based predictive Modeling of Riparian Vegetation in Northern Rocky Mountain Watershed. Wetlands. 30,621-633.

Tarboton D.G., 1997. A new method for the determination of flow directions and upslope areas in grid digital elevation models. Water Resources Research. 33,309-319.

Töyrä J., Pietroniro A ., 2005. Towards operational monitoring of a northern wetland using geomatics-based techniques. Remote Sensing of Environment. 174-191.

Wilson J.P., Gallant J.C., 2000. Secondary topographic attributes. In Wilson JP, Gallant JC (ed) Terrain analysis: Principles and applications, Wiley, New York. 87-131.

Wilson J.P., Aggett G., Deng Y.X., Lam C.S. 2008. Water in the landscape: a review of contemporary flow routing algorithms. In: Zhou Q, Lees B, Tang G (eds) Advances in digital terrain analysis, Springer, Berlin. 213–236.

Winter T. C., Rosenberry D. O. 1995. The interaction of ground water with prairie pothole wetlands in the Cottonwood Lake Area, eastcentral North Dakota, 1979-1990. Wetlands. 193-211.

Yang X., Chapman G.A., Young M.A., Gray J.M., 2005. Using compound topographic index to delineate soil landscape facets from digital elevation models for

comprehensive coastal assessment. In: Zerger A, Argent RM (eds) International Congress on Modeling and Simulation. Modeling and Simulation Society of Australia and New Zealand, ISBN: 0-9758400-2-9, pp 1511–1517 http://www.mssanz.org.au/modsim05/papers/yang_x.pdf

Zhou Q., Liu X., 2002. Error assessment of grid-based flow routing algorithms used in hydrological models. International Journal of Geographical Information Science. 16, 819–8.

Chapter 3: Wetland mapping in the Upper Midwest United States: An object-based approach integrating lidar and imagery data*

This study investigated the effectiveness of using high resolution data to map existing wetlands in three ecoregions in Minnesota. High resolution data included multispectral leaf-off aerial imagery and lidar elevation data. These data were integrated using an Object-Based Image Analysis (OBIA) approach. Results for each study area were compared against field and image interpreted reference data using error matrices, accuracy estimates, and the kappa statistic. Producer's and user's accuracies were in the range of 92-96% and 91-96% respectively and overall accuracies ranged from 96-98% for wetlands larger than 0.20 ha (0.5 acres). The results of this study may allow for increased accuracy of mapping wetlands efforts over traditional remote sensing methods.

* Paper in press: Rampi, L.P., Knight, J. Wetland mapping in the Upper Midwest United States: An object-based approach integrating lidar and imagery data, Photogrammetric Engineering and Remote Sensing, 2013

Introduction

Wetlands are naturally dynamic systems of important value to the environment and society. The U.S. Army Corps of Engineers (USACE) in cooperation with the U.S. Environmental Protection Agency (EPA) have defined wetlands, incorporating technical and policy considerations, as "…those areas that are inundated or saturated by surface or ground water at a frequency and duration to support and under normal circumstances do support, a prevalence of vegetation typically adapted for life in saturated soil conditions" (Federal Register, 1982; 1980).

Wetlands can reduce some of the negative effects of flooding and recharge groundwater by gradually releasing flood water and snow melt (Mitsch and Gosselink, 2000). Wetlands offer habitat that supports wildlife and fishing activities. Wetlands also provide ecosystem services, including educational, aesthetic, and economic opportunities. For example, intact freshwater marshes in Canada have a total economic value of approximately $5,800 per hectare compared to $2,400 when those lands are drained and used for agriculture (Millennium Ecosystem Assessment, 2005; Turner *et al*., 2000).

Due to wetland loss and degradation many of the preceding benefits have been reduced and are increasingly impacted. About 215 million acres of wetlands existed in the United States at the time of European settlement. However, by the mid-1970's, only 99 million acres of the original wetlands remained. Many of the lost wetlands were drained and are currently used for agriculture, resource extraction, urbanization, and other commercial purposes (Dahl and Johnson, 1991; Frayer *et al*., 1983; Stedman and Dahl, 2008).

Minnesota is not an exception to this large national wetland loss. Nearly half of Minnesota's original wetlands were lost due to extensive agricultural drainage and urban development. According to the Minnesota Pollution Control Agency (MPCA) (2006), many original natural wetlands were changed into local storm-water ponds to make additional land available for urban development.

Currently in Minnesota only a few cities have updated wetland inventories. For the rest of Minnesota the only wetland inventory available is the National Wetlands Inventory (NWI).

The Minnesota NWI maps were completed in the late 1980's using aerial photos (some black and white) collected between 1979 and 1988 (LMIC, 2007). Several 7.5 quadrangles in northwestern Minnesota and a much larger area in northeastern Minnesota were mapped based on 1970's 1:80,000 scale black-and-white photos (MPCA, 2006). Changes in the landscape have occurred which limit the use of the NWI maps due to the outdated data and techniques used to create them. Thus, there is a need to update wetland inventories with accurate boundaries and improved delineation of smaller wetlands. An updated wetland inventory would provide information that could be used to make accurate decisions for the conservation, protection and restoration of wetlands. Though a Minnesota statewide update is underway, it is a heavily image interpretation-based project that is not expected to be completed until 2020. Thus, more automated techniques may be useful in the near term.

A fast and effective method to identify accurate wetland boundaries involves the use of remote sensing data and techniques (Butera, 1983; Corcoran et al., 2011; Knight et al., 2013). To the present time, the majority of wetland mapping efforts using remote sensing data and techniques has been focused on evaluating traditional pixel-methods with medium to coarse resolution data.

In many cases, the use of remote sensing for wetland mapping has resulted in low accuracy estimates, often due to mixed pixels and insufficient spectral resolution (Grenier et al., 2007; Fournier et al., 2007; Lunetta and Balogh, 1999; Ozesmi and Bauer, 2002). Integration of high resolution optical and elevation data has been shown to reduce the mixed pixel problem (Frohn et al., 2009; Maxa and Bolstad, 2009).

Some studies have integrated optical and elevation data to map wetlands using traditional pixel-based methods. However, their accuracy results were low for wetland classification due to the use of low to medium spatial resolution data and pixel-based techniques (Baker et al., 2006; Ozesmi and Bauer, 2002).

An object-based approach may be a better option to integrate high resolution data and overcome some limitations, including the mixed pixel problem and salt-and-pepper effect of traditional pixel-based techniques (Myint et al., 2011; Zhou and Troy, 2008). Object Based Image Analysis (OBIA) segmentation and classification techniques have been considered as an alternative to pixel-based methods since the late 1990's because of their ability to include contextual information, human knowledge, and experience to interpret the objects of interest (Baatz et al., 2008; Blaschke, 2003; Blaschke, 2010).

The foundation of the OBIA approach is an initial image segmentation that uses pixel-based features to create statistically homogeneous image objects (Benz et al., 2004; Fournier et al., 2007). These homogenous objects, also called geo-objects or segments, can be classified into land-cover classes using attributes of the objects such as spectral, textural, contextual and shape characteristics (Burnett and Blaschke, 2003; Bruzzone and Carlin 2006; Hay and Castilla, 2008). The OBIA approach can be used to generate vector polygons from the classification and directly incorporate them into a geographic information system (GIS) (Castilla, et al., 2008; O'Neil-Dunne et al., 2012).

The aim of this research was to investigate the effectiveness of using high resolution leaf-off aerial imagery and lidar data to map wetlands in three different ecoregion study areas in Minnesota.

Study Area and Data

Study Area Description

Due to the complexity and variety of wetlands in Minnesota, we selected three study areas to evaluate the OBIA approach to map wetlands. The first study area was the Minnesota River Headwaters watershed located in the Northern Glaciated Plains ecoregion and within Big Stone, Traverse, and Stevens counties (Figure 3-1). This watershed is 717 km² in size and the main land use is agriculture.

A large portion of the watershed is characterized by a rolling prairie of till plain, clay loam soils and a combination of poorly and well drained soils (Minnesota Department of Natural Resources, 2006). The average precipitation is 640 mm/year and

360 mm during the growing season (May to September). Many shallow lakes and wetlands are common features of the landscape in this watershed. These lakes and wetlands are perfect settings to support and nurture wildlife habitat and viewing opportunities for a variety of bird and duck species (Midwest Community Planning LLC, 2012).

The second study area was the Swan Lake watershed located in the Western Corn Belt Plains ecoregion and within Nicollet County (Figure 3-1). It has an area of 204 km² and the main land use is agriculture. A large portion of the watershed consists of glacial till plain with level to gently rolling prairie uplands.

This area is characterized by clay loam soils and fertile deep soils with a high level of organic matter (Minnesota Department of Natural Resources, 2006). The average precipitation is 740 mm/year and 460 mm during the growing season (May to September). This watershed has one of the biggest prairie pothole marshes in the United States, providing habitat for different species, storm water retention and education opportunities (Nicollet County, 2008).

The third study area is the Thompson Reservoir St. Louis River watershed located in the Northern Lakes and Forest, between St. Louis and Carlton counties (Figure 3-1). It is 53 km² in size and the main land use is forested land. A large portion of the watershed is characterized by drumlins covered with forest, poorly drained wetland depressions, and fine sandy loam soils. The average precipitation is 710 mm/year and 440 mm during the growing season (May to September).

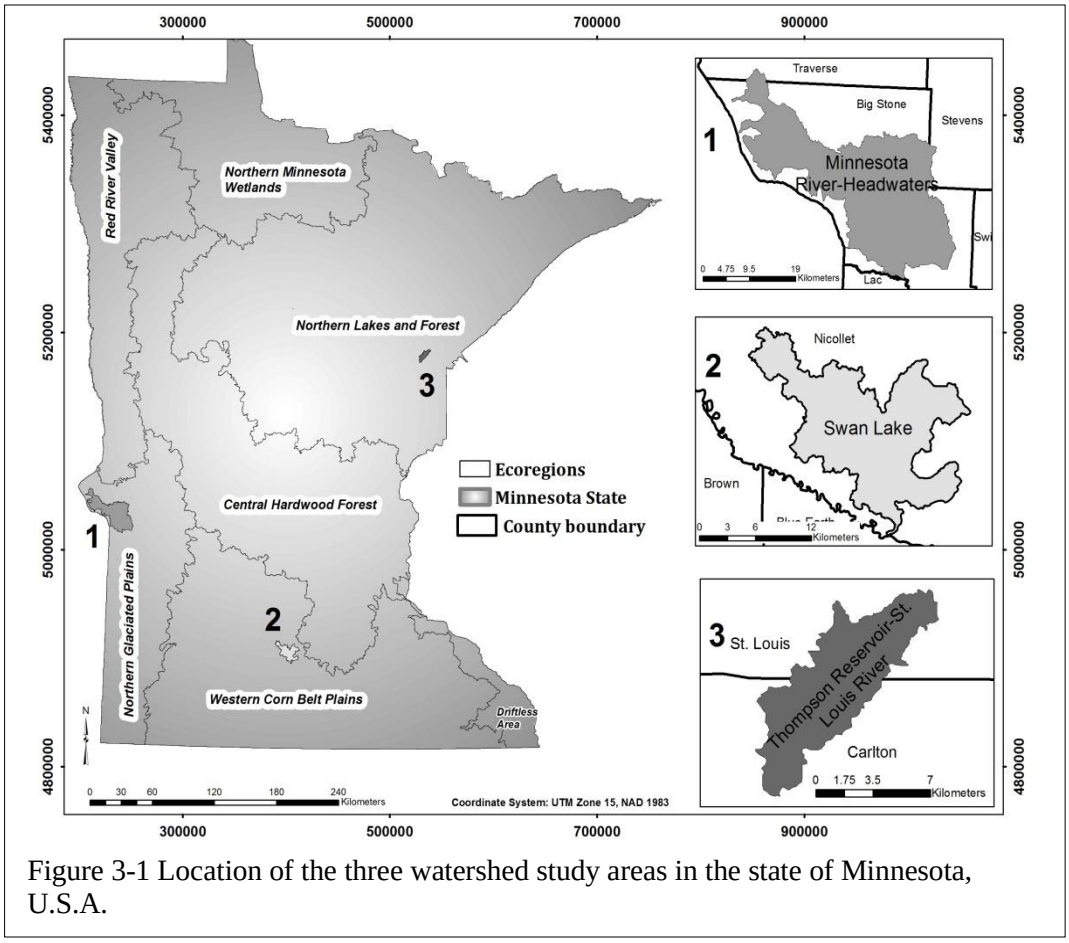

Figure 3-1 Location of the three watershed study areas in the state of Minnesota, U.S.A.

Data acquisition

We used two data sources to investigate the effectiveness of integrating multiple datasets to map wetlands in the three study areas. These sources included lidar data and orthorectified digital aerial photography (0.5 m). The half-meter orthorectified imagery used for Swan Lake and the Minnesota River Headwaters was collected by Surdex Corporation between 12 April 2011 and 16 May 2011.

This imagery was provided by the vendor to the Minnesota Department of Natural Resources (MDNR) as a radiometric/orthorectified ready product. The Minnesota Department of Transportation (MnDOT) separately tested the horizontal positional accuracy of this imagery and obtained a root mean square error (RMSE) of 0.819 m with an NSSDA of 1.418 m (95% confidence level).

This imagery was acquired with an Intergraph DCM (digital mapping camera) from an altitude of about 3000 m, capturing four multispectral bands (red, green, blue and near infrared). The half-meter orthorectified imagery used for the Thompson Reservoir St. Louis River watershed was collected by Keystone Aerial Surveys Inc. in May 2009. This imagery was provided by the vendor to the DNR as a radiometric/orthorectified ready product. The DNR separately tested the horizontal positional accuracy of this imagery and obtained an RMSE of 2 m with an NSSDA of 3.5 m (95% confidence level).

This imagery was acquired with a Vexcel UltraCamX camera from an altitude of about 7300 m, capturing four multispectral bands (red, green, blue and near infrared).

The lidar data (point cloud data, lidar DEM and lidar hybrid intensity) used for the Minnesota River Headwaters study area was obtained through the International Water Institute (IWI) lidar download portal.

The lidar data for the Minnesota River Headwaters was collected in the spring of 2010 during leaf-off conditions by Fugro Horizons Inc. The data were collected with a Leica sensor ALS50-II MPiA (Multiple Pulses in Air), at an altitude of 2400 m above mean terrain (AMT), and with an average post spacing of 1.35m. The horizontal accuracy for these data was of +/- 1 m (95% confidence level), and a vertical accuracy RMSE of 15.0 cm. For this study area, we used the 1 m DEM and hybrid intensity images provided by the IWI. The DEM was produced by interpolating the bare earth LAS files delivered by the vendor using the 'Raster to ASCII' command in ArcGIS 10.1.

The hybrid intensity layers were created from lidar intensity and raw lidar/hillshade by the vendor. Hybrid intensity images were created by interpolating the infrared reflectance value attributed for each point. The lidar data (point cloud data, lidar DEM and lidar intensity) used for Swan Lake and Thompson Reservoir St. Louis River watershed were acquired from the Minnesota Geospatial Information Office (MnGeo) FTP site.

The lidar data for the Swan Lake study area were collected between 26 April and 28 April 2010 by AeroMetric, Inc. The data were collected using a multiple fixed wing aircraft lidar system at an altitude of 1700 m AMT, and an average post spacing of 1.3 m.

The horizontal accuracy for these data was of +/- 0.3 m (95% confidence level), and a vertical accuracy RMSE of 10.0 cm.

The lidar data collected for the Thompson Reservoir St. Louis River study area were collected between 3 May and 5 May, 2011 by Woolpert Inc. The data were collected at an altitude of about 2400 AMT with an average post spacing of 1.5 m. The horizontal accuracy for these data was +/- 1.2 m (95% confidence level), and vertical accuracy RMSE was 5 cm. In this study we used the 1 m DEM provided by the Minnesota DNR, which produced the DEM by extracting bare earth points from the point cloud data. The DEM was also hydro flattened using the edge of the water breaklines.

Methods

We mapped wetlands by using an OBIA approach through the creation of rulesets for each study area. We used the Cognition Network Language (CNL) within the software package Definiens eCognition Developer version 8.8.0 to develop the three rulesets. The eCognition Server 64-bit package was used to execute in a batch mode all the tile stacks for each study area.

The first subsection of the methods used in this study describes the data preparation performed for each study area. The next subsection explains the design of the ruleset created for each study area. Finally, the last subsection addresses the accuracy assessment procedures used to evaluate results in each study area.

Data preparation

Before the creation of the three ruleset, we performed four data preparation steps needed prior to develop the OBIA approach. First, we generated several raster layers from the lidar point cloud data and DEM. The raster layers included: a digital surface model (DSM), a lidar intensity layer, the compound topographic index (CTI). These raster layers were chosen because of their topographic information, which is useful to differentiate wetland from other cover classes.

We used Quick Terrain (QT) Modeler version 7.1.6 to generate the 3 m DSM raster layer using the point cloud data for each study area. The natural-neighbor

interpolation algorithm method, the maximum Z value of the first return for all the classes were used to create the DSM l ayer. We exported the DSM into a raster geoTIFF file with 3 m spatial resolution.

The lidar intensity images for Swan Lake and the Thompson Reservoir St. Louis River study areas were also generated in QT Modeler with the grid statistic tool, using the mean intensity values of all the lidar returns. We exported the intensity grid layer into a raster geoTIFF file with 3 m spatial resolution. The lidar intensity image for the Minnesota River Headwaters study area was obtained directly from the IWI download website.

The CTI layers for each study area were created using the DEM layer for each study area. We used the following formula to compute the CTI given by Beven and Kirkby (1979) study: $CTI = \ln [(\alpha)/ (\tan (\beta)]$. In this equation α represents the local upslope area draining through each cell and β represents the local slope gradient.

The CTI represents the potential distribution of the water movement and water accumulation across the landscape (Moore *et al*., 1991). The CTI is used to identify parts of the landscape where sufficient wetness could allow for the formation of wetlands (Rodhe and Seibert, 1999).

Figure 3-2 shows a map of the Minnesota River-Headwaters study area representing CTI values, where higher CTI values represent water accumulation (potential wetland formation) and lower CTI values represent dryness or steep places where water would not likely accumulate based on topography. The choice of the flow direction algorithm used to calculate α (local upslope area) can affect the accuracy of the CTI.

For example, single flow direction algorithms allow flow to pass only to one neighboring downslope cell while multiple flow direction algorithms allow water to flow into multiple neighboring cells. This multidirectional flow effect creates more realistic water flow patterns in different topographic settings, including convex and concave hillslopes (Erskine et al., 2006; Gruber and Peckham, 2008; Wilson et al., 2008).

Thus, in this study we used the triangular multiple flow direction algorithm proposed by Seibert and McGlynn (2007) to compute the local upslope area. We used the Whitebox open-source software version 1.0.7 to calculate the contributing area (local upslope area) and local slope layers needed for the CTI. The slope layer was modified by adding a minimum value of 0.0001 to avoid division by zero for CTI calculations. It is important to clarify that the DEM for the Swan Lake and Thompson Reservoir St. Louis River areas was obtained directly as a raster layer, already mosaicked, from the MnGeo FTP site. However, for the Minnesota River Headwaters areas we had to mosaic each

DEM and hybrid intensity tile contained within this area. Mosaicking was necessary because these data were provided by the IWI in raster tiles of 2000 by 2000 m. We used ERDAS image 2011 to mosaic and exported the DEM and intensity layers as geoTIFF files. We also exported the DEM for the Swan Lakes and the Thompson Reservoir St. Louis River study areas to geoTIFF format. Second, after calculating all the lidar layers, we used the MosaicPro tool from the ERDAS Image 2011 software to mosaic the orthorectified aerial imagery for each study area.

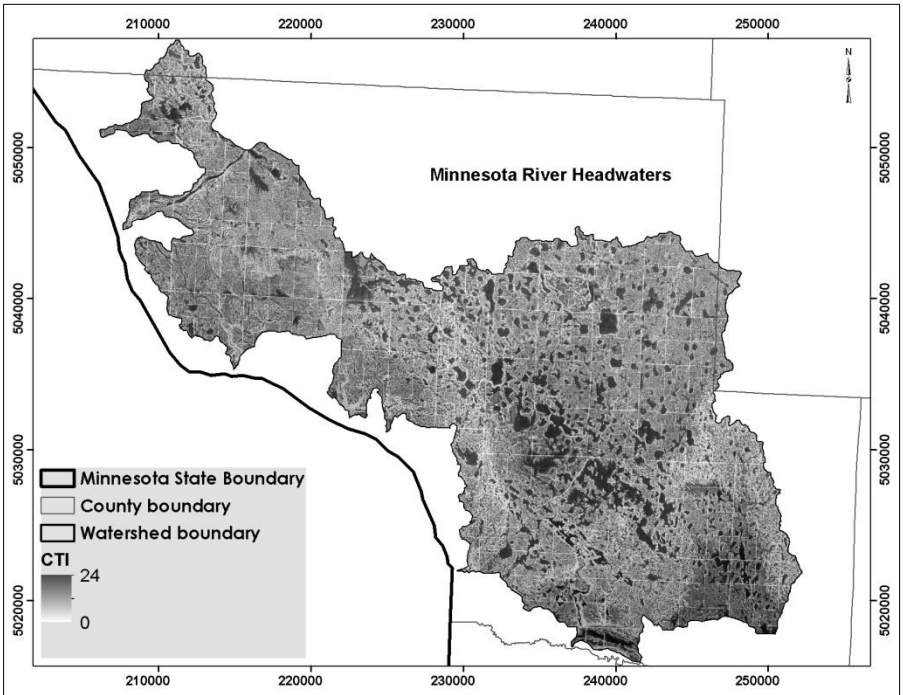

Figure 3-2 CTI index for Minnesota River-Headwaters study area.

Third, once all the previous lidar and imagery layers were prepared, we used a watershed boundary shapefile layer for each study area to subset all the raster layers in ERDAS Image version 2011. The watershed boundaries were obtained from the Minnesota Department of Natural Resources (DNR). Finally, we produced a tile generation for each study area. The tile generation was carried out in ERDAS Image version 2011, using the Dice tool with the following parameters: tile size of 3000 m x 3000 m and an overlap of 300 m between adjacent tiles on all four sides. Each study area had a tile stack of four lidar product layers (DEM, DSM, CTI, and Intensity) and four spectral bands (NIR, R, G, B) of imagery layers (Figure 3-3). The following tile stacks were created: 224 for the Minnesota River Headwaters, 49 for Swan Lake and 20 for the Thompson Reservoir St. Louis River

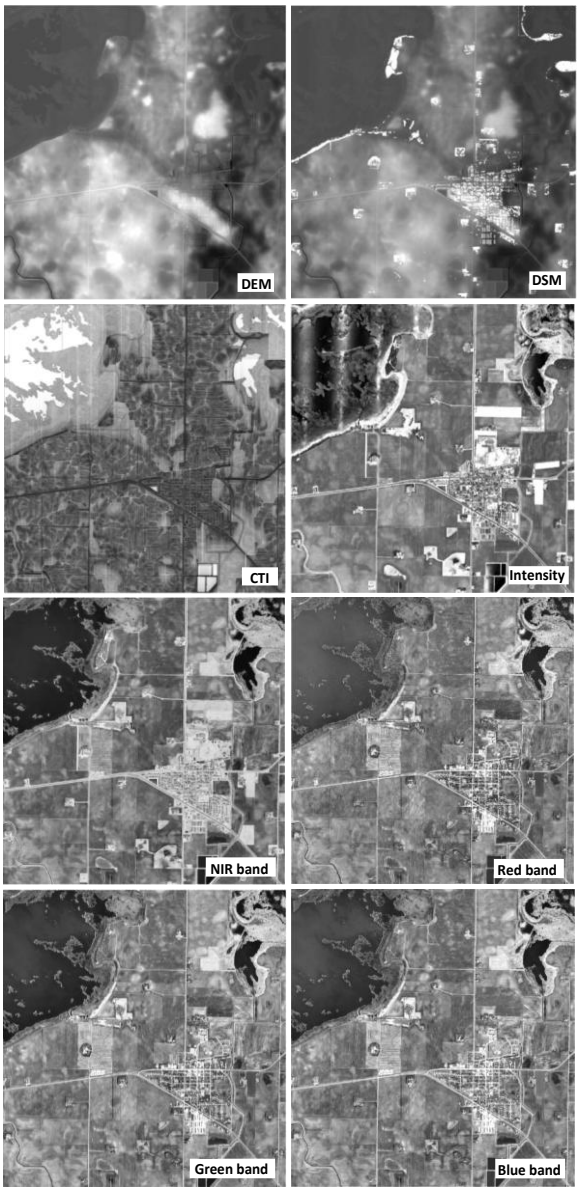

Figure 3-3 Tile stack of the dataset used for the OBIA approach.

Ruleset Creation and Classification

Before the creation of rulesets for each study area, we developed a customized import routine in eCognition developer software to import all the tile stacks of layers for each study area. Each ruleset was developed through a trial and error process using small subset areas (500 x 500 pixels). We used a *divide and conquer* approach (Quinlan, 1990; O'Neil-Dunne, et al., 2012), which is a multiscale iterative method where objects vary in size, shape, and spectral attributes. While the two major steps performed in the ruleset development were the creation of objects and the classification of those objects, further steps were required for the classification of each object to be assigned to the class of interest (wetland class vs. non-wetland class). Each ruleset consisted of four main components: 1) image processing, 2) segmentation and classification, 3) export operation, and 4) cleanup operation.

In the image processing phase, we carried out the following tasks: calculation of the normalized Digital Surface Model (nDSM) = DSM-DEM, and application of a median filter to the nDSM and intensity layers, and computation of the Green Ratio Vegetation Index (GRVI) using the eCognition developer software tools for object features. The GRVI was computed using the NIR and green bands of the aerial imagery as the ratio of the NIR divided by the green band (Sripada et al., 2006).

This index was chosen for two reasons: first, it is known that vegetation indices such as the Normalized Difference Vegetation Index (NDVI) can be useful for discriminating wetlands from other upland classes (Hodgson et al., 1987, Wright and Gallant, 2007). Second, after testing several vegetation indices including the NDVI, the Green Normalized Difference Vegetation Index (GNDVI), the Difference Vegetation Index (DVI), and the GRVI to determine which index would be more helpful in differentiating wetland features from non-wetland features. Our unpublished results indicated that the GRVI was more accurate than the other indices to differentiate and exclude areas that were topographically suitable for wetlands but contain impervious cover (non-vegetated). GRVI index was assessed using traditional accuracy assessment methods, including error matrices, overall accuracy, producer's accuracy, and user's accuracy.

In the segmentation and classification phase, we performed the following tasks: we created preliminary objects using the multiresolution segmentation algorithm (Baatz and Schape, 2000) with the following parameter values: scale 30, shape 0.3, and compactness 0.5. A weight value of 1 was given to the three visible optical bands and a weight value of 2 to the NIR band. The scale value of 30 was chosen because we wanted medium size preliminary objects. The shape value of 0.3 was chosen because more weight was given to the influence of color on the segmentation process. The NIR band was given a higher weight value because of its ability to spectrally separate potential non-water objects from water objects.

After creating the preliminary objects, the second step was to refine those objects by applying a spectral difference segmentation algorithm, based on a maximum spectral difference value. The spectral difference algorithm merges neighboring objects based on a maximum spectral difference value parameter (Definiens Imaging, 2009).

A value of 14 was chosen as the maximum spectral difference parameter for this difference segmentation. This value was chosen after visually assessing different values. The third step was to classify the preliminary objects into temporary classes, including wet vs. dry, bright vs. dark, and short vs. tall. We used the following attributes of each dataset to create the temporary classes: min, max, and mean threshold values of the CTI, nDSM, intensity, NIR band, imagery brightness, and GRVI.

The CTI, GRVI and NIR layers were specifically used to separate wet vs. dry classes with the following threshold values: NIR ≤ 45, GRVI ≤ 0.9, and CTI ≥ 10.78. These threshold parameters were determined through a series of trial-and-error efforts in combination with photo-interpretation to determine whether different "wet classes" (potential wetland classes) across the three different ecoregions were sufficiently separated from dry classes (potential non-wetland classes).

The threshold of 10.78 resulted after testing several threshold values at different DEM resolutions including 3 m lidar data. Our unpublished results indicated that the most accurate CTI threshold values to separate wetness (potential wetland) from dryness (upland) was the mean plus ½ standard deviation of the CTI range of values**.** Also, this

CTI threshold value of 10.78 agrees with the value that Galzki et al., (2008) found in their study based on field work.

The imagery brightness, intensity, and GRVI layer were used to classify bright vs. dark objects using the spectral difference segmentation algorithm with a maximum spectral difference parameter of 12. The NDSM layer was used to separate short vs. tall objects using the contrast split segmentation algorithm with the following parameters: a minimum threshold value of 2, a max threshold value of 5, and a step size of 1. Previous parameters were determined after several trial-and-error experiments and a detailed visual assessment for separating bright vs. dark classes and short vs. tall classes.

Finally, we used contextual information from the different temporary classes to achieve the final desired classes. Final classes included wetlands, agriculture, forest, and urban classes. These classes were chosen to allow for easier discrimination between wetland boundaries and upland boundaries due to the spectral, contextual and shape differences between classes. The contextual information was based on the spatial relationships of an individual object to neighboring objects. For example, small bright objects located in the middle of agriculture fields (unlikely to be impervious surfaces) were reclassified as agriculture classes based on contextual information (neighboring relationship).

In the export operation phase, we exported the final classes into raster and vector formats. In addition, we improved the wetland polygon's appearance by applying the smoothing and generalizing tools from the advanced editing toolbar in the ArcGIS software.

Accuracy assessment

We assessed the classification results for the three study areas using a single pixel based approach based on the analysis of the error matrix (Congalton and Green, 2009). The following accuracy assessment estimators were computed in ERDAS Imagine for each study area: overall accuracies, producer's accuracy, user's accuracy, and kappa coefficient.

The classification results were evaluated using independent stratified randomly generated points for each study area. Each sample point was interpreted by a trained analyst, who gave the point a value of forest, agriculture, impervious, or wetland. The analyst used aerial photos and field data. In the summer of 2009 and 2011, a team from the Remote Sensing and Geospatial Analysis Laboratory at the University of Minnesota collected field reference data of independent randomly selected points of wetland/upland from different parts of Minnesota including the three study areas used in this study.

The field data collected contained the following information: Plant type and percent coverage, land-cover/land-use type, UTM coordinates, 5-6 photos of the area, and Cowardin wetland type (Cowardin et al., 1974). Upland types included crop fields, other agriculture, forests, grasslands, urban areas, construction areas, bare areas, and others.

We generated 289 reference data points for the Minnesota River Headwaters, 118 for Swan Lake and 117 for the Thompson Reservoir St. Louis River study areas.

Results

Results for the three study areas are summarized in Tables 3-1 through 3-5, and Figures 3-4 and 3-5. Overall accuracy results for the OBIA classification were consistently high (90-93%), throughout the three study areas, with little confusion between the four classes.

Within the classification scheme of the four classes, we obtained producer and user accuracies of 92-96% respectively for the wetland class that included wetlands larger than 0.20 ha (0.5 acres) across the three ecoregions. In addition to the OBIA accuracy assessment classification, a comparison assessment was performed to compare the

accuracy of the original NWI and the OBIA classification using only two classes (wetland/upland) for the same study areas. It is important to acknowledge that this comparison of the NWI results and our OBIA results is not a direct and fair comparison.

The temporal and methodological differences between the two datasets are significant. Thus, our main objective was to offer an alternative method (OBIA) that will allow for improvements to the accuracy of wetland classification boundaries compared to current wetland boundaries. Updated accurate boundaries of wetlands are necessary, particularly for organizations that currently use older NWI maps as a tool to monitor and regulate wetland management and conservation.

The comparison assessment was done using the kappa-based Z-statistic test described in Congalton and Green (2009). Additionally, the overall accuracy, user's accuracy and producer's accuracies for wetland and upland classes were computed for both classifications. These comparison results demonstrated that there was a statistically significant difference between the OBIA and the NWI classification at an alpha level of 0.05.

For this classification scheme of two classes, the comparison results also indicated that the OBIA wetland class always had a higher user's accuracy (92-94%) and producer's accuracy (91-96%) across the three study areas compared to the NWI user's accuracy (56-71%) and producer's accuracy (57-79%) for the wetland class.

Table 3-1 shows a full error matrix and accuracy estimates of the four classes in the Minnesota River-Headwater study area using the OBIA method. The overall accuracy was 90%, with a kappa score of 0.84 and low errors of commission and omission. The wetland class was accurately identified with producer's and user's accuracies values at 92%. Figure 3-4 (a) shows a final OBIA classification map with four classes for the Minnesota River-Headwater study area.

Table 3-2 shows a full error matrix and accuracy estimates of the four classes for the Swan Lake study area. The overall accuracy was 93% with a kappa score of 0.90, and with low errors of commission and omissions for the majority of the classes. Figure 3-4 (c) displays a final OBIA classification map with four classes for this study area. The wetland class in this study area was the least confused compared to other classes (Table

2). Overall, the most confused class pair was agriculture and urban because these classes can be relatively similar spectrally and spatially close in proximity to each other (e.g., an unpaved road bordering or in the middle of an agricultural field).

Table 3-3 shows a full error matrix and accuracy estimates of the four classes for the Thompson Reservoir St. Louis River study area. The overall accuracy was 91% with a kappa value of 0.87, and with low errors of commission and omissions for all the classes. Figure 3-4 (b) displays a final OBIA classification map with four classes for the third study area.

Table 3-4 shows accuracy estimators of the NWI classification and OBIA classification with two classes (upland vs. wetland) for the three study areas, indicating a higher overall accuracy for the OBIA classifications (97-98%) compared to the NWI classification (74-85%). In addition, the total amount (hectares) of wetlands for the Minnesota River-Headwaters area, revealed an underestimation of wetlands within the NWI classification.

This underestimation also is confirmed by the wetland omission error (43%) and low wetland producer's accuracy (57%) obtained for the NWI wetland class in this area. The total amount (hectares) of wetlands for the Swan Lake and Thompson Reservoir St. Louis River areas exposed an overestimation of the current amount of wetlands compared to the total area amount of wetlands within the NWI classification. This overestimation also is confirmed by the wetland commission error (35-44%) and low wetland user's accuracy (56-65%) estimators obtained for the NWI wetland class in these areas.

Table 3-5 shows the significance test (Z-test) comparison of the two classification methods for each study area; the results were found to be statistically different in each study area at a 95% confidence level. Figure 3-5 shows a comparison of the NWI polygons and OBIA polygons for a small portion of the Minnesota River-Headwaters area. This figure exposes significant differences between NWI and OBIA wetland boundaries, revealing greater amount of wetland omission area for the NWI classification. Although this comparison may be unfair between the NWI and our OBIA results, this comparison confirms the assumption that NWI maps are of limited utility due to their inaccuracy in wetlands vs. upland boundaries.

Table 3-1 OBIA classification error matrix for Minnesota River-Headwater study area.

		Reference Data					
		Wetlands	Agriculture	Forest	Urban	Row Total	User's Accuracy
Map data	Wetlands	**47**	4	0	0	51	92%
	Agriculture	2	**148**	1	5	156	95%
	Forest	1	10	**31**	0	42	74%
	Urban	1	5	0	**34**	40	85%
	Column Total	51	167	32	39	**289**	Overall Accuracy
	Producer's Accuracy	92%	89%	97%	87%		**90 %**

Overall Kappa Statistic: 0.84

Table 3-2 OBIA classification error matrix for Swan Lake study area.

		Reference Data					
		Wetlands	Agriculture	Forest	Urban	Row Total	User's Accuracy
Map data	Wetlands	**27**	1	0	0	28	96%
	Agriculture	1	**46**	0	0	47	98%
	Forest	0	0	**23**	0	23	100%
	Urban	0	5	1	**14**	20	70%
	Column Total	28	52	24	14	**118**	Overall Accuracy
	Producer's Accuracy	96%	88%	96%	100%		**93%**

Overall Kappa Statistic: 0.90

Table 3-3 OBIA classification error matrix for Thompson Reservoir St. Louis River study area.

		Reference Data					
		Wetlands	Agriculture	Forest	Urban	Row Total	User's Accuracy
Map data	Wetlands	**32**	0	2	0	34	94
	Agriculture	1	**20**	3	0	24	83
	Forest	2	0	**37**	0	39	95
	Urban	0	2	1	**17**	20	85
	Column Total	35	22	43	17	**117**	Overall Accuracy
	Producer's Accuracy	91%	92%	86%	100%		**91%**

Overall Kappa Statistic: 0.87

Table 3-4 Overall accuracy and wetland user and producer's accuracy for two mapping classification results (Classification scheme: wetland/upland).

Land cover classification	Overall accuracy	Wetland user's accuracy	Wetland producer's accuracy	Total area for wetlands in ha
OBIA-Minnesota River-Headwaters	97%	92%	92%	7,620.90
NWI-Minnesota River-Headwaters	88%	71%	57%	6,526.38
OBIA-Swan Lake	98%	96%	96%	4,794.52
NWI-Swan Lake	85%	65%	79%	5,812.04
OBIA- Thompson Reservoir St. Louis River	96%	94%	91%	1,927.29
NWI-Thompson Reservoir St. Louis River	74%	56%	66%	2,233.42

Table 3-5 Significance Test (Z-test) for comparing two mapping classification scheme (wetland/upland) using the same independent reference data points for each study area.

Land cover classification	**Kappa1 vs. Kappa2**	**Z-Value**
OBIA vs. NWI for Minnesota River-Headwaters	0.91 Vs. 0.56	4.61*
OBIA vs. NWI for Swan Lake	0.98 vs. 0.61	3.88*
OBIA vs. NWI for Thompson Reservoir St. Louis River	0.90 vs. 0.42	4.83*

* A Z-value over 1.96 indicates that there is a significant difference at 95% confidence level.

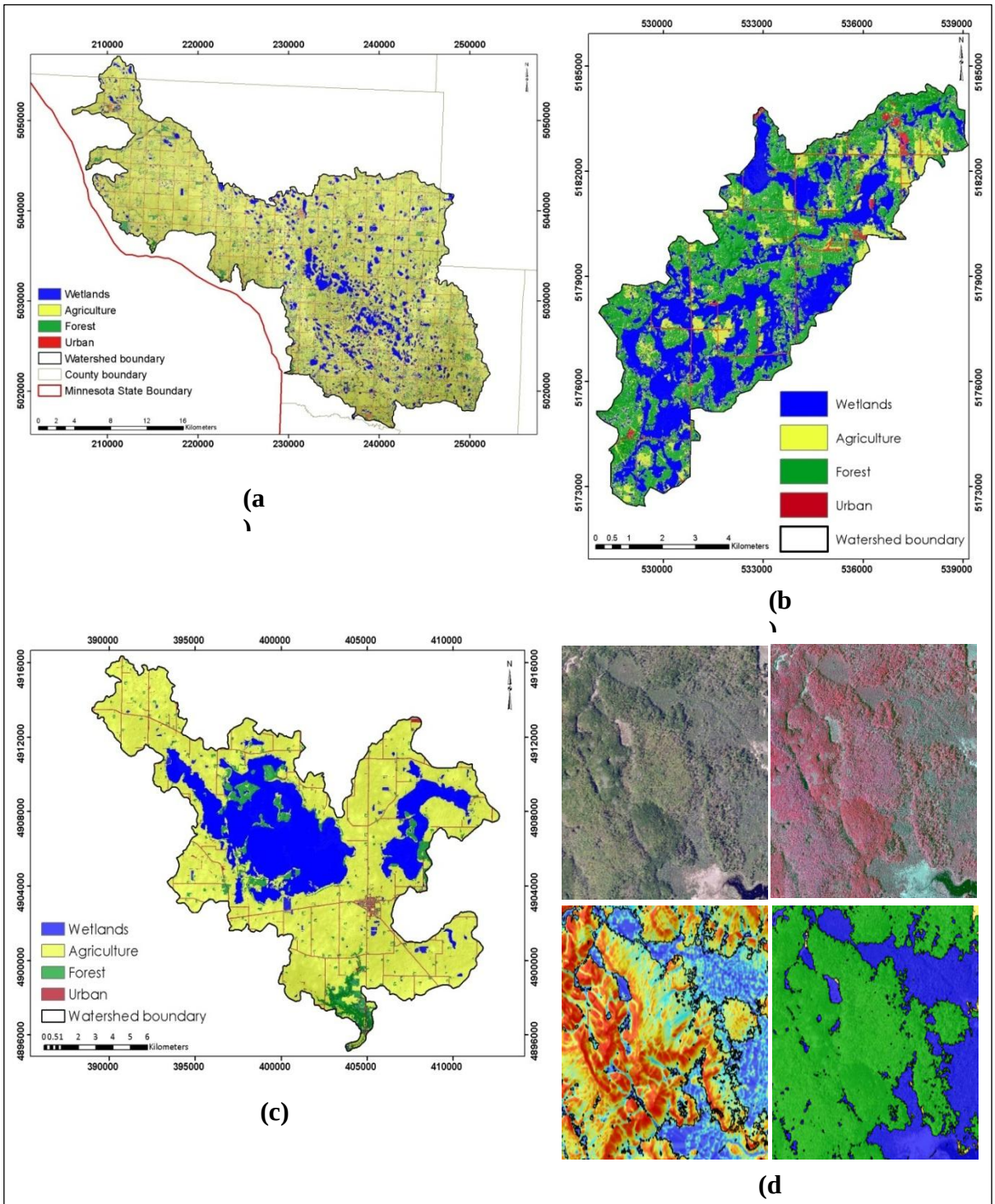

Figure 3-4 OBIA classification maps for Minnesota River-Headwaters (a), Thompson Reservoir St. Louis River (b), and Swan Lake (c). Comparison of layers for a small portion of the Thompson Reservoir St Louis River study area, top left visible bands, top right NIR band, bottom left CTI, and bottom right OBIA classes (wetland/upland) (d).

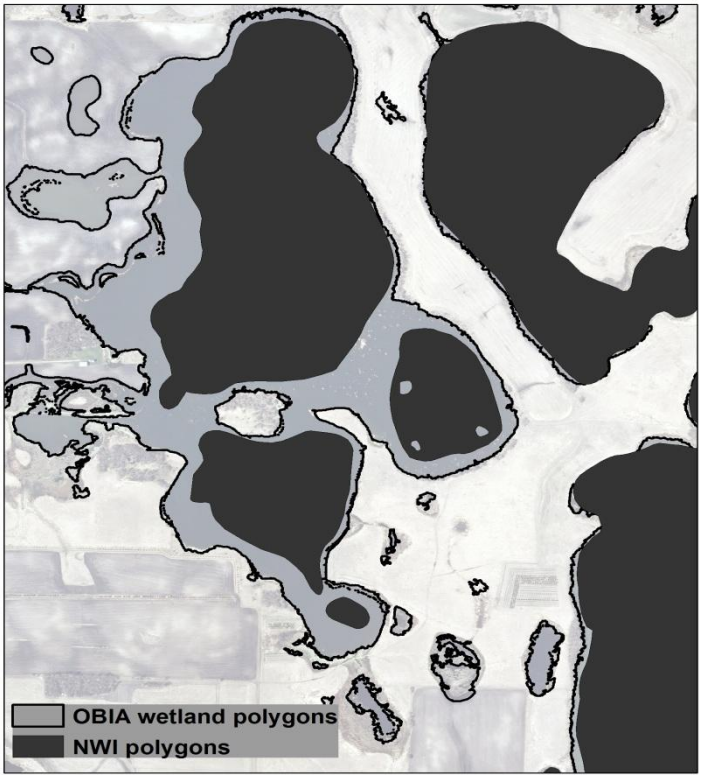

Figure 3-5: Comparison map of the original NWI polygons and OBIA polygons for a small portion of the Minnesota River-Headwaters with a background of an aerial imagery.

Discussion and Conclusions

In this study, we have evaluated an OBIA approach to map and differentiate wetlands from other classes through the design of a ruleset for each study area. The OBIA approach used in this study, across three different ecoregions, provided an adequate platform to integrate different types of high resolution data for accurately detecting wetlands that were greater than 0.20 ha (0.5 acres).

OBIA classification maps corresponded well with the reference data for each study area, obtaining high overall accuracy percentages between 90-93% for the four classes. The results of this study reinforced previous findings regarding the value and importance of high resolution data to improve wetland classification accuracy. Previous

studies have concluded that high resolution data including lidar, aerial and satellite imagery are very advantageous to distinguish between wetlands and non-wetlands classes. These studies have found less confusion between wetlands and upland classes due to the reduction in mixed pixels and addition of high resolution elevation data to separate wetlands from uplands (Everitt et al., 2004; Huan and Zhang 2008; Laba et al., 2008).

The integration of high resolution imagery and lidar data helped to improve classification of wetlands in two ways. First, the use of high resolution data including optical and lidar through an OBIA approach helped to improve the accuracy of wetland classification over traditional pixel-based techniques. For example, Corcoran et al., (2011) integrated high resolution imagery with coarse topographic data using a decision-tree classifier to map wetlands, in a similar area to our third study area in the Northern lakes and forest ecoregion area in Minnesota.

The Corcoran *et al*. (2011) results were lower in overall accuracy (72%) for wetland/upland classification compared to our OBIA results for wetland/upland classification (96%). Sader et al. (1995) compared four satellite image classification methods, including a GIS rule-based model to delineate forest wetlands and other wetlands in Maine. Their results were lower in overall accuracy, ranging from 72% to 82% for their two study areas. Similarly, other studies have used coarse resolution imagery data including satellite data to map wetlands, but obtained low accuracy estimates for wetland classification because of mixed pixels with similar spectral reflectance (Jensen et al., 1993; Lunetta and Balogh, 1999).

Our study demonstrated that an OBIA approach is more suitable than traditional pixel-based methods to take advantage of the high resolution data available to map wetlands (Dechka et al., 2002; Halabisky et al., 2011; Knight et al. 2013; Maxa and Bolstad 2009). The OBIA approach used in this study incorporated contextual, spectral, and shape information that came from homogenous objects instead of pixel units.

It is important to note that all the high resolution data used in this study were available to the public free of charge. This free high resolution data can be advantageous to many governmental and non-governmental organizations interested in wetland conservation and protection.

Second, the integration of high resolution imagery and lidar data helped to improve classification of wetlands because of the use of high resolution lidar to calculate derivatives such as the CTI. In a qualitative visual assessment of all the data layer inputs, the CTI layer provided additional discrimination between wetland and other non-wetland classes because of its ability to separate low terrain areas from steep terrain areas based on topography (Figure 3-5). For example, forested vegetation in local low areas were often confused spectrally with forested vegetation in upland areas, but were easier to separate with the addition of the CTI data layer.

Other studies have shown similar results when adding topographic data and optical data, resulting in a greater improvement of the wetland accuracy classification. For example, in a study by Knight et al. (2013), in an area similar to our third study area, different input datasets including optical and topographic data were evaluated to determine if the addition of different data types would improve the accuracy of wetland classification.

The Knight et al. (2013), results indicated that topographic data and derivatives including the CTI helped to significantly improve the accuracy of wetland/upland classification compared to other data type scenarios including radar and optical data.

That and other similar studies (e.g. Baker et al., 2006; Murphy et al., 2007) reinforce our results regarding the value of using topographic data, which can be categorized as one of the major factors to determine and accurately predict the potential location of wetlands across different ecoregions settings.

It is important to acknowledge that most existing research (e.g. Frohn et al., 2009; Moffett and Gorelick, 2013) using an OBIA approach to classify wetlands and other land cover has focused more on segmentation techniques, while our study focused more on the development of a customized ruleset appropriate to each specific ecoregion setting.

The OBIA multiscale iterative approach used in this study involved the design of a customized ruleset, allowing us the incorporation of contextual and expert knowledge information through the CNL in the eCognition Developer software.

Rulesets can be complex and unique to each area; however, they are adaptable with newer data and transferable to similar areas. Despite the fact that traditional pixel-based techniques are often preferred to study wetlands because of the reduction in analyst time over the classification process, OBIA offers a way to combine the experience and knowledge of the analyst with computer assistance to classify wetlands more accurately in a semi-automated way.

Experience and expert knowledge are critical for mapping wetlands, because these ecosystems tend to have a high variability of physical properties. In addition, this experience and knowledge were necessary in our study to obtain and develop crucial contextual information that was not available through traditional pixel-based techniques. In addition to the high accuracy of the results, the output maps were more aesthetically pleasing than pixel-based maps.

Our OBIA results were significantly improved over the original NWI for the three study areas, with lower rates of wetland omissions. Though it is not fair to make a direct comparison between the NWI and the OBIA results, the OBIA approach used in this study suggests an alternative technique to improve the accuracy of wetlands boundaries.

Results from this study included a landcover classification map with four classes and wetlands polygons for each study area. Lidar data in combination with high resolution imagery significantly improved the accuracy of wetland classification across the three different ecoregions in Minnesota.

Our results provide evidence that diverse ecosystems such as wetlands of different sizes can be identified and classified accurately using an OBIA approach with high resolution data across the three different ecoregions studied in this paper. These results are encouraging and useful as an initial classification of wetland habitats but further research is encouraged to classify wetland types, using recently acquired remote sensing data and OBIA rulesets techniques.

The OBIA approach presented here to map wetlands offers an alternative, semi-automated and improved method over traditional pixel based techniques and the original NWI. Furthermore, this OBIA approach may be suitable for extension to a larger range of wetlands located in areas such as the ones used in this study, with similar land-use, topography and ecoregions.

Acknowledgements

This research was funded by the Minnesota Environment and Natural Resources Trust (ENRTF), the Minnesota Department of Natural Resources (MNDNR), and the United States Fish and Wildlife Services (USFWS: Award 30181AJ194).

References

Baatz M., Schäpe A., 2000. Multiresolution segmentation: An optimization approach for high quality multi-scale image segmentation. Angewandte Geographische Informationsverarbeitung XII (J. Strobl and T. Blaschke, editors), Wichmann, Heidelberg. 12–23.

Baatz M., Hoffmann M., Willhauck G., 2008. Progressing from object-based to object-oriented image analysis, Object Based Image Analysis (T. Blaschke, S. Lang, and G.J. Hay, editors), Springer, Heidelberg, Berlin, New York. 12-23.

Baker C., Lawrence R., Montagne C., Patten D., 2006. Mapping wetlands and riparian areas using Landsat ETM+ imagery and decision-tree-based models. Wetlands. 26, 465–474.

Beven K.J., Kirkby M.J., 1979. A physically based, variable contributing area model of basin hydrology. Hydrological Sciences journal. 24, 43-69.

Benz U., Hoffman P., Willhauck G., Lingenfelder I., Heynen M., 2004. Multi-resolution, object-oriented fuzzy analysis of remote sensing data for GIS-ready information. ISPRS Journal of Photogrammetry and Remote Sensing. 58, 239-258.

Burnett C., Blaschke T., 2003. A multi-scale segmentation/object relationship modeling methodology for landscape analysis. Ecological Modelling. 168, 233-249.

Butera M., 1983. Remote Sensing of Wetlands. IEEE Transactions on Geoscience and Remote Sensing. 21, 383-392.

Blaschke, T., 2003. Object-based contextual image classification built on image segmentation, Proceedings of the 2003 IEEE Workshop on Advances in Techniques for Analysis of Remotely Sensed Data, 27-28 October, Washington D.C., pp. 113-119.

Blaschke T., 2010. Object based image analysis for remote sensing. ISPRS Journal of Photogrammetry and Remote Sensing. 65, 2-16.

Bruzzone L., Carlin L., 2006. A multilevel context-based system for classification of very high spatial resolution images. IEEE Transactions on Geoscience and Remote Sensing. 44, 2587-2600.

Castilla G., Hay G.J., Ruiz-Gallardo J.R., 2008. Size-constrained region merging (SCRM): An automated delineation tool for assisted photointerpretation. Photogrammetric Engineering and Remote Sensing. 74, 409-419.

Congalton R.G., Green K., 2009. Assessing the accuracy of remotely sensed data: principles and practices, 2nd ed. Boca Raton, Florida: CRC Press/Taylor and Francis.

Corcoran J.M.,. Knight J.F, Brisco B., Kaya S., Cull A., Murnaghan K. 2011. The integration of optical, topographic, and radar data for wetland mapping in northern Minnesota. Canadian Journal of Remote Sensing. 37, 564-582.

Cowardin L.M., Carter V., Golet F.C., LaRoe E.T., 1974. Classification of wetlands and deepwater habitats of the United States, U.S. Department of the Interior, Fish and Wildlife Service, Washington, D.C.

Dahl T.E., Johnson C.E., 1991. Status and trends of wetlands in the conterminous United States, mid-1970's to mid-1980, U.S. Department of the Interior, Fish and Wildlife Service, Washington, DC. 28.

Definiens Imaging, 2009. eCognition Imaging Developer version 8. ECognition User Guide.

Dechka J.A., Franklin S.E., Watmough M.D., Bennett R.P., Ingstrup D.W., 2002. Classification of wetland habitat and vegetation communities using multi-temporal Ikonos imagery in southern Saskatchewan, Canadian Journal of Remote Sensing, 28(5):679:685.

Erskine R.H., Green T.R., Ramirez J.A., MacDonald L.H., 2006. Comparison of grid-based algorithms for computing upslope contributing area. Water Resources Research. 42, W09416.

Everitt J. H., Yang C., Fletcher R.S., Davis M.R., Drawe D.L., 2004. Using Aerial Color infrared Photography and QuickBird Satellite Imagery for Mapping Wetland Vegetation. Geocarto International. 19, 15 - 22.

Frayer W.E., Monahan T.J., Bowden D.C., Graybill F.A., 1983. Status and trends of wetlands and Deep-water habitats in the conterminous United States, 1950's to 1970's Colorado State University, Fort Collins, CO.

Federal Register 1980. 40 CFR part 230: Section 404b (1) guidelines for specification of disposal sites for dredged or fill material. 45, 85352-85353.

Federal Register 1982. Title 33: Navigation and navigable waters; chapter II, regulatory programs of the corps of engineers. 47, 31810.

Fournier R.A., Grenier M., Lavoie A., Helie R., 2007. Towards a strategy to implement the Canadian Wetland Inventory using satellite remote sensing Canadian Journal of Remote Sensing. 33, S1-S16.

Frohn R., Reif M., Lane C., Autrey B., 2009. Satellite remote sensing of isolated wetlands using object-oriented classification of LANDSAT-7 data. Wetlands. 29, 931-941.

Galzki J., Nelson J., Mulla D., 2008. Identifying critical landscape areas for precision conservation in the Minnesota River Basin. In: (R. Khosla, ed.), Proc. 9th International Conf. Prec. Agriculture. Denver, CO.

Grenier M., Demers A.M., Labrecque S., Benoit M., Fournier R.A., Drolet B., 2007. An object-based method to map wetland using RADARSAT-1 and Landsat ETM images: Test case on two sites in Quebec, Canada. Canadian Journal of Remote Sensing. 33,S28-S45.

Gruber S. Peckham S., 2008. Land-surface parameters and objects in hydrology. In: Hengl, T. and Reuter, H.I. (eds.) Geomorphometry: concepts, software, applications. Elsevier, Amsterdam, Netherlands. 171-194.

Halabisky M., Moskal L.M., Hall S.A, 2011. Object-based classification of semi-arid wetlands, Journal of Applied Remote Sensing. 5, 053511-1 – 053511–13.

Hay G.J., Castilla G., 2008. Geographic object-based image analysis (GEOBIA): A new name for a new discipline, object-based image analysis-spatial concepts for knowledge-driven Remote Sensing Applications (T. Blaschke, S. Lang, and G.J. Hay, editors), Springer-Verlag, Berlin. 75-89.

Hodgson M. E., J.R. Jensen, H.E. Mackey, and M.C. Coulter, 1987. Remote sensing of wetland habitat: A wood stork example. Photogrammetric Engineering and Remote Sensing. 53, 1075-1080.

Huan Y., Zhang S., 2008. Applications of high resolution satellite imagery for wetlands cover classification using object-oriented method. The International Archives of the Photogrammetry, Remote Sensing and Spatial Information Sciences. 37, 521-526.

Jensen J.R., Cowen D.J., Althausen J.D., Narumalani S.,Weatherbee O., 1993. The detection and prediction of sea level changes on coastal wetlands using satellite imagery and a geographic information system. Geocarto International 4:87–98.

Knight J.F., Tolcser B.T., Corcoran J.M., Rampi L.P., 2013. The effects of data selection and thematic detail on the accuracy of high spatial resolution wetland classifications. Photogrammetric Engineering and Remote Sensing. 79, 613-623.

Laba M., Downs R., Smith S., Welsh S., Neider C., White S., Richmond M., Philpot W., Baveye P., 2008. Mapping invasive wetland plants in the Hudson River National Estuarine Research Reserve using QuickBird satellite imagery, Remote Sensing of Environment. 112, 286–300.

Land Management Information Center (LMIC), 2007. Metadata for the National Wetlands Inventory, Minnesota.

Lunetta R. S., Balogh M.E., 1999. Application of Multi-Temporal Landsat 5 TM Imagery for wetland identification, Photogrammetric Engineering and Remote Sensing. 65, 1303–1310.

Maxa M., Bolstad P., 2009. Mapping northern wetlands with high resolution satellite imagery and lidar. Wetlands. 29, 248–260.

Midwest Community Planning, LLC, 2012. Big Stone County Water Plan. URL: http://www.bigstonecounty.org/environmental/waterplanning/BigStoneCountyWaterPlan.pdf, accessed on March 05 2013.

Millennium Ecosystem Assessment, 2005. Ecosystems and human well-being: wetlands and water Synthesis, World Resources Institute, Washington, DC.

Minnesota Department of Natural Resources, 2006. Tomorrow's Habitat for the Wild and Rare: An Action Plan for Minnesota Wildlife, Comprehensive Wildlife Conservation Strategy. Division of Ecological Services, Minnesota Department of Natural Resources.

Mitsch W. J., Gosselink J. G., 2000. Wetlands (Third ed.). New York: Wiley.938

Moffett, K., Gorelick S., 2013. Distinguishing wetland vegetation and channel features with object-based image segmentation, International Journal of Remote Sensing. 34, 1332-1354.

Moore I. D., Grayson R. B., Ladson A. R., 1991. Digital terrain modeling: a review of hydrological, geomorphological, and biological applications, Hydrological Processes. 5, 3-30.

MPCA 2006. A Comprehensive Wetland Assessment, Monitoring and Mapping Strategy for Minnesota. Saint Paul, MN: Minnesota Pollution Control Agency.

Murphy P. N. C., Ogilvie J., Connor K., Arp P.A., 2007. Mapping wetlands: a comparison of two different approaches for New Brunswick, Canada. Wetlands. 27, 846-854.

Myint S.W., Glober P., Brazel A., Grossman-Clarke S., Weng Q., 2011. Per-pixel vs. object-based classification of urban land cover extraction using high spatial resolution imagery. Remote Sensing of Environment. 115, 1145–1161.

Nicollet County, 2008. Nicollet county local water management plan. URL: http://www.co.nicollet.mn.us. Accessed on March 6, 2013.

O'Neil-Dunne J.P.M., MacFaden S.W., Royar A. R., Pelletier K.C., 2012. An object-based system for LiDAR data fusion and feature extraction. Geocarto International. 1-16.

Ozesmi S. L., Bauer M.E., 2002. Satellite remote sensing of wetlands, Wetlands Ecology and Management. 10, 381-402.

Quinlan J.R., 1990. Decision trees and decision-making, IEEE Transactions on Systems, Man and Cybernetics. 20, 339-346.

Rodhe A., Seibert J., 1999. Wetland occurrence in relation to topography: a test of Topographic indices as moisture indicators. Agricultural and Forest Meteorology. 98-99, 325-340.

Sader S. A., Ahl D., Liou W.S., 1995. Accuracy of Landsat- TM and GIS rule-based methods for forest wetland classification in Maine, Remote Sensing of Environment, 53(3):133-44.

Seibert J., McGlynn B., 2007. A new triangular multiple flow direction algorithm for computing upslope areas from gridded digital elevation models. Water Resources Research. 43,1-8.

Sripada R. P., Heiniger R.W., White J.G., Meijer A.D., 2006. Aerial color infrared photography for determining early in-season nitrogen requirements in corn. Agronomy Journal. 98, 968-977.

Stedman S., Dahl T.E., 2008. Status and trends of wetlands in the coastal watersheds of the Eastern United States 1998-2004. National Oceanic and Atmospheric Administration, National Marine Fisheries Service and U.S. Department of the Interior, Fish and Wildlife Service. 1-32.

Story M., Congalton R.G., 1986. Accuracy assessment: A user's perspective, Photogrammetric Engineering and Remote Sensing. 52, 397-399.

Turner R. K., van den Bergh J. C. J. M., Soderqvist Barendregt T., A., van der Straaten J., Maltby E., van Ierland E. C., 2000. Ecological-economic analysis of wetlands: scientific integration for management and policy. Ecological Economics. 35, 7-23.

Wilson J.P., Aggett G., Deng Y.X., and C.S. Lam, 2008.Water in the landscape: a review of contemporary flow routing algorithms. (Q. Zhou, B. Lees and G. Tang, editors) Advances in digital terrain analysis. Springer, Berlin, DE. 213-236.

Wright C., Gallant A., 2007. Improved wetland remote sensing in Yellowstone National Park using classification trees to combine TM imagery and ancillary environmental data, Remote Sensing of Environment. 107, 582-605.

Zhou W., Troy A., 2008. An object-oriented approach for analyzing and characterizing urban landscape at the parcel level. International Journal of Remote Sensing. 29, 3119-3135.

Conclusions and implications of Dissertation Research

This dissertation investigated the use and accuracy of lidar and high resolution imagery with application to mapping wetlands and lidar building footprints to provide valuable and significant information to the general public and scientific community regarding the use of these data for practical applications.

The goal of the first chapter of this dissertation was to determine whether low or high lidar posting densities would influence on the accuracy and quality of lidar derived building footprints and DEM across the metro region in Minnesota. This goal was achieved by comparing the lidar building footprints and DEM to traditional techniques including manual digitization and ground survey collection. Quantitative statistical results of the building analysis indicated that using low and high lidar posting density to create building footprints will overestimate and underestimated the building area size by a small, statistically insignificant percentage.

There was a small tendency for building footprints created from low lidar density to underestimate the areas of buildings and for building footprints created from high lidar density to overestimate their areas. On the other hand, qualitative assessment results showed that lidar building footprint created from higher lidar density presented more defined, sharper outlines of the buildings. The main conclusion for this building analysis is that the areas of exiting commercial buildings across the metro region can be estimated from the Minnesota DNR lidar building footprints with a small percentage of overestimation or underestimation.

The implication of this finding is that lidar building footprints present an alternative free data type for an updated inventory of commercial building inventory compared to traditional techniques such as photo-interpretation and heads-up digitization.

Statistical results of the ground elevation analysis demonstrated that elevation changes that occurred within the low lidar density DEM were very similar to the ground survey elevations taken at the same locations. In the same way, elevation changes that occurred within the high lidar density DEM were very similar to the ground survey elevation points.

The statistical tests reported an insignificant difference between the changes that occurred in both datasets using low and high lidar density. The main conclusion of this elevation analysis is that accurate DEMs can be computed from low and high lidar densities (1.4 pt/m² and 11.4 pt/m²). The implication of this result is that lidar data collected in the state of Minnesota can be used by governmental and non-governmental organizations to create accurate DEMs from low or high lidar densities and use this accurate elevation information different aplications such as urban planning, engineering, and enviromental applications.

The goal of the second chapter was to determine which flow direction algorithms would yield higher accuracy results in the application of the CTI derived from a lidar DEM for mapping wetlands in three different ecoregions. This goal was accomplished by comparing and evaluating the accuracy of seven CTIs based on single and multiple flows direction algorithms.

In general, accuracy assessment results demonstrated that CTI based maps can accurately map wetlands using lidar DEM information alone in the range of 81% and 92% overall accuracy. Also, visual quality assessment of the seven CTI maps for wetland vs. upland showed clear variations such as unrealistic parallel flow patterns that were not assessed in the quantitative accuracy assessment.

The main conclusion of this chapter is that the CTI in the three different ecoregions study areas can significantly improve the accuracy of potential wetlands location, and using multiple flow direction algorithms (D-∞, MD-∞, Mass Flux) will visually help to determine more accurate location of potential wetlands. Using a multiple flow direction algorithm to calculate the CTI helps to define the real pattern of water movement and distribution throughout the landscape, and this will influence the identification of potential wetlands, particularly for depressional wetlands.

The implication of this chapter is that Lidar derived CTIs can offer a fast, practical, and cost-effective technique to estimate potential wetlands and update current wetland inventories such as the NWI.

The goal of the third chapter was to evaluate an OBIA method to integrated lidar data and high resolution imagery with the purpose of mapping and differentiating

wetlands from other classes in three different ecoregions. This goal was completed by using an OBIA customized ruleset and a multiscale iterative approach that incorporated spectral, elevation, contextual, and shape information from the two data types used in this study. Accuracy assessment results showed that wetland greater than 0.20 ha (0.5 acres) in the three different ecoregions can be accurately maps with overall accuracy of 90-93% using four classes to differentiate wetlands from forest, agricultural and urban areas.

The main conclusion of this chapter was that an OBIA approach should be preferred over traditional pixel-based methods to integrate different types of high resolution data including lidar data for mapping wetlands and other land cover classes.

In this study, the OBIA technique for mapping wetlands demonstrated that higher accuracy results in all the three study areas were reachable compared to the results of the second chapter of this research using the CTI alone.

The implication of the results of the third chapter is that complex diverse wetland ecosystems of different sizes, located in different ecoregions can be accurately identified using lidar data and high resolution imagery in an OBIA approach. The OBIA method created in this research can be adapted to map wetlands in other areas that have similar topography and land cover. Furthermore, the fact that an OBIA can combine the knowledge and experience of the analyst can help to further improve the accuracy of complex wetlands such as forested wetlands.

It is important to acknowledge the fact that in Minnesota there are two different systems normally used to classify wetlands, these include: the Circular 39 system, developed by the U.S. Fish and Wildlife Service in 1956, and the Cowardin classification system, developed by the U.S. Fish and Wildlife Service in 1979 (Eggers and Reed, 1997). Although, our research focused only on mapping wetland's boundaries vs. other upland classes; it is important to recognize that we included all types of wetlands in our assessment by classifying all the type of wetlands as wetlands only.

We found that some study areas had higher overall accuracy than others for mapping wetland boundaries and location. These differences can be explained by the following points:

Methodology used in chapter two was limited to use only lidar elevation data via the CTI for identifying wetlands. Thus, the use of only topography information resulted in partiality to have higher accuracy results for all types of wetlands (majority depressional wetlands) located in the study areas within the northern Glaciated Plains ecoregion and Central Hardwood Forest ecoregion.

The majority of wetlands types found in these two study areas according with the Circular 39 system are type 3, 4, and 5, including: open water wetlands, shallow marshes, and deep marshes.

On the other hand, we had lower overall accuracy results in the study area located in the Northern Lakes and Forest ecoregion. This can be explained because of the wetlands types located in this area which includes type 2, 7 and 8. Example of type 2 wetland found in our study area was calcareous fens and sedge meadows, for type 7 were hardwood and coniferous swamps, and for type 8 were coniferous bogs. These types of wetlands (2, 7, and 8) are groundwater recharge (seepages) which make them less sensitive to topography influence and inundation events as they are located at an elevation above floodplain.

Methodology used in chapter three was less limited to identifying different types of wetlands compared to methodology in chapter two because of the integration of optical data and lidar elevation data. In general, the combination of spectral data and topographic information helped to improve the overall accuracy across the three study areas located in different ecoregions.

The combination of both data types through an OBIA approach helped to increase the overall accuracy particularly for the study areas located in the Western Corn Belt Plains ecoregion and the Northern Lakes and Forest.

The western Corn Belt plains study area had type 1 and 2 wetlands types, including: seasonal wetlands and wet meadows. These type of wetland often occurred on relatively flat slopes. Thus, CTI alone would have not been able to capture these wetlands but the use of high resolution leaf-off data particularly when areas have been inundated helped in the process of classifying accurately these types of wetlands using the OBIA

approach. Same increase in overall accuracy was found for the Northern Lakes and Forest especially for forested wetlands.

Finally, the NWI maps are the most available inventory accessible to the general public, governmental and non-governmental entities. Thus, the techniques investigated in this research can be used to update wetland inventories using high resolution data.

It is important to recognize that all the data used in this study was free of cost and available statewide in Minnesota. Such data, combined with appropriate analysis techniques, can be used to update inventories necessary to take accurate decisions to protect and monitor valuable ecosystems such as wetlands.

References

Ackermann F., 1999. Airborne laser scanning-present status and future expectations. ISPRS Journal of Photograpmmetry and Remote Sensing. 54,64-67.

Anderson E.S., Thompson J., Crourse D.A., Austin R.E., 2006. Horizontal resolution and data density effects on remotely sensed lidar-based DEM. Geoderma. 132, 406–15.

Anteau M.J., Afton A.D., 2009. Wetland Use and feeding by lesser Scaup during spring migration across the upper midwest, USA. Wetlands 29,704-712.

Antonarakis A.S., Richards K.S., Brasington J., 2008. Object-based land cover classification using airborne Lidar. Remote Sensing of Environment. 2988-2998

Aguilar F.J., Agüera F., Aguilar M.A., Fernando C., 2005. Effects of terrain morphology, sampling density**,** and interpolation methods on grid DEM accuracy. Photogrammetric Engineering & Remote Sensing. 7, 805–816.

Aguilar F.J., Mills J.P., Delgado J., Aguilar M.A., Negreiros J.G., Perez J.L., 2010. Modelling vertical error in LiDAR-derived digiral elevation models. ISPRS Journal of Photogrammetric and Remote Sensing. 65, 103-110.

Awrangjeb M., Zhang C., Fraser C.S., 2013. Automatic extraction of buildings roofs using LIDAR data and multispectral imagery. ISPRS Journal of Photogrammetric and Remote Sensing. 83, 1-18.

Baatz M., Schäpe A., 2000. Multiresolution segmentation: An optimization approach for high quality multi-scale image segmentation. Angewandte Geographische Informationsverarbeitung XII (J. Strobl and T. Blaschke, editors), Wichmann, Heidelberg. 12–23.

Baatz M., Hoffmann M., Willhauck G., 2008. Progressing from object-based to object-oriented image analysis, Object Based Image Analysis (T. Blaschke, S. Lang, and G.J. Hay, editors), Springer, Heidelberg, Berlin, New York. 12-23.

Baker C., Lawrence R., Montagne C., Patten D., 2006. Mapping wetlands and riparian areas using Landsat ETM+ imagery and decision-tree-based models. Wetlands. 26, 465–474.

Banskota A., Wynne R. H., Johnson P., Emessiene B., 2011. Synergistic use of very high-frequency radar and discrete-return lidar for estimating biomass in temperate hardwood and mixed forests. Annals of Forest Science. 68, 347–356.

Barling R.D., Moore I.D., Grayson R.B., 1994.A quasi-dynamic wetness index for characterizing the spatial distribution of zones of surface saturation and soil water content. Water Resources Research. 30, 1029-1044.

Bauer J., Rohdenburg H., Bork H.R., 1985. Ein Digitales Reliefmodell als Vorraussetzung fuer ein deterministisches Modell der Wasser- und Stoff-Fluesse. In: Bork, H.R. & Rohdenburg H(eds) Parameteraufbereitung fuer deterministische Gebiets-Wassermodelle, Grundlagenarbeiten zu Analyse von Agrar-Oekosystemen. Technische University Braunschweig. 1-15.

Benz U., Hoffman P., Willhauck G., Lingenfelder I., Heynen M., 2004. Multi-resolution, object-oriented fuzzy analysis of remote sensing data for GIS-ready information. ISPRS Journal of Photogrammetry and Remote Sensing. 58, 239-258.

Beven K.J, Kirkby M.J., 1979. A physically based, variable contributing area model of basin hydrology. Hydrological Sciences journal. 24, 43-69.

Bilskie M.V., Scott C.H., 2013. Topographic accuracy assessment of bare earth lidar-derived unstructured meshes. Advances in water resources. 52, 165-177.

Burnett C., Blaschke T., 2003. A multi-scale segmentation/object relationship modeling methodology for landscape analysis. Ecological Modelling. 168, 233-249.

Butera M., 1983. Remote Sensing of Wetlands. IEEE Transactions on Geoscience and Remote Sensing. 21, 383-392.

Blaschke, T., 2003. Object-based contextual image classification built on image segmentation, Proceedings of the 2003 IEEE Workshop on Advances in Techniques

for Analysis of Remotely Sensed Data, 27-28 October, Washington D.C., pp. 113-119.

Blaschke T., 2010. Object based image analysis for remote sensing. ISPRS Journal of Photogrammetry and Remote Sensing. 65, 2-16.

Bridgham S.D., Pastor J., Dewey B., Weltzin J.F., Updegraff K., 2008. Rapid Carbon Response of Peatlands to Climate Change. Ecology. 89, 3041-3048.

Bruzzone L., Carlin L., 2006. A multilevel context-based system for classification of very high spatial resolution images. IEEE Transactions on Geoscience and Remote Sensing. 44, 2587-2600.

Cavalli M., Tarolli P., Marchi L., Fontana G.D., 2008. The effectiveness of airborne LiDAR data in the recognition of channel-bed morphology. Catena. 73, 249-260.

Bartier P.M., Keller C.P., 1996. Multivariate interpolation to incorporate thematic surface data using inverse distance weighting (IDW). Computers & Geosciences. 22, 795–799.

Caruso C., Quarta F., 1998. Interpolation methods comparison, Computers and Mathematics with Applications. 35,109–126.

Castilla G., Hay G.J., Ruiz-Gallardo J.R., 2008. Size-constrained region merging (SCRM): An automated delineation tool for assisted photointerpretation. Photogrammetric Engineering and Remote Sensing. 74, 409-419.

City of Chanhassen Surface Water Management Plan (2006) In: The Second Generation Surface Water Management Plan - Chanhassen, Minnesota: http://www.ci.chanhassen.mn.us/serv/cip/swmp/wetlandsmanagement.htm. Accessed 25 May 2013.

Congalton R.G., Green K., 2009. Assessing the accuracy of remotely sensed data: principles and practices, 2nd edn. Boca Raton, Florida: CRC Press/Taylor and Francis.

Coops N.C., Wulder M.A., Culvenor D.S., St-onge B., 2004. Comparison of forest attributes extracted from fine spatial resolution multispectral and lidar data. Canadian Journal of Remote Sensing. 30, 855-866.

Corcoran J.M., Knight J.F., Brisco B., Kaya S., Cull A., Murnaghan K., 2011. The integration of optical, topographic, and radar data for wetland mapping in northern Minnesota. Canadian Journal of Remote Sensing. 37, 564-582.

Costa-Cabral M., Burges S.J., 1994. Digital elevation model networks (DEMON): a model of flow over hillslopes for computation of contributing and dispersal areas. Water Resources Research. 30,1681-1692.

Cowardin L.M., Carter V., Golet F.C., LaRoe E.T., 1974. Classification of wetlands and deepwater habitats of the United States, U.S. Department of the Interior, Fish and Wildlife Service, Washington, D.C.

Chaplot V., Walter C., 2003. Subsurface topography to enhance the prediction of the spatial distribution of soil wetness. Hydrological processes. 2567-2580.

Charman D.J., 2009. Peat and Peatlands. Elsevier Inc. 541-548.

Chen Q., 2010.Retrieving vegetation height of forests and woodlands over mountainous areas in the Pacific Coast region using satellite laser altimetry," Remote Sensing of Environment. 114, 1610–1627.

Chow T.E.,Hodson M.E., 2009. Effects of lidar post-spacing and DEM resolution to mean slope estimation, International Journal of Geographical Information Science. 23, 1277-1298. DOI: 10.1080/13658810802344127

Dahl T.E., Johnson C.E., 1991. Status and trends of wetlands in the conterminous United States, mid-1970's to mid-1980's. U.S. Fish and Wildlife Service, Washington, DC. 28.

Dahl T.E., 2006. Status and trends of wetlands in the conterminous United States 1998 to 2004, U.S. Department of the Interior; Fish and Wildlife Service, Washington, D.C. 112.

Definiens Imaging, 2009. eCognition Imaging Developer version 8. ECognition User Guide.

Dechka J.A., Franklin S.E., Watmough M.D., Bennett R.P., Ingstrup D.W., 2002. Classification of wetland habitat and vegetation communities using multi-temporal Ikonos imagery in southern Saskatchewan, Canadian Journal of Remote Sensing, 28(5):679:685.

Deshpande S.S., 2013. Improved Floodplain Delineation Method Using High-Density LiDAR Data. Computer-Aided Civil and Infrastructure Engineering. 28, 68–79.

Dubayah R.O., Drake J.B., 2000. Lidar remote sensing for forestry. Journal of Forestry. 98, 44-46.

Eggers S. D., Reed D. M., 1997. Wetland plants and plant communities of Minnesota and Wisconsin (Second ed.). St. Paul Distric.

Erskine R.H., Green T.R., Ramirez J.A., MacDonald L.H., 2006. Comparison of grid-based algorithms for computing upslope contributing area. Water Resources Research. 42, W09416.

Everitt J. H., Yang C., Fletcher R.S., Davis M.R., Drawe D.L., 2004. Using Aerial Color infrared Photography and QuickBird Satellite Imagery for Mapping Wetland Vegetation. Geocarto International. 19, 15 - 22.

Fairfield J., Leymarie P., 1991. Drainage networks from grid digital elevation models. Water Resources Research. 27,709-717.

Federal Register 1980. 40 CFR part 230: Section 404b (1) guidelines for specification of disposal sites for dredged or fill material. 45, 85352-85353.

Federal Register 1982. Title 33: Navigation and navigable waters; chapter II, regulatory programs of the corps of engineers. 47, 31810.

Fiocco G., Smullin L.D., 1963. Detection of scattering layers in the upper atmosphere (60-140 kn) by optical radar. Nature. 199, 1275-1276. doi:10.1038/1991275a0

Fournier R.A., Grenier M., Lavoie A., Helie R., 2007. Towards a strategy to implement the Canadian Wetland Inventory using satellite remote sensing Canadian Journal of Remote Sensing. 33, S1-S16.

Flood M., 2001. Laser altimetry, from science to commercial lidar mapping. Photogrammetric Engineering and Remote Sensing. 67, 1209-1217.

Frayer W.E., Monahan T.J., Bowden D.C., Graybill F.A., 1983. Status and trends of wetlands and Deep-water habitats in the conterminous United States, 1950's to 1970's Colorado State University, Fort Collins, CO.

Frohn R., Reif M., Lane C., Autrey B., 2009. Satellite remote sensing of isolated wetlands using object-oriented classification of LANDSAT-7 data. Wetlands. 29, 931-941.

Galzki J., Nelson J., Mulla D., 2008. Identifying critical landscape areas for precision conservation in the Minnesota River Basin. In: (R. Khosla, ed.), Proc. 9th International Conf. Prec. Agriculture. Denver, CO.

García-Quijano M.J., Jensen J.R., Hodgson M.E., Hadley B.C., Gladden J.B., Lapine L.A., 2008. Significance of Altitude and Posting Density on Lidar-derived elevation accuracy on Hazardous waste sites. Photogrammetric Engineering and Remote Sensing. 74, 1137-1146.

Ghilani C.D., Wolf P.R., 2012. Elementary surveying: an introduction to geomatics. 13th edition, Prentice Hall.

Goodwin N.R., Coops N.C., Culvenor D.S., 2006. Assessment of forest structure with airborne LiDAR and the effects of platform altitude. Remote Sensing of Environment. 103, 140–152.

Guntner A., Seibert J., Uhlenbrook S., 2004. Modeling spatial patterns of saturated areas: An evaluation of different terrain indices. Water Resources Research. 40,W05114.

Guo Q., Li W., Yu H., Alvarez O., 2010. Effects of topographic variability and Lidar sampling density on several DEM interpolation methods. Photogrammetric Engineering and Remote Sensing. 76, 701-712.

Grabs T., Seibert J., Bishop K., Laudon H., 2009. Modeling spatial patterns of saturated areas: A comparison of the topographic wetness index and a dynamic distributed model. Journal of Hydrology. 373,15-23.

Grenier M., Demers A.M., Labrecque S., Benoit M., Fournier R.A., Drolet B., 2007. An object-based method to map wetland using RADARSAT-1 and Landsat ETM images: Test case on two sites in Quebec, Canada. Canadian Journal of Remote Sensing. 33,S28-S45.

Gruber S., Peckham S., 2008. Land-surface parameters and objects in hydrology. In: Hengl T, Reuter HI (eds) Geomorphometry: concepts, software, applications, Elsevier, Amsterdam, Netherlands. 171-194.

Halabisky M., Moskal L.M., Hall S.A, 2011. Object-based classification of semi-arid wetlands, Journal of Applied Remote Sensing. 5, 053511-1 – 053511–13.

Hay G.J., Castilla G., 2008. Geographic object-based image analysis (GEOBIA): A new name for a new discipline, object-based image analysis-spatial concepts for knowledge-driven Remote Sensing Applications (T. Blaschke, S. Lang, and G.J. Hay, editors), Springer-Verlag, Berlin. 75-89.

Haugerud R.A., Harding D.J., Johnson S.Y., Harless J.L., Weaver C.S., Sherrod B.L., 2003. High-resolution lidar topography of the Puget Lowland-A bonanza for earth science. Geological Society of America Today. 13, 4–10.

Heidemann H. k., 2012. Lidar Base Specification version1.0: U.S. Geological Survey Techniques and Methods, Book 11. United States Geological Survey, Washington D.C.

Hodgson M. E., J.R. Jensen, H.E. Mackey, and M.C. Coulter, 1987. Remote sensing of wetland habitat: A wood stork example. Photogrammetric Engineering and Remote Sensing. 53, 1075-1080.

Hodson M.E., Bresnahan, P., 2004, Accuracy of airborne lidar-derived elevation, empirical assessment and error budget. Photogrammetric Engineering and Remote Sensing. 70, 331–339.

Huan Y., Zhang S., 2008. Applications of high resolution satellite imagery for wetlands cover classification using object-oriented method. The International Archives of the Photogrammetry, Remote Sensing and Spatial Information Sciences. 37, 521-526.

Jenkins R.B., Frazier P.S., 2010. High-Resolution Remote Sensing of Upland Swamp Boundaries and Vegetation for Baseline Mapping and Monitoring. Wetlands. 30, 531-540.

Jensen J.R., Cowen D.J., Althausen J.D., Narumalani S.,Weatherbee O., 1993. The detection and prediction of sea level changes on coastal wetlands using satellite imagery and a geographic information system. Geocarto International 4:87–98.

Knight J.F., Tolcser B.T., Corcoran J.M., Rampi L.P., 2013. The effects of data selection and thematic detail on the accuracy of high spatial resolution wetland classifications, Photogrammetric Engineering and Remote Sensing. 79, 613-623.

Laba M., Downs R., Smith S., Welsh S., Neider C., White S., Richmond M., Philpot W., Baveye P., 2008. Mapping invasive wetland plants in the Hudson River National Estuarine Research Reserve using QuickBird satellite imagery, Remote Sensing of Environment. 112, 286–300.

LaBaugh J.W., Winter, T. C., Rosenberry, D. O.,1998. Hydrologic Functions of Prairie Wetlands. Great Plains Research: A Journal of Natural and Social Sciences.17-37.

Land Management Information Center (LMIC)., 2007. Metadata for the National Wetlands Inventory, Minnesota.

Lang M.W., McCarty G.W., 2009. Lidar intensity for improved detection of inundation below the forest canopy. Wetlands. 29,1166–1178.

Lang M.W., McDonough O., McCarty G.W., Oesterling R., Wilen B., 2012. Enhanced Detection of Wetland-Stream ConnectivityUsing LiDAR. Wetlands 32:461-473

Lang M.W., McCarty G.W., Oesterling R., Yeo I., 2013. Topographic Metrics for Improved Mapping of Forested Wetlands. Wetlands. 33, 141-155.

Lea N.L., 1992. An aspect driven kinematic routing algorithm. In: Parsons AJ, Abrahams AD, (eds) Overland flow: hydraulics and erosion mechanics, Chapman & Hall, New York. 393–407.

Lee H., Younan N.H., 2003. DEM extraction of lidar returns via adaptive processing. IEEE Transactions on Geoscience and Remote Sensing. 41,2063–2069.

Liu X., Zhang Z., 2008. LIDAR data reduction for efficient and high quality DEM generation Paper presented at the ISPRS Congress Beijing 2008, Beijing, China (http://eprints.usq.edu.au/4569/)

Liu X., Zhang Z., Peterson J., Chandra S., 2007. Lidar-derived high quality ground control information and DEM for image orthorectification. GeoInformatica. 11,37–53.

Lohani B., Singh R., 2008. Effect of data density, scan angle, and flying height on the accuracy of building extraction using LiDAR data. Geocarto International. 23, 81-94. DOI: 10.1080/10106040701207100

Lunetta R. S., Balogh M.E., 1999. Application of Multi-Temporal Landsat 5 TM Imagery for wetland identification, Photogrammetric Engineering and Remote Sensing. 65, 1303–1310.

Lloyd C.D., Atkinson P.M., 2002. Deriving DSMs from lidar data with kriging. International Journal of Remote Sensing. 23, 2519–2524.

Ma R. 2005. DEM generation and building detection from lidar data. Photogrammetric Engineering and Remote Sensing.71, 847-854.

Minnesota Geospatial Information Office (MnGeo). Minnesota Geospatial Information Office. www.mngeo.state.mn.us. Accessed 2013 October 15.

Maxa M., Bolstad P., 2009. Mapping northern wetlands with high resolution satellite imagery and lidar. Wetlands. 29, 248–260.

Means J. E., Acker S. A., Harding D. J., Blair J. B., Lefsky M. A., Cohen W. B., Harmon M. E., McKee W. A., 1999. Use of large-footprint scanning airborne lidar to estimate forest stand characteristics in the Western Cascades of Oregon. Remote Sensing of Environment. 67, 298–308

Midwest Community Planning, LLC, 2012. Big Stone County Water Plan. URL: http://www.bigstonecounty.org/environmental/waterplanning/BigStoneCountyWaterPlan.pdf. Accessed on March 05 2013.

Millennium Ecosystem Assessment, 2005. Ecosystems and human well-being: wetlands and water Synthesis, World Resources Institute, Washington, DC.

Minnesota Department of Administration (Admin MN) Office of geographic and demographic analysis state demographic center, 2010 census: Minnesota city profiles. http://www.demography.state.mn.us/CityProfiles2010/index.html. Accessed May 20, 2013

Minnesota Department of Natural Resources, 2006. Tomorrow's Habitat for the Wild and Rare: An Action Plan for Minnesota Wildlife, Comprehensive Wildlife Conservation Strategy. Division of Ecological Services, Minnesota Department of Natural Resources.

Mitsch W. J., Gosselink J. G., 2000. Wetlands (Third ed.). New York: Wiley.938

Moffett, K., Gorelick S., 2013. Distinguishing wetland vegetation and channel features with object-based image segmentation, International Journal of Remote Sensing. 34, 1332-1354.

Moore I. D., Grayson R. B., Ladson A. R., 1991. Digital terrain modeling: a review of hydrological, geomorphological, and biological applications, Hydrological Processes. 5, 3-30.

Moore I.D., Gessler P.E., Nielsen G.A., Peterson G.A., 1993. Soil attribute prediction using terrain analysis. Soil Science Society of America Journal. 57, 443-452.

MPCA 2006. A Comprehensive Wetland Assessment, Monitoring and Mapping Strategy for Minnesota. Saint Paul, MN: Minnesota Pollution Control Agency.

Murphy P. N. C., Ogilvie J., Connor K., Arp P.A., 2007. Mapping wetlands: a comparison of two different approaches for New Brunswick, Canada. Wetlands. 27, 846-854.

Myint S.W., Glober P., Brazel A., Grossman-Clarke S., Weng Q., 2011. Per-pixel vs. object-based classification of urban land cover extraction using high spatial resolution imagery. Remote Sensing of Environment. 115, 1145–1161.

Nicollet County, 2008. Nicollet county local water management plan. URL: http://www.co.nicollet.mn.us. Accessed on March 6, 2013.

Næsset 2004. Effects of different flying altitudes on biophysical stand properties estimated from canopy height and density measured with a small-footprint airborne scanning laser. Remote Sensing of Environment. 9, 243–255

O'Callaghan J.F., Mark D.M.m 1984. The extraction of drainage networks from digital elevation data. Computer Vision, Graphic and Image Processing. 28, 328-344.

Oehlert G. W., 2010.A First Course in Design and Analysis of Experiments. New York: W. H. Freeman and Company. http://users.stat.umn.edu/~gary/book/fcdae.pdf

O'Neil-Dunne J.P.M., MacFaden S.W., Royar A. R., Pelletier K.C., 2012. An object-based system for LiDAR data fusion and feature extraction. Geocarto International. 1-16.

Ozesmi S. L., Bauer M.E., 2002. Satellite remote sensing of wetlands, Wetlands Ecology and Management. 10, 381-402.

Pan F., Peters- Lidar C.D., Sale M.J., King A.W., 2004. A comparison of geographical information system-based algorithms for computing the TOPMODEL topographic index. Water Resources Research. 40,1–11.

Quinlan J.R., 1990. Decision trees and decision-making, IEEE Transactions on Systems, Man and Cybernetics. 20, 339-346.

Quinn P., Beven K., Chevallier P., Planchon O., 1991. The prediction of hillslope flow paths for distributed hydrological modeling using digital terrain models. Hydrological Processes. 5,59–80.

Raber G.T., Jensen J.R., Hodgson M.E., Tullis J.A., Davis B.A., Berglund J., 2007. Impact of lidar nominal post-spacing on DEM accuracy and flood zone delineation. Photogrammetric Engineering & Remote Sensing. 73, 793–804.

Rampi L.P., Knight J.F., 2013. Wetland mapping in the Upper Midwest United States: An object-based approach integrating lidar and imagery data. PhotogrammetricEngineering and Remote Sensing. In review.

Rodhe A., Seibert J., 1999. Wetland occurrence in relation to topography: a test of Topographic indices as moisture indicators. Agricultural and Forest Meteorology. 98-99, 325-340.

Rutzinger M., Rottensteiner F., Pfeifer N., 2009.A Comparison of Evaluation Techniques for Building Extraction From Airborne Laser Scanning. IEEE Journal of selected topics in applied earth observations and remote sensing. 2, 11-20.

Sader S. A., Ahl D., Liou W.S., 1995. Accuracy of Landsat- TM and GIS rule-based methods for forest wetland classification in Maine, Remote Sensing of Environment, 53(3):133-44.

Seibert J, McGlynn B., 2007. A new triangular multiple flow direction algorithm for computing upslope areas from gridded digital elevation models. Water Resources Research. 43,1-8.

Sripada R. P., Heiniger R.W., White J.G., Meijer A.D., 2006. Aerial color infrared photography for determining early in-season nitrogen requirements in corn. Agronomy Journal. 98, 968-977.

Sørensen R., Seibert J., 2007. Effects of DEM resolution on the calculation of topographical indices: TWI and its components. Journal of Hydrology. 79–89.

Stedman S., Dahl T.E., 2008.Status and trends of wetlands in the coastal watersheds of the Eastern United States 1998 - 2004. National Oceanic and Atmospheric Administration, National Marine Fisheries Service and U.S. Department of the Interior, Fish and Wildlife Service, 32 pages

Schmidt F., Persson A., 2003. Comparison of DEM data capture and topographic wetness indices. Precision Agriculture. 4,179-192.

Shoutis L., Dunca T.P., McGlyn B., 2010. Terrain-based predictive Modeling of Riparian Vegetation in Northern Rocky Mountain Watershed. Wetlands. 30,621-633.

Smith S.L., Holland D.A., Longley P.A., 2004. The importance of understanding error in lidar digital elevation models. International Archives of the Photogrammetry, Remote Sensing and Spatial Information Sciences. 35, 996–1001.

Story M., Congalton R.G., 1986. Accuracy assessment: A user's perspective, Photogrammetric Engineering and Remote Sensing. 52, 397-399.

Tarboton D.G., 1997. A new method for the determination of flow directions and upslope areas in grid digital elevation models. Water Resources Research. 33,309-319.

Töyrä J., Pietroniro A ., 2005. Towards operational monitoring of a northern wetland using geomatics-based techniques. Remote Sensing of Environment. 174-191.

Tournaire O., Brédif M., Boldo D., Durupt M., 2010. An efficient stochastic approach for building footprint extraction from digital elevation models. ISPRS Journal of Photogrammetry and Remote Sensing. 65, 317-327.

Turner R. K., van den Bergh J. C. J. M., Soderqvist Barendregt T., A., van der Straaten J., Maltby E., van Ierland E. C., 2000. Ecological-economic analysis of wetlands: scientific integration for management and policy. Ecological Economics. 35, 7-23.

USGS Center for LIDAR Information Coordination and Knowledge. http://lidar.cr.usgs.gov/. Accessed 2013 October 15.

Webster T.L., Forbes, D.L., Dickie, S., 2004. Using topographic lidar to map flood risk from storm-surge events from Charlottetown, Prince Edward Island. Canadian Journal of Remote Sensing. 30, 64–76.

Wehr, A., Lohr U., 1999. Airborne laser scanning-An introduction and overview. ISPRS Journal of Photograpmmetry and Remote Sensing 54:68-82.

Wilson J.P., Gallant J.C., 2000. Secondary topographic attributes. In Wilson JP, Gallant JC (ed) Terrain analysis: Principles and applications, Wiley, New York. 87-131.

Wilson J.P., Aggett G., Deng Y.X., Lam C.S. 2008. Water in the landscape: a review of contemporary flow routing algorithms. In: Zhou Q, Lees B, Tang G (eds) Advances in digital terrain analysis, Springer, Berlin. 213–236.

Winter T. C., Rosenberry D. O. 1995. The interaction of ground water with prairie pothole wetlands in the Cottonwood Lake Area, eastcentral North Dakota, 1979-1990. Wetlands. 193-211.

Wright C., Gallant A., 2007. Improved wetland remote sensing in Yellowstone National Park using classification trees to combine TM imagery and ancillary environmental data, Remote Sensing of Environment. 107, 582-605.

Yang X., Chapman G.A., Young M.A., Gray J.M., 2005. Using compound topographic index to delineate soil landscape facets from digital elevation models for comprehensive coastal assessment. In: Zerger A, Argent RM (eds) International Congress on Modeling and Simulation. Modeling and Simulation Society of Australia and New Zealand, ISBN: 0-9758400-2-9, pp 1511–1517 http://www.mssanz.org.au/modsim05/papers/yang_x.pdf

Zhou Q., Liu X., 2002. Error assessment of grid-based flow routing algorithms used in hydrological models. International Journal of Geographical Information Science. 16, 819–8.

Zhang K., Yan j., Chen S., 2006. Automatic Construction of Building Footprints From Airborne LIDAR Data. IEEE Transactions on geoscience and remote sensing. 44, 2523-2533.

Zhou W., Troy A., 2008. An object-oriented approach for analyzing and characterizing urban landscape at the parcel level. International Journal of Remote Sensing. 29, 3119-3135.